Department of Urology

Ulm University

Medical Director: Prof. Dr. Christian Bolenz

The role of TKS5 in bladder cancer and chromosome instability

Dissertation

submitted for the degree of Doctor in Medicine (Dr. med.)

at the Medical Faculty of Ulm University

Wenya Wang

Born in Shandong, P. R. China

2021

Current Dean: Prof. Dr. Thomas Wirth

First Supervisor: Prof. Dr. Cagatay Günes

Second Supervisor: Prof. Dr. Franz Oswald

Day of thesis defense: 22.07.2022

Content

Abbreviations I

1. Introduction 1

1.1 Overview of bladder cancer (BC) 1

1.2 Chromosome instability 3

1.2.1 Causes of chromosomal instability 4

1.2.2 Chromosome instability in BC 7

1.3 The biological role of invadosome 8

1.3.1 Invadopodia in cancer progression 9

1.3.2 Invadopodia: The mechanisms of formation and function 9

1.3.3 Invadopodia in BC 11

1.4 TKS5 adaptor proteins and their roles in invadopodia formation ..11

1.4.1 Roles of TKS5 in cancer progression 13

1.4.2 Pathological and physiological processes related to TKS5 14

1.4.3 Significance of TKS5 in pathway regulation 15

1.5 Aims of the study 17

2. Materials and Methods 18

2.1 Materials 18

2.2 Methods 31

3. Results 46

3.1 The role of TKS5 in ploidy control and genome stability of urothelial cells 46

3.1.1 Decreased TKS5 in urothelial cells leads to aneuploidy 46

3.1.2 Decreased TKS5 expression results in increased number of micronuclei 47

3.1.3 Decreased TKS5 expression in Y235T results in abnormal cell division 48

3.2 Expression of TKS5 in human and mouse urothelial tissues and cells 53

3.2.1 TKS5 expression in immortalized urothelial cell strains and established BC cell lines *53*
3.2.2 TKS5 expression in normal urothelial tissues and tumor tissues of mice and humans *54*
3.3 The biological role of TKS5 in urothelial cells and BC cells 57
3.3.1 Knockdown of TKS5 in Y235T and RT4 cell lines *57*
3.3.2 Overexpression of TKS5 in UMUC-3 and BFTC-905 cell lines *58*
3.3.3 The impact of TKS5 on viability *59*
3.3.4 TKS5 is involved in the formation of invadopodia *60*
3.3.5 TKS5 regulates matrix degradation and invasion ability *62*
3.3.6 TKS5 regulates migration ability of RT4 cells and UMUC-3 cells in wound healing assay *65*
3.4 Pathway analysis in Y235T, RT4 and UMUC-3 cells 67
4. Discussion **69**
4.1 The expression of TKS5 in normal and tumor tissues or cells 69
4.2 The roles of TKS5 in cell viability/survival 71
4.3 The roles of TKS5 in invasion, migration and invadosome formation 73
4.4 TKS5 knockdown causes chromosome instability 76
4.5 Possible signal pathways and gene regulation that TKS5 involved 77
5. Summary **80**
6. Bibliography **82**
7. Appendix **97**
8. Acknowlegements **101**
9. Curriculum Vitae **101**

Abbreviations

ADAM12	A disintegrin and metalloproteinase-12
ADAM15	A disintegrin and metalloproteinase-15
ADAM19	a disintegrin and metalloproteinase-19
ADAMs	a disintegrin and metalloproteinases
ADFP	adipose differentiation-related protein
Arp2/3	Actin related protein 2/3
AXL	AXL Receptor Tyrosine Kinase
Aβ	Alzheimer's disease-related amyloid β-amyloid
BBN	N-butyl-N-(4-hydroxybutyl)-nitrosamine
BC	bladder cancer
BCA	bicinchoninic acid assay
BSA	Bovine Serum Albumin
CDK	cyclin-dependent kinase
cDNA	complementary DNA
Cep192	centrosomal protein 192
CIN	chromosome instablity
DAPI	4',6-diamidino-2-phenylindole
ddH_2O	double distilled water
DMEM	Dulbecco's Modified Eagle Medium – high glucose
DMSO	dimethyl sulfoxide
DNA	deoxyribonucleic acid
e.g.	exempli gratia
ECM	extracellular matrix
EDTA	Ethylenediaminetetraacetic acid
EGF	epidermal growth factor
EGFR	epidermal growth factor receptor
F-actin	filamentous-actin
FBP17	formin-binding protein 17
FBS	Fetal bovine serum
FCS	Fetal calf serum
FISH	five SH3 domains
g	gram
GRB2	Growth Factor Receptor Bound Protein 2
HBEC	human bronchial epithelial cell
HBSS	Hanks' Balanced Salt Solution
HEPES	4-(2-hydroxyethyl)-1-piperazineethanesulfonic acid
HOFI	Homolog of FISH
HRP	Horseradish Peroxidase
HTS	high-throughput sequencing

i.e.	id est
IF	Immunofluorescence
IRS-4	Insulin receptor substrate 4
ISUP	international society of urology pathology
KO	knockout
LB medium	Lysogeny Broth medium
MAD2	mitotic arrest deficient 2
MAPK	mitogen-activated protein kinase
MEF	mouse embryonic fibroblasts
mg	milligram
MIBC	muscle invasive bladder cancer
ml	milliliter
MT1-MMP	membrane type I matrix metalloprotease
MTT	Methylthiazolyldiphenyl-tetrazolium bromide
Nck1	non-catalytic region of tyrosine kinase adaptor protein 1
NEA	non-essential amino acids
NMIBC	non-muscle invasive bladder cancer
N-WASP	neural Wiskott–Aldrich syndrome protein family members
PBS	phosphate buffered saline
PCR	polymerase chain reaction
PEI	polyethyleneimine
PI (3,4) P2	Phosphatidylinositol 3,4-bisphosphate
PI3K	phosphoinositide 3-kinase
PKC	protein kinase C
PLK1	polo-like kinase 1
PLK4	polo-like kinase 4
PRM	proline-rich motifs
PUNLMP	papillary urothelial neoplasm of low malignant potential
PVDF	Polyvinylidene fluoride
PX	Phox
REST	repressor 1-silent transcription factor
RNAi	RNA interference
rpm	Revolutions per minute
RPMI	Roswell Park Memorial Institute
RT-qPCR	real-time quantitative reverse transcription polymerase chain reaction
SAC	spindle assemble checkpoint
SAS-6	spindle assembly abnormal protein 6 homolog
SDS	Sodium dodecyl sulfate
SH3	SRC Homology 3
SH3PXD2A	SH3 and PX domain-containing protein 2A
SH3PXD2B	SH3 and PX domain-containing protein 2B
SMC1	structural maintenance of chromosomes 1

SMC3	structural maintenance of chromosomes 3
SRC	non-receptor tyrosine kinase
SRC-3T3 cells	SRC-transformed mouse fibroblasts
STAG1	stromal antigen 1
STAG2	stromal antigen 2
SV40	simian virus 40
SV40-LT	simian virus 40 large T antigen
TBST	Tris-Buffered Saline, with 0.1% Tween
TCGA	The Cancer Genome Atlas
TEMED	Tetramethylethylenediamine
TERT	Telomerase Reverse Transcriptase
TKS	tyrosine kinase substrate
TKS4	tyrosine kinase substrate 4
TMA	tissues microarrays
TNM	tumor lymph-node metastasis
TUBB3	Type III β-tubulin
VSMCs	vascular smooth muscle cells
WASP	Wiskott–Aldrich syndrome protein family members
WIP	WASP interacting protein
ZEB1	zinc finger E-box binding homeobox 1
ZEB2	zinc finger E-box binding homeobox 2
µg	Microgram
µl	Microliter

1. Introduction

1.1 Overview of bladder cancer (BC)

BC is one of the leading causes of mortality in men with more than 357,000 new cases and more than 130,000 deaths worldwide every year [73]. Moreover, BC is the fifth common cancer and the ninth paramount cause of cancer-related deaths in men in the US [58]. Pathogenic factors for the development of BC include occupational exposure, chemotherapy drugs and pelvic radiation therapy, etc., but tobacco use is a generally recognized risk factor. A majority of BC are urothelial cancers, which are non-muscle invasive (75%) at the beginning of the diagnosis, corresponding to muscle infiltration or spread (25%), about 50% of non-muscle invasive tumors are low-grade tumors, while muscle invasive tumors are high-grade tumors [73]. The classification of high-grade or low-grade tumors is based on cell structure and cytological atypia. The WHO's 2004 classification, which includes a third category, namely papillary urothelial tumors with low malignant potential is currently the most widely used classification [63]. At the time of diagnosis, most BCs (about 60%) are low-grade non-muscular invasive papillary tumors [63]. Stage T1 tumor refers to the tumor that has penetrated the epithelial basement membrane but has not yet affected the muscles (Figure1) [63]. Muscle invasive bladder cancers (MIBCs; approximately 20% at the time of diagnosis) are mostly high-grade tumors. Non-muscle invasive bladder cancers (NMIBCs) often relapse (50–70%), but rarely progress to invasion (10–15%), and the five-year survival rate is approximately 90% [94].

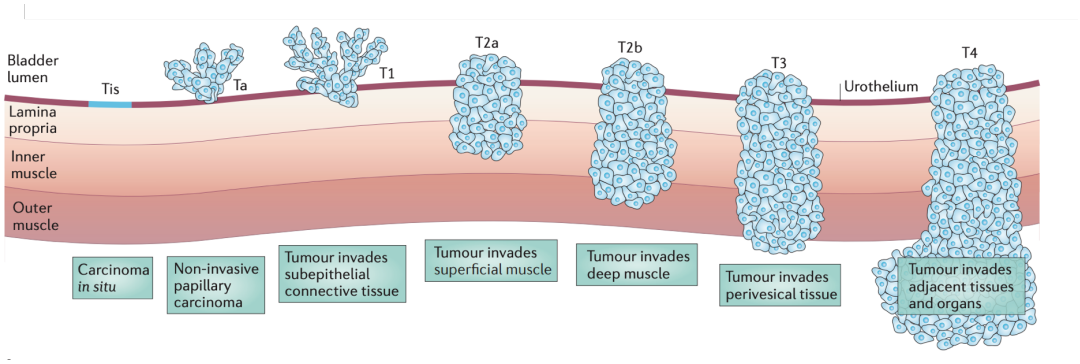

Figure 1. The grading and staging of bladder tumors. Bladder tumors gradually penetrate into the muscle layer from the urothelial [63].

Despite the relatively good 5-year survival rate of NMIBC, BC is the leading cause of death of patients with urinary tract diseases [120]. The majority of death in BC patients are attributed to recurrence of NMIBC with metastasis. In addition, MIBC accounts for 25-40% of all BCs and can spread from the bladder to the pelvic lymph nodes and then to the internal organs [132]. Even if radical cystectomy is possible, the 5-year survival rate of MIBC patients with lymph node metastasis is much lower than that of MIBC patients without lymph node metastasis [123, 52]. The metastasis to lymph nodes and distant organs is a complex multi-molecular mechanism and multi-step processes, involving the mutation of various genes, and the upstream and downstream regulatory modification at the microscopic level, as well as the spread of cancer cells to the lymphatic vessels, the transportation of cancer cells, settlement and colonization expansion of cancer cells at the macroscopic level [21,60].

Improved treatments require a detailed understanding of the molecular mechanisms of the pathogenesis and progression of urothelial carcinoma. However, the biological characteristics and molecular mechanisms of BC cell invasion and metastasis are still largely unknown.

1.2 Chromosome instability

The vast majority of tumors are aneuploid due to errors in chromosome segregation. Aneuploidy refers to abnormal number of single chromosomes in a cell or organism, and is a common form of chromosome instability (CIN). David Hansemann first described mitotic defects in tumor cells with aneuploidy more than a century ago [51]. Subsequently, Theodor Boveri compared the defects in sea urchin embryos that had undergone multipolar division and reported that "some abnormal chromatin structure", regardless of its origin, "will lead to the occurrence of malignant tumors" [11]. In addition, Theodor Boveri observed that an abnormal number of centrosomes can cause chromosomal misalignment, which is harmful to cells in most cases [11]. However, only a "specific, wrong combination of chromosomes" can cause unlimited growth. In this regard, Boveri assumed that there are chromosomes that promote and suppress cancer [11]. As we understand today, chromosomes contain tumor-promoting genes and tumor suppressor genes. Therefore, the observation made by Hansemann and Boveri is to define cancer as a genetic disease and lay the foundation for subsequent research work involving chromosomal missense segregation as the origin of cancer.

For the aim of this project, I concentrate on the definition of CIN as a whole chromosome missegregation, although chromosome structural rearrangement may also be associated with missegregation.

Since CIN means loss of fidelity of chromosome segregation during mitosis, there is a need to review the features of mitosis that support correct chromosome segregation. Mitosis is well-designed to make sure that all sister chromatids are evenly separated into daughter cells (Figure 2) [113]. Sister chromatid cohesion, established during DNA replication through the deposition of adhesin complexes, is the core of this cellular programming. Maintaining cohesion in the G2 and M

phases of the cell cycle is required in correct chromosome segregation, and then abruptly disrupted at the beginning of the later period. The coordinated activity of cyclin-dependent kinase (CDK) and spindle assembly checkpoint (SAC) determines the exact timing of sister chromatid cohesion destruction during mitosis [113]. The chromosomes that are not correctly connected to the spindle microtubules send signals to maintain the activity of CDKs, thereby inhibiting later occurrence and retaining chromatid cohesion [99].

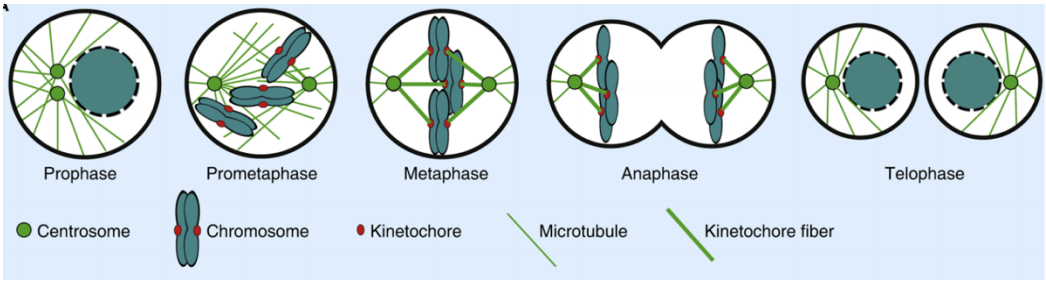

Figure 2. Chromosome segregation in mitosis. After the nuclear membrane breakdown, the chromosomes combine with the spindle microtubules. The spindle assembly checkpoint is accountable for inhibiting the start of anaphase until all chromosomes form the correct bidirectional orientation on the spindle microtubules. The destruction of cohesion causes the separation of sister chromatids and initiates the anaphase. To ensure high-fidelity chromosome separation, all sister chromatids should be separated into the same daughter cell [113].

1.2.1 Causes of chromosomal instability

It is conceivable that damage to the SAC will cause the sister chromatid to separate prematurely, leading to chromosomal missegregation and aneuploidy [67, 83]. In fact, it has already been demonstrated by removing the mitotic arrest deficient 2 (MAD2) allele in human colorectal carcinoma cell line HCT116, a colon cancer cell line with stable chromosomes, which leads to persistent chromosomal misalignment and is therefore sufficient to cause CIN [77]. Similar to the damage of SAC, chromosomal missegregation and CIN are also caused by abnormal sister chromatid cohesion. A ring-shaped adhesion protein complex holds the sister chromatids together during DNA replication, it is composed of Stromal antigen 1 (STAG1) or Stromal antigen 2 (STAG2), RAD21, structural maintenance of chromosomes 1 (SMC1) and structural maintenance of

chromosomes 3 (SMC3), which bind to the chromosomes during DNA replication [90, 95].

In fact, the incidence of premature separation of sister chromatids in human cancer is very low, likely due lethal outcome. Therefore, it is commonly accepted that some additional mechanisms may be responsible for the main cause of widespread chromosomal misalignment events in cancer cells. The most prevalent phenotype observed in mitotic cancer cells, which causes chromosomal misalignment is the so-called lagging chromosomes that appear in anaphase [114]. Lagging chromosomes are caused by incorrect attachment of microtubule-kinetochore, which cannot be resolved before the anaphase onset [25]. In this respect, it is necessary to emphasize that there are two main causes leading to chromosome misalignment. One relies on errors in correction mechanisms, which leads to the maintenance of erroneous kinetochore attachments, and the other is due the increase of erroneous kinetochore attachments, overwhelming the error correction machinery [6]. As has been demonstrated in recent studies, supernumerary centrosomes contribute significantly to erroneous kinetochore attachments [44, 108]. Most recently, there is increasing evidences that the increase in the rate of microtubule plus end assembly in the mitotic spindle plays a critical role in the formation of CIN in human cancer cells [36]. In fact, increasing microtubule plus end dynamics are sufficient to cause transient aberration in spindle geometry, which results in higher rates of mis-attachments, despite as the presence of functional error correction mechanism [36].

In addition to impairments arisen during mitosis, which directly cause chromosomal missegregation, errors originating from the interphase may indirectly cause chromosomal missegregation defects. As discussed above, as a result of a supernumerary centrosome that appears during mitosis, erroneous microtubule-kinetochore attachments can result, leading to chromosomal

missegregation. Supernumerary centrosomes are created when centrosome replication cycle is defective in the interphase [76]. Centrosomes are duplicated once every cell cycle, this process begins with centriole replication, which occurs along with the transition from G1 to S phase of DNA replication. In the process of centriole replication, there are proteins like centrosomal protein 192 (Cep192), spindle assembly abnormal protein 6 homolog (SAS-6) and polo like kinase 4 (PLK4) that are needed [3]. It has been shown that the overexpression of these important centriole replication factors will lead to centriole replication and can be found in human cancers [3].

There is mounting evidences that the rampant activation of oncogenic transcription factors like H-RAS or C-MYC or the inactivation of tumor suppressor proteins such as p53 can result in cell cycle disorders and cause genome instability. There are also other transcription factors are associated with transcription disorders that directly affect genes involved in the process of mitosis. For example, the repressor 1-silent transcription factor (REST) restricts the transcription of MAD2, and REST is degraded by the ubiquitin protease pathway during G2 to allow the proper expression of MAD2, MAD2 has been showed that deficiency can lead to CIN [49]. In addition, damage to the S-phase replication fork process and replication pressure are also considered as sources of chromosomal missegregation during mitosis [17]. In fact, studies have shown that several genes on chromosome 18q in cancer cells that display CIN, serve as suppressors of CIN [91].

Great progress has been made in understanding the regulation of chromosome segregation of which defects may cause chromosomal missegregation in cancer cells. However, the exact mechanisms how these defects contribute to the control of cellular ploidy is not well understood. Given the variety of pathways leading to aneuploidy phenotype it is of importance to delineate exact mechanisms that

contribute to CIN inhibition and therefore to the prevention of the progression of cancer.

1.2.2 Chromosome instability in BC

CIN is increasing with the malignant potential of urothelial tumors. While NMIBC exhibit low grade of CIN, MIBCs are highly aneuploidy and show increased levels of CIN [40]. Although CIN represents the transition from urothelial to aggressive cancer type, its causes remain poorly understood. Nevertheless, studies have identified several factors that are associated with CIN in BC. STAG2, as one of the four components of the cohesin complex, mainly plays a role in the cohesion and separation of sister chromatids. STAG2, the most frequently mutated cohesin subunit, is now known to be frequently altered in urinary bladder cancer. STAG2 knockdown in immortalized urothelial cells which have a stable karyotype will lead to aneuploidy [4, 109]. This cell line was found to have an unstable karyotype and significant changes in its chromosome number upon knockdown of STAG2. In RT4 urothelial cancer cells, shRNA-mediated knockdown of STAG2 also led to significant chromosome number changes [4, 109]. The disturbances of centrosome function may lead to aneuploidy, defects in cell cycle checkpoints and p53 mutations in invasive urothelial carcinoma contribute to centrosome dysfunction and aneuploidy [40]. BUBR1 is a critical component of mitotic spindle checkpoint machinery, Yamamoto and colleagues showed that overexpression of BUBR1 in BC is significantly correlates with higher malignant histological grades and high cell proliferation [130]. Similarly, Polo-like kinase 1 (PLK1) plays a role in the formation of bipolar spindles and mitosis and Yamamoto et al. showed that elevated expression of PLK1 correlates with high-grade tumors and multiple tumors, suggesting that PLK1 promotes the progression of urothelial cancers [131]. Type III β-tubulin (TUBB3) is a component of microtubules involved in chromosome segregation. The study of Hinsch et al. demonstrated that TUBB3 expression is associated with a specific subtype of urinary BC

characterized by increased genetic instability, alterations to the p53 gene, and rapid cell proliferation [53].

1.3 The biological role of invadosome

Invadopodia were first observed in fibroblasts transformed by Rous sarcoma virus [30]. The term invadopodia refers to structures formed within cancerous cells, whereas podosome refers to similar structures produced in non-cancerous cells, including dendritic cells, macrophages, endothelial cells, bronchial epithelial cells, neural crest cells, vascular smooth muscle cells (VSMCs) and osteoclasts [16, 22, 30, 43, 50, 59, 72, 78, 80, 126]. A few reports have described differences between invadopodia and podosomes. For example, Invadopodia can survive in culture for hours, while podosomes only survive for a short time [32, 81]. Despite participating in a variety of different cellular processes, they have a common function in regulating pericellular proteolytic activity, which sets them in contrast to other structures involved in migration and adhesion, such as lamellipodia and filopodia [89]. Invadosome is a term that has recently been used to refer both types of structures and similar structures generated in normal cells through transformation with the non-receptor tyrosine kinase (SRC) [31, 69, 101]. Invadosomes are complex molecular structures composed of a dense filamentous-actin (F-actin) core, which contains actin regulatory proteins, including polymerization activators, filament cross-linking agents and nucleators, surrounded by proteins involved in regulation, adhesion and scaffolding, including integrins and adaptor proteins [33, 41, 81]. The Key components of invadosomes are scaffold protein tyrosine kinase substrate 5 (TKS5), the actin regulators cortactin, wiskott–Aldrich syndrome protein family members (WASP) and cofilin, and membrane type I matrix metalloprotease (MT1-MMP or MMP14) [89].

Previous researches showed that podosomes play roles in embryonic and postnatal development [81], in angiogenesis and remodeling of the vasculature [26], in maturation of the postsynaptic membrane [102], in antigen sampling and recognition [47], and in cell–cell fusion mechanisms [85]. Invadopodia involve in multiple steps of the cancer metastatic process. In the following part, I will focus on the role of invadopodia to expand the narrative.

1.3.1 Invadopodia in cancer progression

Invadopodia are the main drivers of some tumor cell phenotypes, and they are the focus of many signals that control tumor cell behavior [35]. Therefore, Invadopodia is a sign that tumor cells undergo systemic spread and metastasis.

The process of cancer metastasis requires the spread of primary tumor cells to other organs and involves a variety of biological processes. To reach distant organs, cancer cells must first pass through the basement membrane of the primary tumor cell, and then migrate while degrading in the extracellular matrix (ECM). To cross blood vessels, these cells must penetrate the basement membrane of vascular endothelium, pass through the vascular endothelial cells and the gap between adjacent endothelial cells, a process known as trans-endothelial migration [92]. Cancer cells can invade lymphatic vessels outside the primary tumor mass as well [92]. Invadopodia's participation in this process is still un-sufficiently understood.

1.3.2 Invadopodia: The mechanisms of formation and function

Formation of invadopodia is triggered by ligand-induced activation of tyrosine kinase receptors, such as epidermal growth factor receptor (EGFR) and AXL receptor tyrosine kinase (AXL) [97, 128], which trigger diverse signaling pathways that are activated by SRC kinase and protein kinase C (PKC) [12, 61]. The neural wiskott–aldrich syndrome protein family members (N-WASP) activator protein is

also required for the formation of invadopodia, and activated EGFR stimulates the formation of invadopodia through the N-WASP/WASP interacting protein (WIP)/actin related protein 2/3 (Arp2/3) signal pathway mediated by Nck1 [127]. The TKS5 SH3 domains bind to N-WASP, and SRC-phosphorylated TKS5 associates with non-catalytic region of tyrosine kinase adaptor protein 1 (Nck1), promoting F-actin assembly of invadopodia and degradation of ECM [84, 104, 112]. The step of TKS5 recruitment is also crucial for transforming short-lived actin-based precursors into matrix degradation-competent invasion cells [35, 105]. TKS5 interacts with phosphatidylinositol-3,4-bisphosphate (PI (3,4) P2) in the plasma membrane, leading to recruitment of actin modulators Nck1 and cortactin at the membrane [82]. These in turn activate the local polymerization of actin, and then recruit MT1-MMP, thereby initiate matrix degradation and direct the local secretion of vesicles containing different metalloproteinases [5, 82].

Soon after the initial actin core is assembled, integrins and their associated adhesion components are recruited and subsequently form an adhesive ring around the actin core. Continuous polymerization of the actin core was reported to be an important driving force that pushes invadopodia outward and pushes it to penetrate into the surrounding ECM [82, 103]. The molecular structure of invadopodia provide basic functional clues on invasive activities. The ring-shaped adhesion makes the protrusion of membrane locally attached to the ECM, while the membrane-bound and secreted metalloprotease and other proteinases degrade the nearby matrix, making it more susceptible to mechanical interference. In addition, the protruding actin polymerization creates a compressive force, which effectively pushes the tip of Invadopodia into the matrix [96].

1.3.3 Invadopodia in BC

The MIBC is a type of epithelial tumor that has a high rate of metastasis. For bladder tumor cells to reach the muscle layer, the cells must penetrate both the urothelial cell monolayer and the basement membrane. It is not yet known exactly how trans-urothelial invasion occurs.

Invadopodia are actin-based filamentous membrane protrusions that degrade the matrix and allow muscle to invade. The ability of invasive BC cells to form invadopodia is greater than that of non-invasive cells [57]. The BC cells featuring abrogation of cortactin showed reduced invasive invadopodia formation as well as a significantly reduced ability to invade through the urothelial cell monolayer which indicate that the formation of invadopodia is an essential event for the muscle infiltration of invasive BC cells [57]. Furthermore, a study demonstrated that BC cell extravasation into the lungs is reduced when cortactin is knockdown, such findings suggest that formation of invadopodia is key to extravasation [116]. Yamamoto et al. demonstrated that invadopodia formation of BC cells requires recruitment of dynamin-2 that is mediated by formin-binding protein 17 (FBP17), indicating that FBP17 plays a key role in BC invasion via invodopodia formation [129].

1.4 TKS5 adaptor proteins and their roles in invadopodia formation

The TKS molecules are large adaptor proteins and act as tyrosine kinase substrates (TKS) for SRC kinase [18, 43, 104]. There are two TKS factors, tyrosine kinase substrates 4 (TKS4) and TKS5, respectively. They contain the phox homology (PX) domain, conserved linear motifs, such as several proline-rich motifs (PRM) and four (TKS4) or five (TKS5) SRC homology 3 (SH3) domains, respectively. Other names for TKS5 are SH3 and PX domain-containing protein 2A (SH3PXD2A) and five SH3 domains (FISH), while TKS4 is also known

as SH3 and PX domain-containing protein 2B (SH3PXD2B), or Homolog of FISH (HOFI) [1, 70].

The PX domain links the TKS scaffold protein to the cell membrane by binding PI (3,4) P2 [2, 18]. The SH3 domains act as signal molecule binding sites and coordinate protein-protein interactions [65]. The proline-rich motif (PRM) of the TKS proteins represent the contact site of the molecule contained in the SH3 domain (Figure 3). TKS adaptor proteins are expressed in various tissues, but TKS4 is not expressed in testis tissues and TKS5 is not expressed in spleen and testis tissues [18, 70]. Increased expression of TKS proteins were also observed in some transformed cell lines [18, 66].

Some studies have reported the presence of TKS5 isoforms, such as those lacking the PX domain in mice, because of transcription from intronic initiation sites [22, 68]. Different TKS5 isoforms, such as $TKS5_{short}$ and TKS5β, which lack the PX domain, as well as the classic TKS5α/$TKS5_{long}$, which contain PX domain, were also reported [22]. In most of the normal mouse tissues, all Tks5 isoforms can be found. Importantly elevated expression of TKS5α/$TKS5_{long}$ was shown to correlate with malignant transformation, metastasis and formation of invadopodia [22, 68].

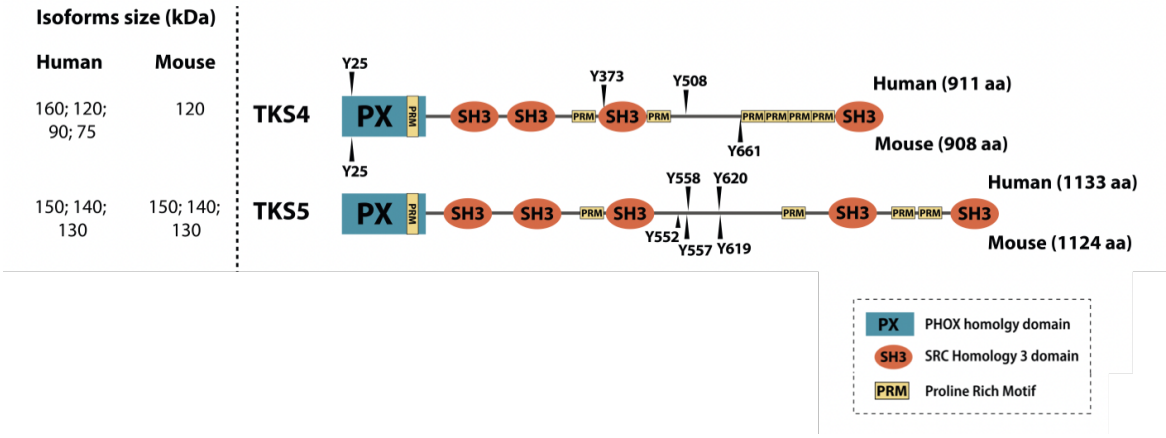

Figure 3. Schematic of the TKS adaptor proteins. The architecture of TKS5 (bottom) and TKS4 (top) is shown, illustrating the PX and SH3 domains, SRC phosphorylation sites (Yxxx) and proline-rich motifs (PRM). The left side shows the molecular weight and Amino acid sequence length in human and mouse respectively. Modified from [64], CC BY 4.0, https://creativecommons.org/licenses/by/4.0/

1.4.1 Roles of TKS5 in cancer progression

The TKS proteins TKS4 and TKS5 are believed to play a critical role in a variety of physiological and pathological processes, such as cell migration and invasion, as well as cancer progression. These proteins contain both PX and SH3 domains, and they function as adaptor proteins that help keep membranes and cellular components near structures called invadopodia or podosomes.

Tks5 is crucial for podosome formation and function in SRC-transformed mouse fibroblasts (SRC-3T3 cells), as well as for the invasion of human cancer cells by proteases [104]. Therefore, TKS5 is part of the proteins involved in the formation of invadopodia. Moreover, introduction of TKS5 in non-invasive breast cancer cell lines resulted in strong invadopodia formation [104]. It was shown that the formation of Invadopodia depends on the PX domain of TKS5, which means that lipid binding to the PX domain of TKS5 can initiate the formation of invadopodia [84]. In fact, Oikawa et al. subsequently revealed that formation of Invadopodia begins at the membrane site rich in PI (3,4) P2, which is a lipid known to bind to the PX domain of TKS5 [2, 84]. Other studies have shown that the recruitment of TKS5 and cortactin is the first event in the formation of invadopodia [86].

Previous immunohistochemistry studies have detected TKS5 expression in breast and melanoma cancer tissues [104]. Furthermore, TKS5 was identified as a significant prognostic marker in glial-derived brain tumors [110]. The emerging evidence that TKS5 is a possible prognostic marker of cancer has prompted the analysis of TKS5 expression in the tissues microarrays (TMA) of breast, colon, lung, and prostate cancers, as well as in normal tissues. The Oncomine^{TM} cancer gene microarray database was used to conduct extensive mRNA analysis, showing that TKS5 expression is selectively upregulated in many human cancers, and correlates with increased metastatic potential of tumors and worse survival of patients [111].

1.4.2 Pathological and physiological processes related to TKS5

Apart from its abilities to contribute to tumor progression, TKS5 is also implicated in Alzheimer's disease-related amyloid β-amyloid (Aβ) peptide-mediated neurotoxicity [7, 71]. A disintegrin and metalloproteinase-12 (ADAM12), a disintegrin and metalloproteinase-15 (ADAM15), and a disintegrin and metalloproteinase-19 (ADAM19) are three members of the a disintegrin and metalloproteinases (ADAMs) family that bind the SH3 domain at the C-terminus of TKS5 [2]. Additionally, it was shown that TKS5 is phosphorylated in human neuronal cells that are exposed to toxic Aβ protein, resulting in TKS5-ADAM12 interaction and ultimately into ADAM12 self-cleavage [71]. TKS5 may also play a role in a pathological condition called preeclampsia, according to another recent study [125]. Analysis of the affected and healthy placenta identified two up-regulated factors, namely leptin and TKS5, the authors propose TKS5 as the main organizer of podosome formation, which could be related to the migration of trophoblast cells in the placenta [125]. Thus, preeclampsia may result from damage to the TKS5-dependent pathway in trophoblast cells [28, 88]. During embryonic development, many cell types are migratory and require cell migration to form a developing embryo. In order to study whether TKS5 is also involved in

cell migration during embryonic development, Murphy et al. analyzed zebrafish embryonic development and observed many serious defects which include craniofacial and pigmentation abnormalities, heart malformations, lack of movement and edema in zebrafish embryos with reduced TKS5 expression [82]. This observation indicates that TKS5 plays vital roles in the embryonic development and homeostasis. Many defects are observed in cell types that are derived from neural crest stem cell differentiation. TKS5 is also required for neural crest cell migration in vitro [82]. The data from Courtneidge et al. showed that neural crest cell migration requires the formation of podosomes, which suggests that cell migration involves similar mechanisms during embryogenesis and cancer metastasis [28, 82].

Using gene trapping to disrupt the *Tks5* gene in mice results in neonatal death and a complete cleft in the secondary palate of mice [22, 64]. Analysis of the *Tks5* knockout (KO) mouse model by Cejudo-Martin et al. revealed that in the background of C57Bl/6J mice, the neonatal mortality rate and the incidence of cleft palate rose to 90%, although the remaining 10% of mice did not have a cleft palate, but they die of unknown causes shortly after birth. The authors concluded that strain purity is the determinant of the loss of *Tks5* phenotypic performance [22]. These *Tks5* KO study indicate that *Tks5* plays a pivotal role in normal physiological processes and embryonic development.

1.4.3 Significance of TKS5 in pathway regulation

TKS5 is phosphorylated at tyrosine residues within minutes after EGF treatment and that phosphorylation continues for at least two hours, which indicates that TKS5 is part of the EGF signaling pathway [39]. Moreover, PX domain of TKS5 is considered to be essential for molecules involved in EGFR signaling and phosphorylation of TKS5 by SRC [10, 39]. Several studies indicate that TKS protein can be used as a platform to recruit key players in EGFR signal

transduction pathway (Figure 4) to promote cell proliferation and migration [8, 10, 29, 66, 84]. However, the specific molecular mechanism of TKS5 in regulating tumor disease progression, normal cell physiological functions and embryonic development still needs further exploration and research.

TKS4, the close homolog of TKS5 plays an important role in the formation of functional podosomes [18, 48]. In recent years, it has emerged that TKS4 is an important scaffolding molecule that has the ability to regulate actin cytoskeleton via SRC and EGFR [10, 66]. It is understood that the EGFR plays an important role in many cellular functions, including proliferation and motility, as well as in the development of various human cancers [66].

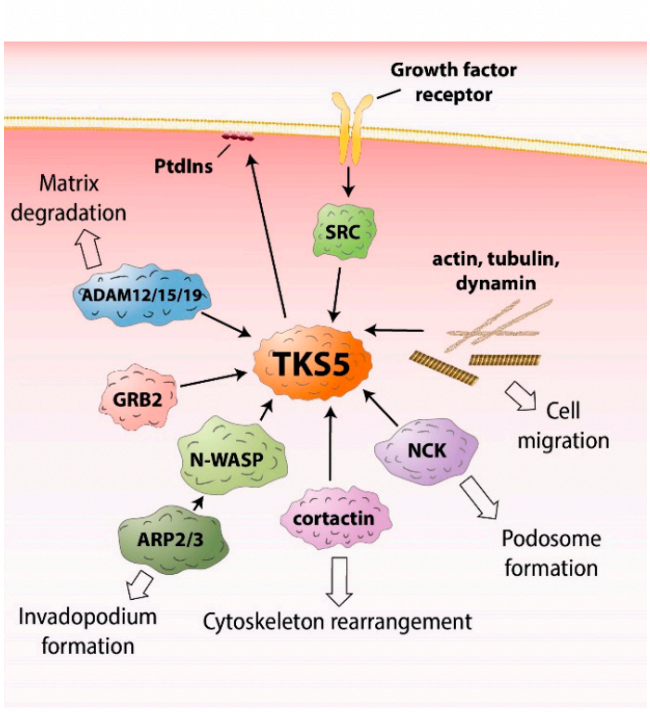

Figure 4. The TKS5 proteins are responsible for recruiting signaling molecules. ADAM12/15/19-a disintegrin and metalloprotease 12/15/19, ARP2/3-actin-related protein 2/3, GRB2–growth factor receptor binding protein 2, NCK-non-catalytic region of tyrosine kinase adaptor protein, N-WASP-neural Wiskott-Aldrich syndrome protein, PtdIns-phosphatidylinositol, SRC-proto-oncogene tyrosine-protein kinase SRC. Modified from [64], CC BY 4.0, https://creativecommons.org/licenses/by/4.0/

1.5 Aims of the study

TKS5 is the member of TKS adaptor proteins and cooperates with SRC tyrosine kinase to promote the formation of invadopodia, which are used by invasive cancer cells to degrade the ECM. Although there are a number of studies showing that TKS5 plays important roles in cancer progression by the formation of invadopodia, especially in breast cancer, lung cancer and melanoma, the functions of TKS5 in BC is still less understood. In our laboratory unpublished results of an RNA interference (RNAi) screen identified TKS5 as a candidate of gene whose knockdown that increase aneuploidy in human cells. But roles of TKS5 in ploidy control and chromosome instability was not reported in previous studies. In order to understand the role of TKS5 in BC initiation and progression more comprehensively, the present study wished to explore following questions: (i) Is TKS5 involved in ploidy control of urothelial cells? (ii) What is the mechanism leading to aneuploidy in response to TKS5 knockdown? (iii) Is TKS5 an oncogene or tumor suppressor gene in the context of BC? (iv) Does TKS5 affect the proliferation, migration and invasion of BC cells? A series of experiments, including gene expression analyses, shRNA-mediated gene knockdown and cell biological, biochemical and immunofluorescence approaches were carried out to better explain the questions raised above.

2. Materials and Methods

2.1 Materials

2.1.1 Chemical reagent, solution and buffers

Accutase ® solution	Pan Biotech, Germany
AceGlow™ Chemiluminescence Substrate	VWR, USA
Acetic acid	VWR, USA
Acrylamide	Sigma-Aldrich GmbH, USA
Agar	Sigma-Aldrich GmbH, USA
Ampicillin	Sigma-Aldrich GmbH, USA
Ammonium Persulfate	Bio-Rad Laboratories, Japan
Bicinchoninic acid	Sigma-Aldrich GmbH, USA
Bovine Serum Albumin Fraction	SERVA, Germany
CnT-Prime Epithelial Culture Medium	CELLnTEC, Switzerland
Copper (II) Sulfate solution	Sigma-Aldrich Chemie GmbH, Germany
Crystal violet solution 1%	Sigma-Aldrich Chemie GmbH, Germany
Complete™ Protease Inhibitor Cocktail Tablets	Roche, Germany
double distilled water (ddH_2O)	Ulm University, Germany

Dimethyl Sulfoxide (DMSO)	Sigma-Aldrich Chemie GmbH, Germany
DMEM (1X) Dulbecco's Modified Eagle Medium	Life Technologies Limited, UK
DMEM/F-12 (1:1) (1X) Dulbecco's Modified Eagle Medium	Life Technologies Limited, UK
DPBS (1X) Dulbecco's Phosphate Buffered Saline	Life Technologies Limited, UK
DNA/RNA dye peqGREEN	VWR, France
DNAZap™	Thermo Fisher Scientific,Lithuania
Entellan	Merck KgaA, Germany
Ethanol	Sigma-Aldrich Chemie GmbH, Germany
Eosine Solution	Waldeck GmbH&Co KG, Germany
Ethylene glycol bis (2 aminoethyl)-tetraacetic acid	Sigma-Aldrich Chemie GmbH, Germany
Fetal calf serum (FCS)	Anprotec, Germany
Formaldehyde solution 37%	VWR, France
Gel Loading Dye Purple (6×)	New England Biolabs, USA
GeneRuler 1kb DNA ladder	Thermo Fisher Scientific, Lithuania
GeneRuler 50bp DNA ladder	Thermo Fisher Scientific, Lithuania
GlutaMAX™ -1 (100×)	Thermo Fisher Scientific, UK

Glutaraldehyde Solution 50% in H_2O	Sigma-Aldrich Chemie GmbH, Germany
Glycine	Sigma-Aldrich Chemie GmbH, Germany
G418 solution	Roche Diagnostics GmbH, Germany
Hanks' Balanced Salt Solution (HBSS)	Thermo Fisher Scientific, UK
4-(2-hydroxyethyl)-1-piperazineethanesulfonic acid (HEPES)	Merck KgaA, Germany
Hydrochloric acid	Merck KgaA, Germany
iTaqTM Universal SYBR®Green supermix	Bio-Rad Laboratories Inc., USA
Lysogeny Broth (LB) medium	Sigma-Aldrich Chemie GmbH, Germany
KaryoMAX™ Colcemid™ Solution in PBS	Life Technologies Limited, UK
Kanamycin solution	Sigma-Aldrich, USA
Mayer’s hemalum solution	Merck KgaA, Darmstadt
Methanol	Sigma-Aldrich Chemie GmbH, Germany
NEB® 5-alpha Competent E. coli (High Efficiency)	New England Biolabs, USA
Non-essential amino acids (NEA)	Biochrom GmbH, Germany
Nuclease free water	Ambion, USA

6× Orange DNA loading Dye	Thermo Fisher Scientific, Lithuania
PageRuler Prestained Protein Ladder	Thermo Fisher Scientific, Lithuania
Penicillin–Streptomycin	Pan- Biotech GmbH, Germany
Puromycin	Life Technologies Corporation, USA
PhosSTOP™ EASYpack Protease Inhibitor	Roche, Germany
Polybrene Transfection Reagent	Merck KgaA, Germany
ProLong™ Gold Eindeckmittel mit 4',6-diamidino-2-phenylindole (DAPI)	Thermo Fisher Scientific, UK
Paraformaldehyde powerder	Roche, Germany
RIPA Buffer	Sigma-Aldrich Chemie GmbH, Germany
Roti®- Histol	CARL ROTH GmbH, Germany
Roswell Park Memorial Institute (RPMI) 1640 Medium	Life Technologies Limited, UK
Sea Plaque™ Agarose	Lonza, USA
Skim Milk Powder	Sigma-Aldrich Chemie GmbH, Germany
Sodium Chloride	Merck Millipore, USA
Sodium dodecyl sulfate (SDS)	Sigma-Aldrich GmbH, USA
SYBR® Green I nucleic acid gel stain	Sigma-Aldrich GmbH, USA

Tetramethylethylenediamine (TEMED)	Bio-Rad Laboratories, Japan
Thiazolyl blue tetrazolium bromide	Sigma-Aldrich Chemie GmbH, Germany
Triton X-100	Sigma-Aldrich Chemie GmbH, Germany
Trizma® (TRIS base)	Sigma-Aldrich Chemie GmbH, Germany
Trypan blue	Sigma-Aldrich GmbH, UK
Tryptone	Sigma-Aldrich Chemie GmbH, Germany
Tween® 20	Sigma-Aldrich Chemie GmbH, Germany
β-Mercaptoethanol	Life Technologies Limited, UK
4x Laemmli sample buffer	Bio-Rad Laboratories, USA

2.1.2 Buffers and solutions to be prepared

Buffers and solutions	**Composition**	**Amount**
0.2% crystal violet	1% crystal violet ddH2O	10ml 90ml
0.5% Glutaraldehyde Solution	50% Glutaraldehyde Solution ddH2O	2ml 198ml
10 x Running buffer	ddH2O Glycine 20% SDS Trisbase	990ml 144.2g 10ml 30.22g

10 x TBST	ddH2O Sodium chloride Tris 1M Tween 20	790ml 80g 200ml 10ml
1 x PBS	10x PBS buffer pH 7.4 ddH2O	100ml 900ml
1 x Running buffer	10x running buffer ddH2O	100ml 900ml
1 x TBST	10x TBST ddH2O	100ml 900ml
1 x Transfer buffer	ddH20 Glycine Methanol Trisbase	800ml 14.42g 200ml 3.02g
1x Tris buffer	ddH2O 1M HCL Sodium chloride Tris base	922ml 78.6ml 170g 121g
70% ethanol	100% ethanol ddH_2O	700ml 300ml
MSB solution	80mM KOH 5mM EGTA in 0.5%Triton x100 1mM Mgcl	10ml 100ml 20ml
75nM KCL	Potassium Chloride powder ddH_2O	1.116g 200ml
4% Paraformaldehyde	Paraformaldehyde ddH_2O	10g 200ml
1% Tritonx100 in PBS	Triton x 100 10 x PBS	1ml 10ml

	ddH_2O	89ml
Bicinchoninic acid–copper (II) sulfate mix	Bicinchoninic acid Copper (II) sulfate	980µL 20µL
Bovine Serum Albumin (BSA) blocking reagent	Albumin bovine fraction V, pH=7.0 1xTBST	5g 100ml
Cell lysis buffer	10x cell lysis buffer Phosphostop EASY pack Protease inhibitor complete tablets	10ml One pill One pill
Complete Dulbecco's Modified Eagle Medium (DEME) medium	DMEM(1x) Fetal Bovine Serum (FBS) (10%) Pen/Strep (1%)	500ml 50ml 5ml
Complete LB medium	LB Broth (Miller) Ampicilin (c_{store}=100mg/ml)	500ml 500µl
Complete RPMI medium	RPMI-1640 medium(1x) Fetal Bovine Serum (10%) Pen/Strep (1%)	500ml 50ml 5ml
Complete DMEM/F-12 medium	DMEM/F-12 (1:1) (1X) Fetal Bovine Serum (10%) Pen/Strep (1%) ITS (1%) FGF (25ng/µl)	500ml 50ml 5ml 50µl 125µl
Freezing medium(10ml)	Fetal Bovine Serum DMSO	9ml 1ml
Laemmli buffer	4x Laemmli sample buffer 2-mercaptoethanol	900µl 100µl
Milk blocking reagent	1x TBST Skim milk powder	100ml 5g

Methylthiazolyldiphenyl-tetrazolium bromide (MTT) cell lysis buffer	Acetic acid DMSO SDS	543µL 90ml 9,05g
MTT solution	1x PBS MTT	1ml 5mg
RPMI plus medium	RPMI-1640 medium(1x) Fetal Bovine Serum (10%) Pen/Strep (1%) GlutaMAX NEA	500ml 50ml 5ml 5ml 5ml
RLT buffer	RLT lysis buffer 2-mercaprtoethanol	990µl 10µl

2.1.3 Kits

Kits	**Company**
Goscript™ Reverse Transcription System	Promega, USA
NucleoBond® Xtra Midi / Maxi	NucleoBond® Xtra Midi / Maxi
Pure Yield™ Plasmid Mini-Prep kit	Promega, USA
QIAamp® DANN Mini Kit	Qiagen, Germany
QIAamp® DANN Micro Kit	Qiagen, Germany
QIAshredder	Qiagen, Germany
Rneasy® Mini Kit	Qiagen, Germany
TGX™ FastCast™ Acrylamide Kit,10%	Bio-Rad Laboratories, USA

2.1.4 Devices and Laboratory Consumables

Devices and Laboratory consumables	**Company**
Analytical blance	VWR, Italy
Biological Safety Cabinets	Thermo Fisher Scientific, Germany
Centrifuge (5417R)	Eppendorf AG, Germany
Centrifuge (5418R)	Eppendorf AG, Germany
Centrifuge (megafuge 40R)	Thermo Fisher Scientific, Germany
Centrifuge (PMC-060)	Tomy Kogyo Co, Ltd, Germany
CO_2 incubator (heracell 240i)	Thermo Fisher Scientific, Germany
Counting chamber	Neubauer, Brand, Germany
Cell counting chamber (0.00025 mm2/0.1mm)	Neubauer, Germany
Cell culture bottles (TC-Flasche T25, T75)	Standard, Sarstedt, Germany
Cell culture dishes (TC-Schale 100)	Cell culture dishes (TC-Schale 100)
Cell culture plates (6-/12-/24-/96- well plates)	Standard, Sarstedt, Germany
Cell scraper	Sarstedt, USA
Coverslips (24mm x 50mm, 24mm x 60mm)	Thermo Fisher Scientific, USA
Cryopure Tube (1.8ml)	Sarstedt, Germany
Culture inserts 4 well	IBIDI, Germany
Digital pH meter 646	Knick, Germany
Electrophoresis chamber	Galileo Bioscience, USA
Electronic orbital shakers	IKA®-Werke GmbH, Germany
Epoch Multi-Volume Spectrophotometer	BioTek, USA

Fusion FX-Western Blot & Chemi imaging	Vilber, France
Filter (0.2µm, 0.45µm)	Sarstedt, Germany
Glass Pasteur Pipettes, 225mm	BrandTech Scientific, Germany
Gloves	Abena A/S, Ireland
Labcycler gradient	SensoQuest, Germany
Laboratory autoclaves	BiomedisLaborserviceGmbH, Germany
Magnetic heating stirrer	Stuart, UK
Mini-PROTEAN®Tetra Vertical	Bio-Rad Laboratories, China
MSC-Advantage™ Class II	Thermo Fisher Scientific, Germany
Masks (operation masks)	Meditrade GmbH, Germany
Masks (FFP3 protection masks)	UVEX, Germany
Microscope slides	Thermo Fisher Scientific, USA
Multiply®-µstrip 0.2ml Chain	Sarstedt, Germany
NEB 5-alpha Competent E. coli	New England Biolabs GmbH, Germany
Pipette Controller accu-jet pro	BrandTech Scientific, Germany
Pipettes Research Plus (2µl, 10µl, 20µl, 100µl, 1,000µl)	Eppendorf AG, Germany
Power supply	Bio-Rad Laboratories, USA
Pipette tips (0.1-10µl)	Nerbe plus GmbH, Germany
Pipette tips (2-20µl, 2-100µl, 2-200µl, 100-1,000µl)	Sarstedt, Germany
PCR tubes	Sarstedt, Germany
Polyvinylidene fluoride (PVDF)	Merck KgaA, Ireland
Rocking Platform shakers	VWR, USA
REAX2 Roller	Heidolph, Germany

Real-time quantitative reverse transcription polymerase chain reaction (RT-qPCR) cycler, Viia7	Applied Biosystems, USA
RT-qPCR plates (MicroAmp Fast 96-well reaction plate, 0.1ml)	Applied biosystems, China
Shaker incubator Certomat®HK	Braun Biotech Inc., Germany
Safe-seal tubes (0.5ml, 1.5ml, 2ml)	Sarstedt, Germany
Serological pipettes (5ml, 10ml, 25ml, 50ml)	Sarstedt, Germany
Silicone Adhesive Film for PCR Plates	VWR, USA
Syringe (5ml, 10ml)	B.Braun Biotech Inc., Germa
Surgical Disposable Scalpels	B.Braun Biotech Inc., Germany
Thermo Shaker	Eppendorf AG, Germany
Thermometer	VWR, USA
Tubes (15ml, 50ml)	Sarstedt, Germany
Transwell inserts (PET 8μm,24-well)	Sarstedt, Germany
Vortex mixer	Bio-Budget Technologies,Germany
Weighing scale (EMB 500-I)	Kern, Germany
ZEISS Axio Imager M2	Carl Zeiss Microscopy GmbH, Germany
ZEISS Axio Vert.A1	Carl Zeiss Microscopy GmbH, Germany
8-strip opt clear flat caps	Sarstedt, Germany

2.1.5 Primers for PCR

Primer	**5'-3' forward sequence**	**5'-3'reverse sequence**
GAPDH (homo sapiens)	aaggtcatccctgagctgaac	acgcctgcttcaccaccttct
GAPDH (mouse)	aaggtcatcccagagctgaac	atgcctgcttcaccaccttct
TKS5 (homo sapiens)	ggaccccaagcaaaggatcat	tgcccggcagtattcatcg
TKS5 (mouse)	gtggtggtgtccaactataa	ttccccagtcttggaggt
CALM2(homo sapiens)	gagcgagctgagtggttgtg	agtcagttggtcagccatgct

2.1.6 Antibodies

Antibody	**Company**	**Dilution ratio**
Anti-α-Tubulin, Mouse monoclonal	Sigma-Aldrich Chemie GmbH, Steinheim	1:2000
Anti-β-Actin, Mouse monoclonal	Sigma-Aldrich Chemie GmbH, Steinheim	1:10000
Anti-TKS5, Rabbit polyclonal	Sigma-Aldrich Chemie GmbH, Steinheim	1:500
Anti-Phospho- Protein kinase B (AKT) (Ser473) Rabbit polyclonal	Cell Signaling Technology, Inc, USA	1:2000
Anti-Phospho-AKT (Thr308) Rabbit polyclonal	Cell Signaling Technology, Inc, USA	1:2000
Anti-p44/42 mitogen-activated protein kinase (MAPK (ERK1/2)), Rabbit monoclonal	Cell Signaling Technology, Inc, USA	1:2000

Anti-Phospho-p44/42 MAPK (ERK1/2) (Thr202/Tyr204), Rabbit monoclonal	Cell Signaling Technology, Inc, USA	1:2000
Anti-Cortactin, Mouse monoclonal	Santa Cruz Biotechnology, Inc	1:500
Anti-Rabbit IgG, HRP-linked Antibody	Cell Signaling Technology, Inc, USA	1:2000
Anti-Mouse IgG, HRP-linked Antibody	Cell Signaling Technology, Inc, USA	1:5000

2.1.7 Cell lines

Cells	**Disease/type**	**Culture medium**	**Source**
RT4	Human urothelial Carcinoma	complete RPMI medium	ATCC® HTB-2™
UMUC-3	Human urothelial carcinoma	complete RPMI medium	ATCC® HTB-4™
BFTC-905	Human urothelial carcinoma	complete DEME medium (20% FBS)	Prof. Wolfgang Schulz from Duesseldorf University, Germany
HEK 293	Human Embryonal Kidney cell	Complete DEME medium (10% FBS)	ATCC®CRL-1573TM
Y235T	Urothelial cells from the human ureter	CnT-Prime epithelial culture medium	Urology department Mannheim university, Germany

HBLAK	Urothelial cells from the human ureter	CnT-Prime epithelial culture medium	Prof. J. Hoffmann from Duesseldorf University, Germany

2.1.8 Plasmids

Plasmids	**Source**
TKS5-WT	Addgene, USA
TKS5-GFP	A gift from Sara A. Courtneidge
PEGFP-C3	Addgene, USA
psPAX2	Addgene, USA
pMD2.G	Addgene, USA
MISSION®pLKO.1-puro-Empty Vector Control Plasmid DNA	Sigma-Aldrich, Inc, Germany
shTKS5(NM_014631.2-3909s21c1)	Sigma-Aldrich, Inc, Germany
shTKS5(NM_014631.2-4314s1c1)	Sigma-Aldrich, Inc, Germany

2.2 Methods

2.2.1 Cell culture

The widely used UROtsa cells were immortalized using a temperature sensitive simian virus 40 large T antigen (SV40-LT) antigen from urothelial cells derived from ureter of a 14-year old patient [87]. In our study, I involved also the Y235T cells (urothelial cells) which have normal karyotype and are immortalized through the ectopic expression of the telomerase catalytic subunit Telomerase Reverse Transcriptase (TERT), and were obtained as a gift from Jennifer Southgate laboratory. The HBLAK cells are spontaneously immortalized and have a near-normal karyotype [54]. BC61, RT4 and RT112 BC cell lines have low or no invasive capacity. UMUC-3, T24, BFTC-905 and J82 are invasive BC cell lines, BC61, RT112, BFTC-905 were gifts from Prof. Wolfgang Schulz, Düsseldorf University.

RT4 cells, UMUC-3 cells, BFTC cells, Y235T cells and T24 cells were cultured in 10cm cell-culture plates at 37°C in a humidified incubator with 5% CO_2 and 95% humidity. RT4, UMUC-3 and T24 cells were cultured in complete RPMI medium which contains 10% Fetal Bovine Serum and 1% pen/strep. BFTC cells were kept in complete DEME supplemented with 20% Fetal Bovine Serum and 1% Pen/Strep. Y235T cells were cultured in 10cm cell-culture plates in CnT-Primer epithelial culture medium. RT4 cells and Y235Tcells were infected with the virus which contains shTKS5 and PLKO-scramble plasmids and then cultured in the complete medium with puromycin 10ug/ml. UMUC-3 and BFTC-905 cells were transfected with TKS5-GFP and pEGFP-C3 plasmids and then were cultured in the complete medium with selection marker G418 1000μg/ml. All cells were detached with trypsin and were splited when the confluency is around 80%-90%

2.2.2 Freezing cells and thawing cells

Preparation of cryopreservation solution, 90%FBS+10%DMSO; Trypsinize cells and suspend cells with pipette, transfer cells suspension into a centrifuge tube, the centrifuge speed is at 1200 revolutions per minute (rpm)/3min; discard the supernatant, add 1ml cryopreservation solution, resuspend cells completely with the pipette and then transfer to the cryopreservation tube, sealing and labeling on the tube; put cryopreservation tubes in the freezing box in -80°C and transfer them into liquid nitrogen after 24 hours.

When cells are needed to be thawed, taking out cells from liquid nitrogen and put them in the water bath with 37°C immediately. Shaking tubes and let it thaw as soon as possible. Then transfer cell suspension to a centrifuge tube with 2ml complete medium, a centrifuge speed with 1200rpm, 3mins. Discarding supernatant and resuspend cells with complete medium, seeding cells to new flasks according to 1:1 or 1:2 ratio.

2.2.3 Cell counting

Tripsinizing cells and neutralizing trypsin with complete medium, transfer cells into a centrifuge tube and centrifuge at 1200rpm/min for 3 minutes. Discarding the supernatant and suspend cells with an appropriate amount of medium. Preparing the counting chamber: Clean the counting chamber and special coverslips 2-3 times with 70% alcohol. Mixing cell suspension and trypan blue solution with ration 1:1. Pipetting 10μl of the mixture and add it between the coverslip and the counting chamber, and count the number of cells in the large squares under the microscope's 10X objective lens. Calculating the cell density according to the following formula. Depending on the needs of different experiments, adjust the required cell density, the number of cells/ml = (the sum of the number of cells in 4 large squares/4) X 10^4.

2.2.4 Bacterial Transformation

The TKS5-GFP plasmid is a gift from Ms. Sara A. Courtneidge. Cut out the filter paper containing the plasmid, then dissolve and dilute it in 10μl WDC water for 20 minutes. NEB 5-alpha Competent E. coli cells were thawed on ice for 10 minutes in advance and used for the transformation. 5μl out of the 10μl plasmid solution was added and mixed gently with the competent cells. Followed by 30 seconds heat shock at 42°C and ice-cooling for 5 minutes. 950μl SOC medium was added and the mixture was incubated at 37°C for 60 minutes with rotating (250rpm/min). The final product was spread onto the pre-warmed and agar pre-coated Kanamycin (50μg/ml) selection plates and incubated overnight at 37 degrees. The colony with kanamycin-resistant clone should grow the next day.

2.2.5 Small-scale preparation of plasmid DNA from E. coli (Miniprep)

The shTKS5 plasmid was purchased from sigma with the form of bacterial glycerol preservation. Taking out 5ul bacterial glycerol store and incubate with 3ml LB medium which contains 50ug/ml ampicillin overnight at 37°C and 225 rpm/min. As for the TKS5 overexpression plasmid, the single colony was picked up from transformation plate and then was incubated with 3ml of LB medium which contains 50μg/ml kanamycin overnight at the condition of 37°C and 225 rpm/min. The plasmid DNA was extracted with Promega Miniprep Kit. Pippeting 2ml bacteria liquid with plasmids and put into 2ml tube, left bacteria liquid was stored in 4 degree as backup. Centrifuging the tube at maximum speed in a microcentrifuge for 1 minute. Discard the supernatant. 600μl water was added to the cell pellet, and resuspend thoroughly. 100μl of cell Lysis Buffer (Blue) is added, and the tubes are inverted six times. And then 350μl of cold neutralization solution (4°C) was added, and that solution should be thoroughly mixed by inversion. Put a microcentrifuge on maximum speed and centrifuge for 3 minutes. The supernatant should be transferred to a PureYield mini-column without disturbing the cell debris pellet. Microcentrifuge at maximum speed for 15 seconds after placing the mini-column into a collection tube. Get rid of the flow-through and place the mini-column in the same collection tube. Fill the mini-column with 200μl of the endotoxin removal wash solution. Perform 15 seconds of centrifugal force at maximum speed. The mini-column should be transferred to a clean 1.5ml microcentrifuge tube and 30μl nuclease-free water added directly to the column matrix. Let it stand in the room for five minutes. Centrifuge for 1 minute to elute plasmid DNA. Cover the centrifuge tube lid, measure the plasmid concentration with a spectrophotometer Epoch, and store the plasmid DNA at -20°C.

2.2.6 Transfection of cells with TKS5 overexpression plasmids

Preparing three 10cm cell-culture plates for each cell line and 500000 cells were seeded in each plate 48 hours before transfection. The mixture of 5μg plasmid DNA, 30μl polyethyleneimine (PEI) (1mg/ml) together with 500ul purified medium (without fetal bovine serum) were needed for transfection in each plate. Normally the 1.5ml tube were used for the preparation of the transfection solution and then let the transfection solution incubate at room temperature for 20 minutes. Adding transfection solution into each plate dropwise. Changing medium with complete cell culture medium on the second day. Starting selection from the third day or on the fourth day if the cell density is low. UMUC-3 and BFTC-905 cells were used for transfection with TKS5-GFP and pEGFP-C3 plasmids. T24 was used for transient transfection with pECE M2-SH3PXD2A WT plasmid (without selection marker).

2.2.7 Transfection and infection for TKS5 knockdown plasmid

HEK293 cells were seeded in a 10cm cell-culture dish at an appropriate ratio of 24 hours or 48 hours in advance. It is better to maintain the cell density at about 60% on the day of transfection. For transfection, 1.8μg packaging vector (psPAX2), 300ng envelop vector (pMD2.G), and 3μg target plasmid, together with 500μl serum-free DMEM were mixed gently, incubated at room temperature for 20 minutes, and dropped wisely over the HEK 293 cells plate.

The medium with transfection reagent should be replaced by a normal 8ml complete medium in 24 hours. Target cells for infection were prepared at the same time and let the confluence reach 60% on the next day. The virus was collected on the second day by using 10 ml syringes and 0.45μM filters. For infection, the old medium was removed and 8 ml virus with 8ug/ml polybrene was put in the 10cm cell-culture dish directly. The virus should be washed three times with DPBS and replaced by normal complete medium on the next day. The

infected cells were moved to the S1 lab and add the selection marker. The working concentration of the selection marker for shTKS5 plasmids is 10µg/ml puromycin, but for the overexpression, the working concentration of G418 is 1000µg/ml.

2.2.8 RNA isolation

The RNA isolation was performed using Qiagen Rneasy Mini Kit according to the protocol of manufacturer. 350µl RLT buffer offered from the kit with 1% 2-mercaptoethanol was used as the lysis buffer. Cells were harvested at maximum number of 1 x 10^7 cells, and the lysis buffer was put into cell pellet or on the cells plate directly. Add the appropriate volume of Buffer RLT (around 350µl). The RNA isolation of Tissues: Do not use more than 30mg tissue. Disrupt the tissue and homogenize the lysate in the appropriate volume of RLT Buffer (around 350µl). Centrifuge the lysate for 3 min at maximum speed. Carefully transfer the supernatant by to a new epi tube, and use it in next step. The centrifuge was pre-cooled to 4°C before using. The mixture of lysis buffer and cells could be stored at -80°C or used for RNA extraction directly for long term store. The lysis mixtures were vortexed, shortly centrifuged, transferred into the 'QIA shredder' column and centrifuged at 14,000rpm/min for 2 minutes. Add a volume of 70% ethanol to the lysate, and mix them using a pipette. Continue immediately with the next step without centrifuging. Put the 700µl of sample into a Rneasy Mini spin column and then put the sample into a 2ml collection tube (supplied). Place the lid on, and centrifuge for 15 seconds at ≥8000Xg. Throw away the flow-through. Add 700µl of RW1 buffer to the Rneasy spin column. Centrifuge at ≥8000Xg for 15 seconds. The filtered liquid was discarded. Add 500µl of RPE buffer to the Rneasy spin column. Centrifuge at ≥8000Xg for 15 seconds. Discard the filtered liquid. Add 500µl of RPE buffer to the Rneasy spin column again. Cover the lid, centrifuge at ≥8000Xg for 2 minutes, and discard the effluent. Centrifuge at full speed for 1 minute. Place the Rneasy spin column in a new 1.5ml collection tube (provided). Add 20-40µl of Rnase-free water directly to the spin column membrane. Cover

the lid, centrifuge at ≥8000Xg for 1 minute to elute RNA, and discard the spin column. RNA was stored at -80°C or used for subsequent production of complementary DNA (cDNA). The concentration and purity of RNA was measured using the spectrophotometer at the following absorptions 260nm, 280nm and 320nm.

2.2.9 Reverse transcription (synthesis of copy DNA)

Reverse transcription of RNA into single-stranded copy DNA in a thermal cycler. Promega's "Goscript Reverse Transcription Kit" was used for cDNA generation. In order to bring the total volume of each reaction mixture to 15µl, the following materials were mixed as master mix (table 1):

Table 1. Reverse transcription (RT)

Nuclease free water	6,1µl
Go Script 5X Reaction buffer	4µl
Mgcl2	2,4µl
Polymerase chain reaction (PCR) Nucleotide Mix	1,0µl
Go Script Reverse Transcriptase	1,0µl
Recombinant Rnasin Ribonuclease Inhibitor	0,5µl
Total	15µl

Thoroughly mix 5µl of 100ng RNA, OligodT primer, Random Primer and nuclease-free water mixture, and incubate at 70°C for 5 minutes. Then pipette 15µl of the master mix into each PCR reaction tube to reach a final total volume of 20µl per tube. The whole reverse transcription program was used as follows: 70°C, 5 minutes; (add master mix) 25°C, 5 minutes; 42°C 1 hour; 70°C, 15 minutes; 4°C, ∞.

2.2.10 Real-time quantitative PCR (RT-qPCR)

RT-qPCR is a common method for detecting relative gene mRNA expression levels. By intercalating between the DNA bases, SYBR® Green is a fluorescent dye commonly used to detect double-stranded DNA molecules. It is used in quantitative PCR since it is possible to measure the amount of DNA that has been

amplified after each cycle. The reaction system of RT-qPCR is as follows (table 2):

Table 2. Master mix for real-time quantitative reverse transcription polymerase chain reaction (RT-qPCR)

		Volume per single 10µl reaction
Master mix	iTaq Universal SYBR Supermix	5µl
	Forward / Reverse primer mix (each 10uM stock)	1µl
	PCR grade water (DEPC)	2µl
	cDNA	2µl

The master mix 8µl was pipetted into the wells of a 96-well microtiter plate, followed by adding the target cDNA 2µl (previously diluted 1:10), to obtain a total volume of 10µl. Pipette each reaction in triplicate. In addition, 2µl Dnase/Rnase-free water was added to the negative control wells. Finally, gently mix the microtiter plate well and place it in the Viia7 Applied Biosystems RT-qPCR cycler after centrifuging. The reaction conditions are as follows (table 3):

Table 3. Real-time quantitative reverse transcription polymerase chain reaction (RT-qPCR) programme

Steps	**Temp**	**Time**	**Cycles**
Pre-incubation	50°C	2 minutes	1
	95°C	10 minutes	1
Denaturation	95°C	15 seconds	40
Annealing	60°C	60 seconds	
Melting	95°C	15 seconds	1
	60°C	1 minutes	1
	95°C	15 seconds	1
	60°C	15 seconds	1
Hold	4°C	∞	

The baseline and threshold are automatically detected by the instrument. Use the ΔΔCT method to calculate the relative expression level of the target gene by the following equation: fold difference = 2-ΔΔCT; ΔΔCT=average ΔCT (control)-ΔCT (treatment); ΔCT = CT (target gene)-CT (reference gene). Use statistical software Prism 6 (GraphPad Software, Inc) to calculate the P value.

2.2.11 Protein preparation for Western blot

500,000 cells were seeded in a 10cm cell culture dish 48 hours before the protein extraction. Wash the target 10cm dish with 5ml ice-cold PBS, and add 80μl lysis buffer containing protease/phosphatase inhibitor mixture (Roche). Place the dish on ice for 5 minutes. Scrape the mixture of cells and lysis buffer with a plastic cell scraper and collect the lysate in a micro-centrifuge tube. The samples were frozen and thawed three times in a refrigerator at -80°C or three times in liquid nitrogen, and then centrifuged at 14,000rpm/min at 4°C for 30 minutes. The supernatant was collected in a 1.5ml Eppendorf tube and stored at -80°C for further analysis. The protein concentration was measured according to bicinchoninic acid assay (BCA) protein determination kit (Thermo Scientific). Spectrophotometer Epoch was used to detect and calculate the protein concentration according to the protein standard curve.

2.2.12 The process of Western blot

40μg protein was used for each sample, together with 5μl 4x Laemmli buffer and lysis buffer consist of 20μl system, then 20μl protein solution was heated at 95°C for 10 minutes for denaturation. The protein was loaded into 10% SDS polyacrylamide gel and put in Mini-PROTEAN®Tetra Cell gel system compartment (BioRad) for separation, which is filled with 1x running buffer and runs at 200V.

For protein transfer, a methanol-activated PDVF membrane (Immobilon-P with a pore size of 0.45μm, Millipore) was used. The structure of the transfer sandwich is as follows: sponge, filter paper, gel, membrane, filter paper, sponge. The transfer process was carried out at 300mA for 2 hours in a cold room at 4°C.

After transfer, in order to block the unspecific antibody binding sites, membranes were incubated with 5% skim milk or BSA in 1x Tris buffered saline-Tween® 20 (TBST) and put on shaker at room temperature for 1-2 hours. After that, the membranes were incubated in target primary antibody diluted in the same blocking solution for overnight at 4°C.

On the next day, membranes were washed in 1x TBST three times (every time 10 minutes) to eliminate the influence of unbound protein. Then incubate in the HRP-conjugated secondary antibody at room temperature for 2 hours. After that, membranes were washed three times with 1xTBST and then detected in the Fusion FX–VILBER LOURMAT' machine with the AceGlow™ Chemiluminescence Substrate (VWR, France).

2.2.13 MTT assay

In order to detect the growth ability of cells, the MTT assay was performed. 5000 target cells in 100μl culture medium were seeded into 96-well plates, and each cell line was repeated with 6 wells. 20ul thawed MTT solution was added to the plate in 24, 48, 72, 96 and 120 hours after seeding the cells. Incubate the plate in an incubator for 2 hours, and discard the supernatant in each well. Add 100μl MTT lysis buffer to the plate and place it on the shaker for 10 minutes in the dark. Absorbance value detected at 570nm.

2.2.14 Wound healing assay

With the ibidi Culture-Inserts, wound healing assays can be done using cells to determine their migration ability. The defined gap size allows for high reproducibility due to the defined size of the cell-free area. Insert Culture-Inserts into 12-well plates. A total of 30.000 to 40.000 cells were seeded into each insert well, and the cells were cultured until optically confluent monolayers were formed. Allow the cell to grow for approximately 24 hours. It is recommended that cells be monitored immediately after the gap is created, in most cases using phase contrast microscopy. It is also possible to take pictures of the gap at different time points (e.g., after 6，12 and 24 hours). Usually, it is sufficient to monitor the cells for 24 hours or less. In order to perform an accurate analysis, the exact gap position must be observed throughout the experiment. By manually analyzing the image data with image J, the data of the pictures have to be further processed and analyzed.

2.2.15 Boyden chamber assay

Boyden chamber assay is a method commonly used to test cell invasion ability, especially tumor cell invasion ability. Matrigel is used to mimic the growth environment of extracellular matrix similar to that in vivo. Prepare 500,000 target cells in culture flask 48 hours before the experiment, and starve them with serum-free medium for 24 hours before the experiment. Gently add 100μl of diluted Matrigel (250μg/ml, diluted with the serum-free medium) into the upper chamber and incubate at 37°C for 2 hours before seeding the cells. 100μl serum-free medium containing 30,000 target cells were added on the upper layer of Matrigel. Add 800μl of 10% FBS complete medium to the bottom of the 24-well cell culture plate. Incubate the plate in the cell culture incubator for 48 hours. The invasive cells in the bottom of chamber membrane were fixed with 5% glutaraldehyde for 30 minutes, and then washed with PBS three times and stained with 0.2% crystal violet for 30 minutes. A cotton swab was used to remove the cells in the upper

chamber. Results of pictures were obtained with the Zeiss microscope under 5X or 10X objectives. Pictures were taken in five selected areas randomly and counts the number of invasive cells in five pictures, analyzed the average number of invasive cells in each view.

2.2.16 Immunofluorescence

As part of the immunohistochemical method of imaging, Immunofluorescence (IF) makes use of fluorophores in order to visualize antigens (such as proteins). With this technology, it is possible to visualize the positioning of cellular components in cells, tissues, and three-dimensional (3-D) structures derived from cultured cells. IF is dependent on fluorophores, compounds that emit light when exposed to specific wavelengths of light. As a means of detecting protein expression, a biological sample is incubated with an antibody specific to the protein of interest, it is possible for an antibody to be conjugated directly to a fluorophore (direct fluorescence) or through a second antibody conjugated to a fluorophore (indirect fluorescence). A fluorescence microscope or confocal microscope can be used to visualize the protein or antigen, and the localization of the protein in cells can be determined optically.

Round cover slips were put in the 12-well cell-culture plate and add 500ml of culture medium each well. 10000-15000 cells were seeded per well in 12-well plate with cover slips, for the analysis of chromosome structure in mitosis, 150000 cells were seeded in each well. Cells were cultured at 37°C incubator with 5% CO_2. After 24–48 hours, discard the culture medium and rinse the cells spread in cover slips 3 times with 500μl 1XPBS. When the immunofluorescence for microtubules was done, cells were treated with 500μl MSB solution and then rinse 3 times with 1xPBS. Then cells were fixed with 400μl 4% paraformaldehyde (pH 7.4) for 15 min at room temperature. Remove paraformaldehyde solution and wash the cells 3 times with 500μl of 1XPBS.

In order to permeabilize the cells, 400µl and 0.1% Triton X-100 in 1XPBS were added, and the cells were incubated for 10 minutes at room temperature. Triton-X-100 should be removed from the cells and washed with 500µl of 1XPBS for 3 minutes. The cells were blocked in 500µl of 0.5% BSA in 1XPBS and incubated at room temperature for 60 minutes (Alternatively, the cells can be incubated at 4°C overnight in 0.5% BSA or 1XPBS before immunostaining). Primary antibody was diluted in 150µl 0.5% BSA and added to the cells, after which they were incubated overnight at 4°C. After removing the primary antibody solution, wash the cells three times with 500µl 0.1% Tween 20 in 1XPBS. Add the desired concentration of fluorescent dye-labeled secondary antibody or along with a compatible counterstain for the cytoskeleton (e.g., rhodamine phalloidin) diluted in 150µl of 0.5% BSA and incubate for 45 min at room temperature protected from light. Cells should be washed three times with 500µl of 0.1% Tween 20 in 1XPBS. In the control, only fluorescent secondary antibody was used, no primary antibody was incubated in order to prevent artifacts from auto-fluorescence of the cells. Prepare the mount for nuclear dye DAPI (containing anti-fade reagent) by drying the coverslip and adding mounting reagent. Keep slides in a dark environment for short periods of time or visualize the target antigen using fluorescence microscopy.

2.2.17 Metaphase assay of chromosome counting

Cells are seeded at low density in a 6-well cell culture plate which has a cover slip in each well and incubated for 48 hours at 37°C, to allow for cell division. Cells were treated with mitotic spindle inhibitor by adding 50ng/ml pre-warmed colcemid and incubating for 4 hours at 37°C. Remove the medium with colcemid out and washed with 1XPBS once. Then it is hypotonic treatment, cells were incubated with 75mM KCL for 45 minutes at room temperature, this will increase cell volume to allow more area for the chromosomes to spread out. The hypotonic solution was replaced with fixative (methanol: Acetic Acid =3:1) solution and put

in room temperature for 10 minutes. The fixative solution was prepared in advance and kept in -20°C.

Cover slips with cells were taken out from 6-well plate and left it dry. Then put a drop of DAPI in the microscopic slides and mount the cover slips on slides and take pictures under microscopy or stored them at dark place.

2.2.18 Gelatin degradation assay

Sterilize the cover slip by immersing it in a 70% ethanol solution, and then dry it. The fluorescent gelatin solution was prepared by diluting the gelatin solution in PBS containing 2% sucrose (prepared by adding 5ml of distilled water to a commercial vial at a concentration of 1mg/ml according to the manufacturer's instructions). Usually the final concentration of gelatin is 0.2mg/ml. Heat the fluorescent gelatin to 60°C before dilution, and keep the working solution away from light and heating during the coating process.

Prepare the gelatin working solution in advance and preheat it at 60°C. Add 100µl of heated fluorescent gelatin solution to the first cover glass, and then put the solution back into the 60°C water bath. Clamp the cover glass with tweezers and rotate, apply the gelatin solution evenly, and drop the excess gelatin on the next cover glass. Place the coverslip in a 12-well plate protected from light. Immediately repeat the same steps for the next cover glass. After applying all the coverslips, let them dry (the coating will look whitish when it dries). Add 1ml of glutaraldehyde pre-cooled solution (diluted with 1XPBS from 0.5% stock solution) to each well, and incubate on ice for 15 minutes. Then remove the glutaraldehyde, and wash the coverslip 3 times with 1XPBS at room temperature. Add 1ml of freshly prepared sodium borohydride solution (5mg/ml in 1XPBS) and incubate at room temperature for 3 minutes. Remove the sodium borohydride. Wash the coverslip 3 times with 1XPBS at room temperature. Transfer the coverslip to another sterile 12-well plate and wash 3 times with 1XPBS. Coverslips can be

used on the same day or stored in 1XPBS with 200μg/ml penicillin and 200μg/ml streptomycin (1:50 stock solution) in the dark at 4°C for up to 2 weeks.

Working under sterilized conditions, transfer the required number of coated coverslips to a new 12-well plate. Wash 3 times with 1XPBS, split the cells and count them. 1ml complete medium with 20,000-40,000 cells were added into a 12-well plate containing a coverslip. Incubate for 48 hours in the incubator.

At the end point, the immunofluorescence method is used to wash, fix, permeate and block. Then, F-actin was diluted with Alexa Fluor 568 Phalloidin (diluted in 1XPBS containing 0.3% BSA and 0.1% Triton X-100 about 1:500 to 1:100) and incubated for 0.5 to 1 hour in the dark place at room temperature. Put the coverslips upside down on a glass slide with a drop of mounting medium containing DAPI to mount the coverslips. The slides can be stored in a dark environment at 4°C for several weeks or be taken pictures under a microscope randomly. The analysis was used imageJ. The measurements associated with the "area fraction" are normalized by comparing them with the number of DAPI nuclei in the same field. The result is referred to as "normalized degradation".

2.2.19 Statistics

GraphPad Prism 6 software (GraphPad, San Diego, California, USA) was used for data collection and statistical analysis. Student's t-test or F-test is used to compare two groups, and analysis of variance (ANOVA) is used to compare multiple groups (more than 2 groups). The statistical significance is set as: $p < 0.05$ (*), $p < 0.01$ (**), $p < 0.001$ (***), $p < 0.0001$ (****)

3. Results

A previous genetic screen in our laboratory identified TKS5 as a potential ploidy-control factor and experiments in the laboratory revealed that the knockdown of TKS5 resulted in an increased aneuploidy in human fibroblasts cells (unpublished results, C. Günes). Since aneuploidy is strongly associated with cancer progression, it was tempting to study the role of TKS5 in bladder cancer (BC) initiation and progression.

3.1 The role of TKS5 in ploidy control and genome stability of urothelial cells

3.1.1 Decreased TKS5 in urothelial cells leads to aneuploidy

Aneuploidy refers to the presence of an abnormal number of chromosomes in a cell, such as a human cell with 45 or 47 chromosomes instead of the usual 46 chromosomes in euploid human cells. In order to clarify whether TKS5 is also involved in ploidy-control in ureter epithelial cells, the number of chromosomes was determined by metaphase spread analysis in the karyotypically normal (46n), telomerase immortalized ureter epithelial cell strain Y235T. Although some variation from the euploid karyotype is observed in control cells (Y235T-shScr) due to the experimental metaphase preparation protocols, the number of chromosomes significantly deviated from the euploid state upon TKS5 knockdown in Y235-shTKS5 cells (Figure 5), indicating that TKS5 may be involved in the maintenance of normal karyotype and thus in the control of genome stability.

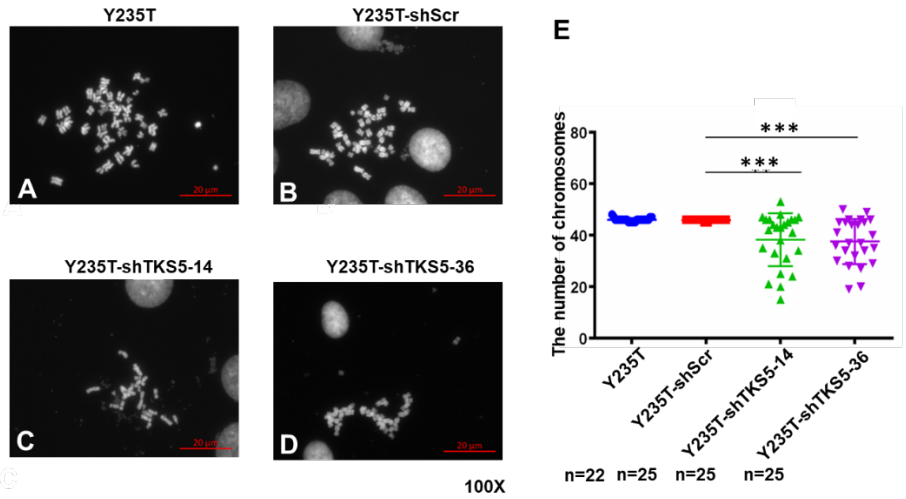

Figure 5. Decreased TKS5 expression results in augmented aneuploidy. A-D) Representative images of chromosomes analyzed by metaphase counting, showing the number of chromosomes in Y235T-shTKS5 cells is different from Y235T-shScr cells. Minor variations from the euploid chromosome number (46 chromosomes) in Y235T control cells is due to experimental conditions. **E)** The number of chromosomes in Y235T-shTKS5 cells is associated with higher variability when compared to the control group. The experiment was repeated in two independent experiments. Pictures were taken with 100X objective. Student's t-test is used to analyze statistical significance. Error bars represent mean +/- SD (***P<0.001).

To strengthen this conclusion, further experiments were performed, such as micronuclei formation or determination of centrosome defects.

3.1.2 Decreased TKS5 expression results in increased number of micronuclei

Micronuclei are commonly observed in cancerous cells as a sign of aneuploidy and their presence indicates genomic damage events that can increase the risk of developmental or degenerative diseases. Micronuclei can simply be counted by DAPI staining of DNA in interphase cells as they appear as small compact DNA structures in close proximity to cell nucleus (Figure 6 A-I). The percent of micronuclei appearing in Y235T-shTKS5 cells were about four to five times more than Y235T control cells (Figure 6 J). These results are in line with the results of the metaphase spread experiments shown above and strengthen the conclusion that TKS5 contributes to genome stability in epithelial cells of human ureter.

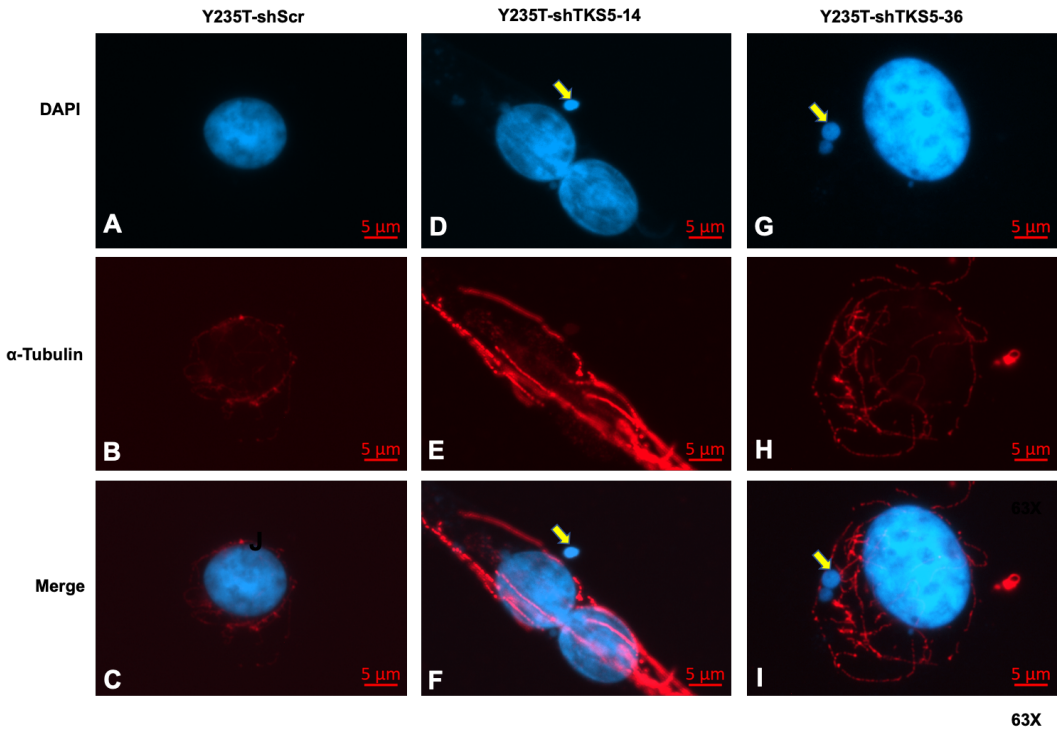

J

	Micronuclei
Y235T-shScr	0.5% (5/1000)
Y235T-shTKS5-14	1.8% (18/1000)
Y235T-shTKS5-36	2.4% (24/1000)

Figure 6. TKS5 knockdown in Y235T cells results in increased micronuclei generation. A, D, G) Nuclei and micronuclei were stained with 4',6-diamidino-2-phenylindole (DAPI)**. B, E, H)** Microtubules were stained with α-Tubulin. **C, F, I)** Two channels of nuclei and microtubules were merged by 4',6-diamidino-2-phenylindole (DAPI) and α-Tubulin. Yellow arrows refer to as the micronuclei. **J)** The percentage of micronuclei in Y235T-shTKS5 cells is 1.8% (18/1000) and 2.4% (24/1000) respectively, and 0.5% of Y235T-shScr cells. Pictures were taken with 63X objective. Representative pictures and micronuclei countings are shown from two independent experiments.

3.1.3 Decreased TKS5 expression in Y235T results in abnormal cell division

In order to understand the impact of TKS5 on chromosome instability, cells in different mitotic stages were observed for abnormal mitosis induced by decreased TKS5. As control, Y235T-shScr cells with normal cell division are shown in metaphase, anaphase and telophase during mitosis (Figure 7). Proper chromosome alignment was present in metaphase in Y235T-shScr cells (Figure 7 A, D, G). In the anaphase, chromosomes are segregated into the opposite poles

symmetrically (Figure 7 B, E, H). Chromatin is divided evenly into two daughter cells in telophase (Figure 7 C, F, I).

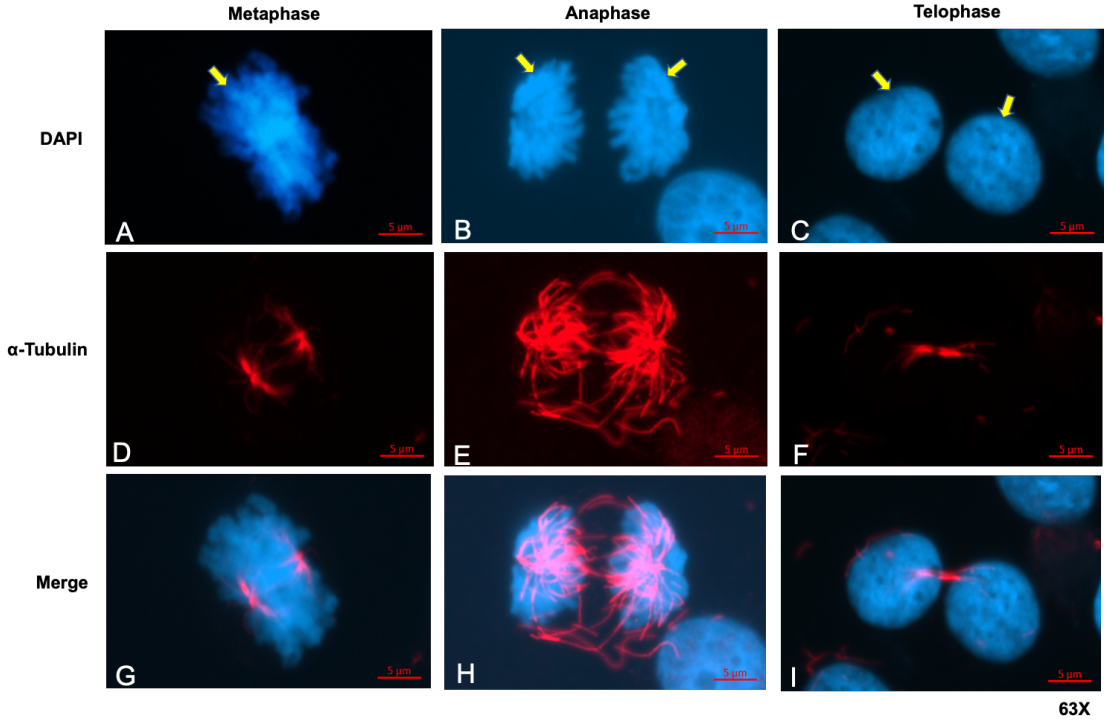

Figure 7. Normal cell division in Y235T-shScr cells. Representative pictures of metaphase, anaphase and telophase in Y235T-shScr cells. **A-C)** The chromosomes were stained with 4',6-diamidino-2-phenylindole (DAPI). **D-F)** The spindle and centrosome were stained by α-Tubulin. **G-I)** The channels of 4',6-diamidino-2-phenylindole (DAPI) and α-Tubulin were merged. The normal chromosome segregation in metaphase, anaphase and telophase during mitosis, yellow arrows indicate accurate chromosome alignment and symmetrical segregation. In the metaphase, normal cell division account for 98.3% (n=59). In the anaphase, normal cell division accounts for 100% of the total (n=41). The proportion of normal cell division in telophase is 97.4% (n=112). Pictures were taken with 63X objective.

In TKS5 knockdown cells, abnormal number of centrosomes appears during mitosis. Before mitosis, two centrosomes separate and migrate to opposite poles of the mitotic cell. Each centrosome is the starting point of a large number of microtubules that form the mitotic spindle apparatus. Decreased TKS5 in Y235T cells (Y235T-shTKS5) results in the generation of multiple centrosomes in the process of mitosis (Figure 8). Triple centrosomes were observed in 2.94% (3/102) of Y235T-shTKS5 cells, while there is no abnormal centrosome observed in control Y235T-shScr cells (0/91) (Figure 8 J).

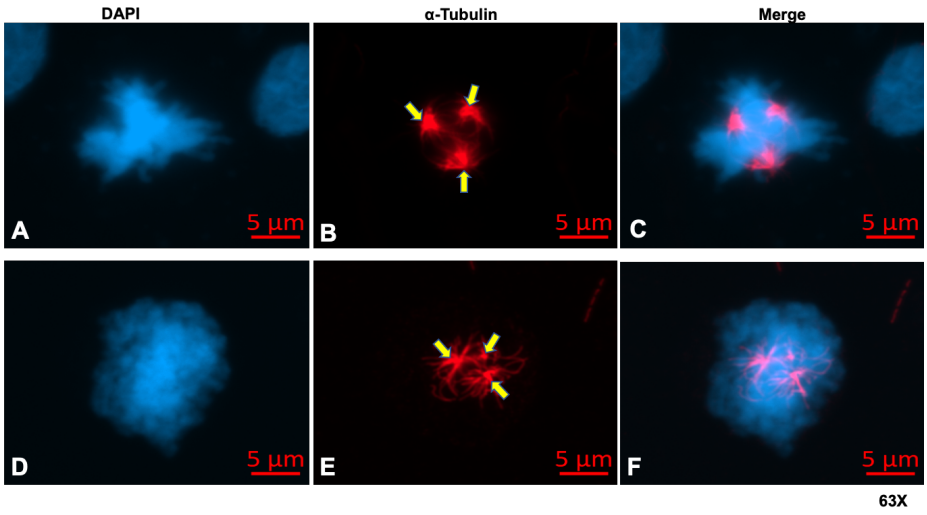

J

Triple centrosomes	Y235T-shScr	(0.0%)0/91
	Y235T-shTKS5	(2.94%)3/102

Figure 8. Abnormal number of centrosomes in mitosis associated by TKS5 knockdown in Y235T cells. Two sets of pictures represent the phenomenon of multiple centrosomes. **A, D**) The chromosomes were stained with 4',6-diamidino-2-phenylindole (DAPI). **B, E)** The centrosomes are visualized by staining with α-Tubulin. **C, F**) 4',6-diamidino-2-phenylindole (DAPI) and α-Tubulin were merged. The pictures demonstrate that TKS5 knockdown in Y235T result in triple-centrosome. Yellow arrows indicate triple centrosomes. Pictures were taken with 63X objective. **J)** The table shows the rate of the abnormal number of multiple centrosomes. Three centrosomes were observed in 2,94% of Y235T-shTKS5 cells (n=102). There was no abnormal number of centrosomes found in Y235T-shScr (n=91). Representative pictures and abnormal metaphase figures are shown from two independent experiments.

TKS5 knockdown in Y235T cells increased the probability of chromosomes missegregation in different stages of mitosis. Chromosome missegregation is used to summarize all abnormal chromosome divisions during mitosis, including chromosomal misalignment, lagging chromosomes, etc. Chromosome misalignment occurs usually by microtubule/kinetochore defects in metaphase during cell division, resulting in lagging chromosomes (Figure 9 A, E, I). Increasing number of lagging chromosomes were observed in the anaphase and telophase of TKS5 knockdown cells (Figure 9 C, G, K, D, H, L). The number of mitotic cells at different stages were counted and evaluated (Figure 9 M). In the metaphase, the probability of chromosome missegregation in TKS5 knockdown

cells is 10.9%, while in control cells it is 1.7%. In anaphase, the incidence of chromosome missegregation is 11.6% and 0% in Y235T-shTKS5 cells and Y235T-shScr cells, respectively. In the telophase, defects in chromosome segregation in TKS5 knockdown cells and control cells are 8.8% and 2.6%, respectively.

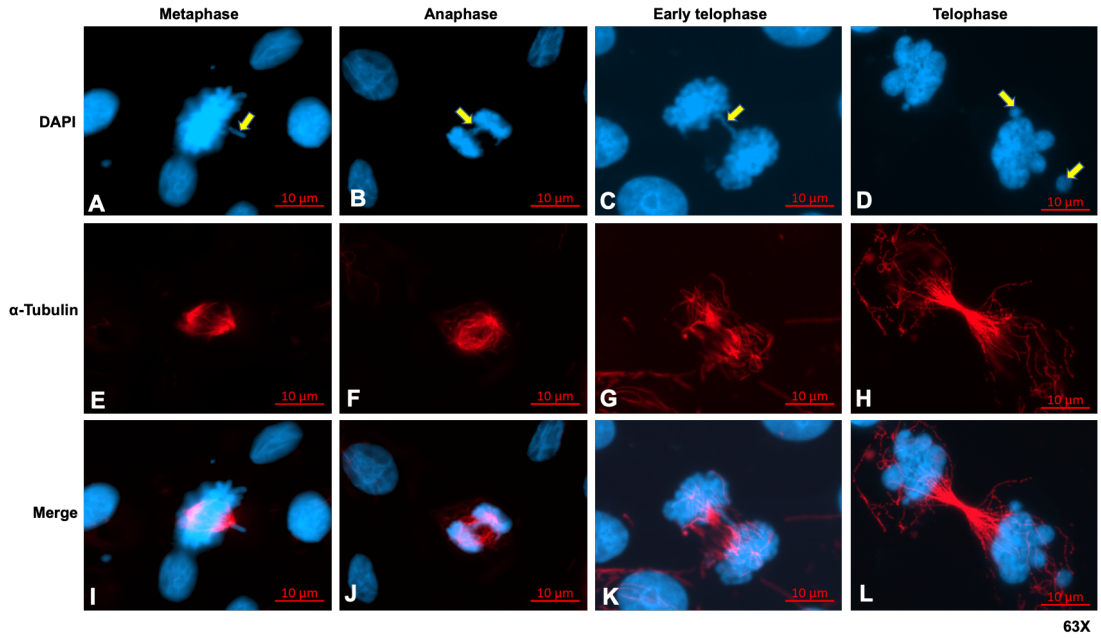

M

		Mitosis		
		Metaphase	Anaphase	Telophase
Y235T-shScr	Chromosome missegregation	1(1.7%)	0(0.0%)	3(2.6%)
	Normal	58(98.3%)	41(100.0%)	112(97.4%)
Y235T-shTKS5	Chromosome missegregation	13(10.9%)	16(11.6%)	20(8.8%)
	Normal	106(89.0%)	122(88.4%)	206(91.2%)

Figure 9. Decreased TKS5 in Y235T cells is associated with impaired cell division. Representative pictures showing chromosome missegregation in metaphase, anaphase and telophase during mitosis are depicted. **A-D)** The chromosomes were stained with 4',6-diamidino-2-phenylindole (DAPI). **E-H)** The spindles and centrosomes were detected by α-Tubulin staining. **I-L)** The channels of 4',6-diamidino-2-phenylindole (DAPI) and α-Tubulin were merged. The pictures show chromosome misalignment and lagging chromosome in mitosis. Yellow arrow in picture A indicate the chromosome misalignment. And yellow arrows in pictures B, C, D illustrate lagging chromosomes. Pictures were taken with 63X objective. **M)** The table shows the events of chromosome missegregation and normal chromosome segregation in different phases during mitosis in control cells and in cells with TKS5 knockdown. Representative pictures, the abnormal metaphase figures and erroneous figure countings are shown from two independent experiments.

Γ-Tubulin is found primarily in centrosomes and spindle pole bodies, and plays an essential role in cell division. The above described results showed a role of TKS5 in cell division. To elucidate the function of TKS5 in mitosis and microtubule alignment, co-localization of γ-Tubulin and TKS5 was assessed in Y235T-shScr cells. The results show that γ-Tubulin and TKS5 signals overlap at the opposite centrosomes in the prophase (Figure 10 A-D), metaphase (Figure 10 E-H), anaphase (Figure 10 I-L) and telophase (Figure 10 M-P).

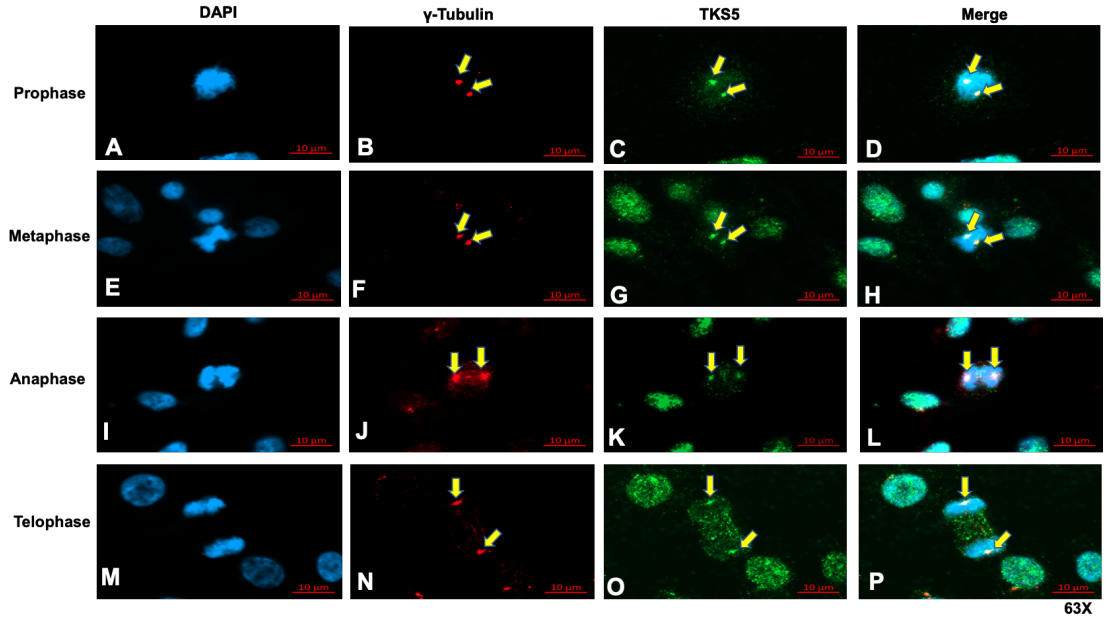

Figure 10. The co-localization of γ-Tubulin and TKS5 during mitosis of Y235T-shScr. A, E, I, M) Chromosomes and chromatids are staining by using 4',6-diamidino-2-phenylindole (DAPI) and showed with blue colour. **B, F, J, N)** Γ -Tubulin is visualized with red colour. **C, G, K, O)** TKS5 is stained with green colour. **D, H, L, P)** The overlap of γ-Tubulin and TKS5 is showed with yellow colour. The co-localization area is marked with yellow arrow. The pictures are taken with 63X objective. Representative pictures and figures are shown from three independent experiments.

3.2 Expression of TKS5 in human and mouse urothelial tissues and cells

3.2.1 TKS5 expression in immortalized urothelial cell strains and established BC cell lines

The above data suggest a contribution of TKS5 in BC progression, potentially by regulating genome stability in bladder epithelium. To gain further insight into the role of TKS5 in BC, next, RT-qPCR method was used to quantitatively determine the expression of TKS5 in immortalized urothelial cells and established BC cell lines. *TKS5* is highly expressed at mRNA level in immortalized urothelial cell lines compared with BC cell lines (Figure 11 A). The TKS5 expression at protein levels in immortalized urothelial cell lines (UROtsa, HBLAK and Y235T) is also higher than BC cell lines (RT4, UMIUC-3, T24 and J82) (Figure 11 B). Interestingly, in contrast to the above-described role of TKS5 in cell migration and invasion, TKS5 levels is inversely correlated with the increased invasive potential of BC cell lines.

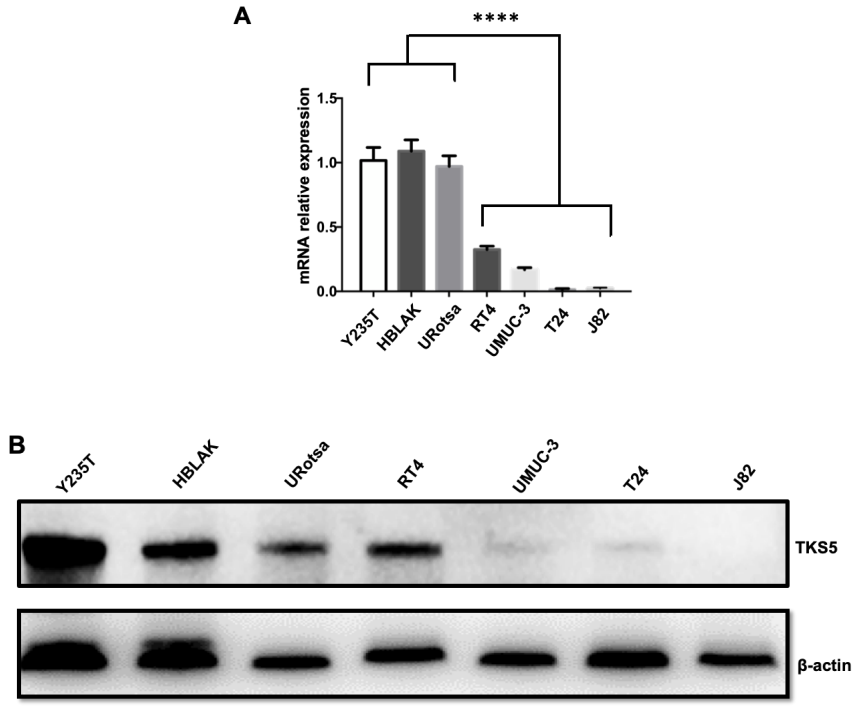

Figure 11. TKS5 expression at mRNA and protein level in immortalized urothelial cell lines and bladder cancer cell lines. A, B) The expression of TKS5 in same cell lines at mRNA level and protein level. The expected size of TKS5 protein is around 130-150kDa and β-actin was used as quality control appears at around 42kDa. The experiments are technically repeated for three times. Analysis of variance (ANOVA) is used to analyze statistical significance. Error bars represent mean +/- SD (**** P<0.0001).

3.2.2 TKS5 expression in normal urothelial tissues and tumor tissues of mice and humans

In order to understand a potential contribution to human BC, *TKS5* expression was also determined in healthy human bladder and bladder tumor using a small set of 20 pairs of matched normal/tumor tissue samples from patients (Figure 12 A). The mRNA samples of 20 pairs' bladder tumour and normal adjacent tissue were a kindly gift from University of Cologne with informed written consent. The experiment was approved by informing written consent and local research ethics committee (239/18). Despite some differences in individual patients in *TKS5* mRNA levels, there was no significant difference between normal tissues and tumor tissues when all samples were compared (Figure 12 B). Nevertheless, the majority of patients had reduced *TKS5* mRNA levels in the tumor sample

compared to normal tissue sample (reduced: n=11, not changed: n=5, and increased: n=4). These data suggest that TKS5 may play a critical role during BC progression in some genetic context.

The administration of the chemical carcinogen N-butyl-N-(4-hydroxybutyl) nitrosamine (BBN) is commonly used to induce bladder tumors in experimental animals, including mice. Depending on the animal species, the spectrum of BBN-induced urothelial lesions is different, yet similar to that observed in humans. In mice, BBN-induced tumors are mostly invasive squamous cell carcinoma of the bladder and to some extend transitional cell carcinoma. In order to analyze potential changes in *Tks5* mRNA levels, *Tks5* expression was determined by RT-qPCR in normal and tumor bladder samples of control mice and BBN-treated mice at different time-points post BBN-treatment (2, 4, 6 and 8 months after start of BBN-administration) to identify changes in *Tks5* mRNA level during tumor progression. Of note, bladder tumors are first detectable after 4 months post-BBN treatment under the conditions used here. The animal experiment was approved by local research ethics committee (35/9185.81-3/1326). According to the pathological results of mice, they are classified as non-tumor and tumor group. Though there is no statistically compared with the expression level of *Tks5* in the non-tumor group, the expression level of *Tks5* in the bladder tissue of different time points of BBN treatment is lower than non-tumor mice (Figure 12 D). Similar to TKS5 expression in human bladder tumor samples, analysis of the gene expression data did not reveal a significant difference in Tks5 between the non-tumor group and the BBN treatment tumor group (Figure 12 E).

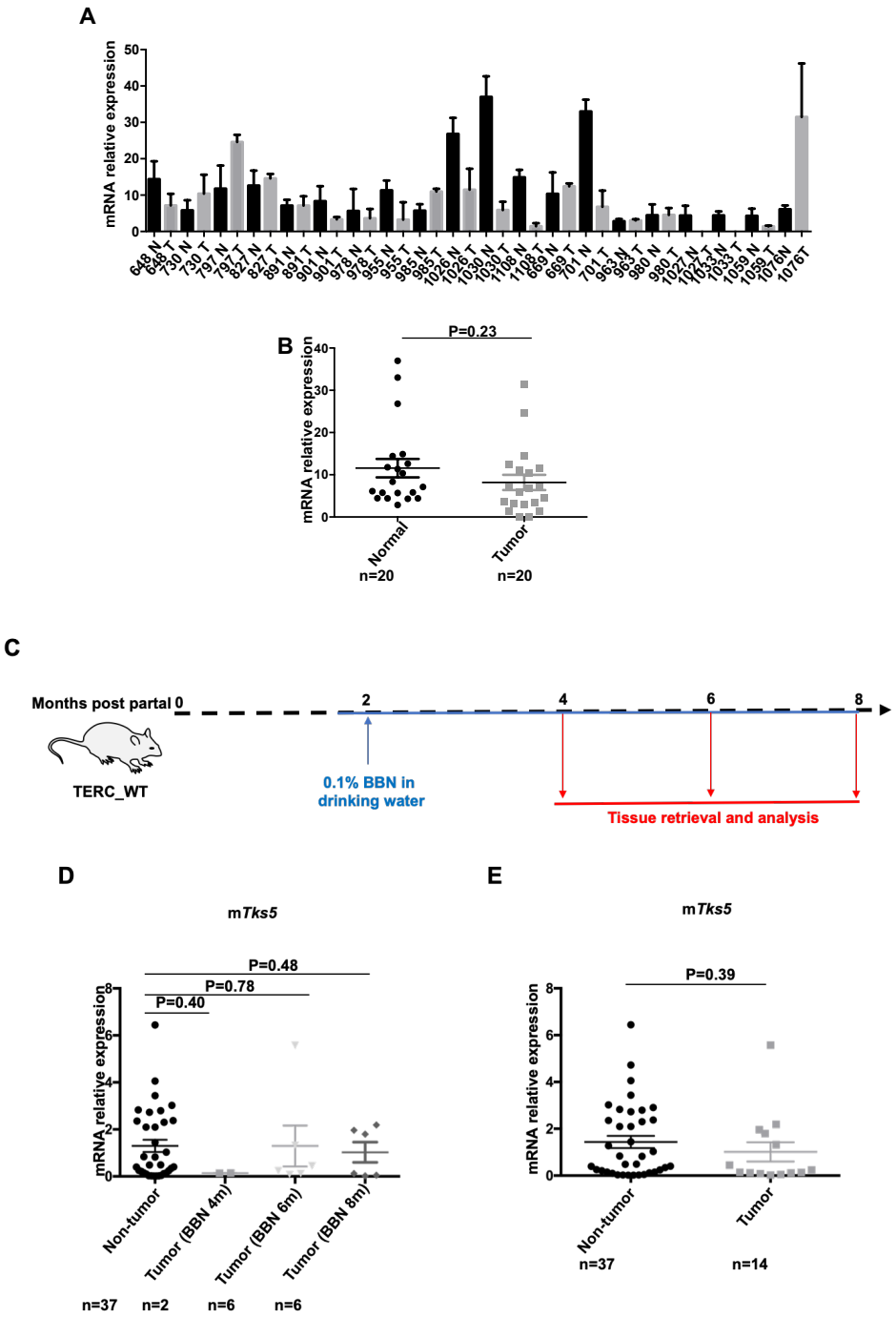

Figure 12. Expression of TKS5 in tissues of human and mice specimens. A, B) Expression of TKS5 in human urothelial bladder tumor (T) tissues and their matched adjacent non-tumor(N) tissues. The numbers indicate the individual patients (pseudonymized). **C)** Schematic diagram of the process of building a bladder cancer model by feeding mice with BBN. **D)** The expression of *Tks5* in non-tumor tissues and bladder tumor tissues with different BBN treatment time is shown. **E)** The expression of *Tks5* in non-tumor mice bladder tissues and BBN induced bladder tumor tissues of mice is presented. The experiments are from three technical repeats. Student's t-test and F-test are used to analyze statistical significance. Error bars represent mean +/- SEM.

3.3 The biological role of TKS5 in urothelial cells and BC cells

In order to gain further insights into the potential roles of TKS5 in urothelial cells, TKS5 expression was abrogated using shRNA technology in Y235T and RT4 cell lines. Conversely, TKS5 was overexpressed in cancer cell lines with low TKS5 levels (UMUC-3 and BFTC-905). In both situations, the impact of TKS5 knockdown or ectopic expression on cell viability, genome stability and invasive/migratory capacities of cells was investigated by functional experiments, such as proliferation-assay, Boyden chamber assay, wound healing assay and gelatin degradation assay.

3.3.1 Knockdown of TKS5 in Y235T and RT4 cell lines

Y235T and RT4 cells were transduced with TKS5-specific shRNAs (shTKS5-14 and shTKS5-36) and cells stably expressing the indicated shRNAs were established. In these cells, *TKS5* mRNA expression was reduced significantly compared to parental cells or compared to cells that were transduced with a scrambled shRNA (Figure 13). The expression efficiency was verified by RT-qPCR and Western blot at both mRNA and protein level (Figure 13 A, B).

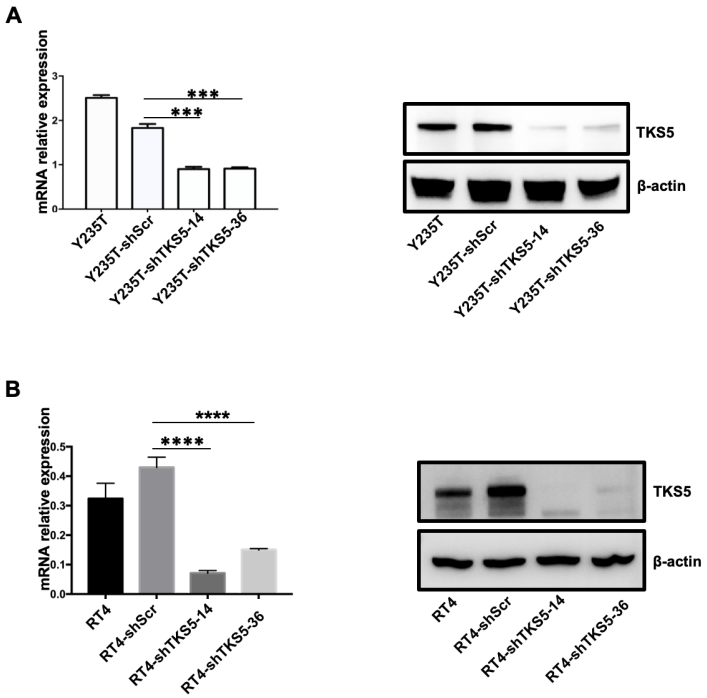

Figure 13. Knockdown of TKS5 in Y235T and RT4 cell lines. A) The RT-qPCR experiment showed the relative *TKS5* mRNA levels and determination of TKS5 protein levels by Western blot in Y235T parental, Y235T scramble control (shScr), Y235T shTKS5-14 and shTKS5-36 cell lines. **B)** The qPCR experiment indicated *TKS5* mRNA expression and detection of TKS5 protein expression by Western blot in RT4 parental, RT4-shScr, RT4-shTKS5-14 and shTKS5 cell lines. *TKS5* expression in Y235T-shTKS5 was reduced significantly in mRNA level compared with Y235T-shScr cells and parental cells. The expression of TKS5 protein was also decreased in Y235T shTKS5 cells. *TKS5* mRNA expression was decreased significantly in RT4 shTKS5 cells compared with RT4 scramble control cells and the protein expression was reduced obviously in RT4 shTKS5 cells as well. The experiments are repeated for three times. Student's t-test and analysis of variance (ANOVA) are used is used to analyze statistical significance. Error bar represents mean+/-SD (*** P<0.001, **** P<0.0001).

3.3.2 Overexpression of TKS5 in UMUC-3 and BFTC-905 cell lines

UMUC-3 and BFTC-905 cells were transfected with the TKS5-GFP-expressing vector and the control empty vector. Successful ectopic TKS5 expression in both cells lines was confirmed by RT-qPCR and Western blot (Figure 14).

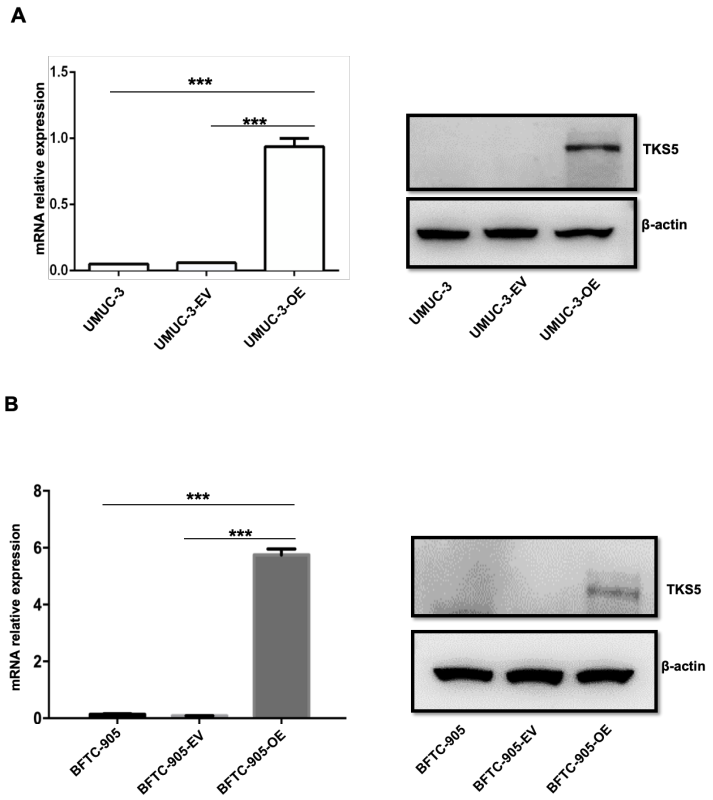

Figure 14. Overexpression of TKS5 in UMUC-3 and BFTC-905 cell lines. A) The RT-qPCR experiment showed the relative *TKS5* mRNA level and the determination of TKS5 protein level by western blot. **B)** *TKS5* mRNA and protein expression was tested in BFTC-905 overexpressing cells. UMUC-3-OE and BFTC-905-OE cells showed significantly higher *TKS5* mRNA level compared to cells with empty vectors. The protein expression of TKS5 was increased in UMUC-3-OE and BFTC-905-OE cell lines compared to UMUC-3-EV and BFTC-905-EV cells. The experiments are repeated for three times. Student's t-test and analysis of variance (ANOVA) are used is used to analyze statistical significance. Error bars represents mean +/-SD (***P<0.001).

3.3.3 The impact of TKS5 on viability

In order to delineate the role of TKS5 in the cell viability of urothelial cells or BC cell lines. MTT assay and cell counting was used to test the cell viability and the result of these experiments show that knockdown of TKS5 reduced growth ability in Y235T cells significantly (Figure 15 A). On the other hand, abrogation of TKS5 in RT4 cells had no effect on cell viability (Figure 15 B). Similarly, increased TKS5 expression in UMUC-3 did not affect the growth ability/viability of these cells (UMUC-3-OE) compared to parental UMUC-3 cells or UMUC-3 cells with the empty vector (UMUC-3-EV) (Figure 15 C).

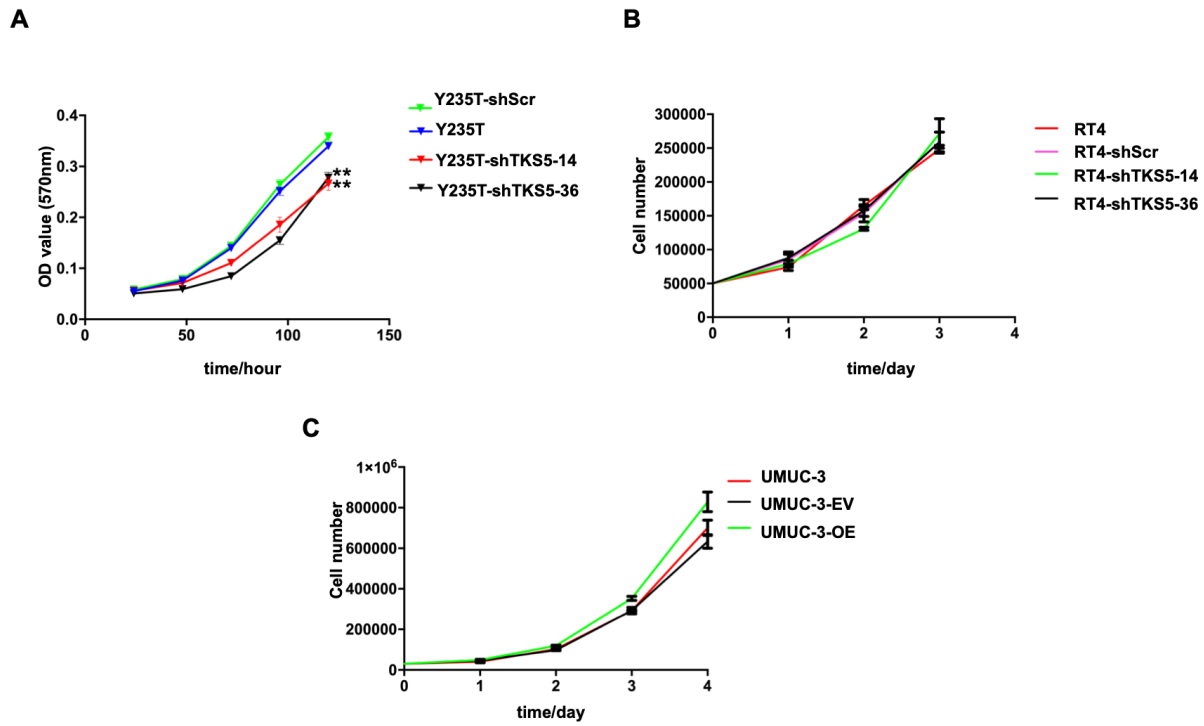

Figure 15. The effect of in TKS5 expression level on bladder cancer cells and normal urothelial cells. A) Abrogation of TKS5 impairs growth ability of Y235T cells, TKS5 knockdown reduced the growth ability in Y235T cells significantly compared to control cell lines (**P<0.01). **B)** Knockdown of TKS5 in RT4 cells did not affect the growth ability. **C)** Overexpression of TKS5 in UMUC-3 cells has no impact on the growth ability. The experiments are technically repeated for three times. Student's t-test is used to analyze statistical significance. Error bars represent mean +/- SEM.

3.3.4 TKS5 is involved in the formation of invadopodia

Cortactin or F-actin are typical markers of invadopodia. In order to visualize the morphology of invadopodia/podosomes, cells were monitored by Immunofluorescence after staining with specific antibodies for cortactin and F-actin, the co-localization of cortactin and F-actin was indicated by punctual staining represent invadopodia/podosomes which are indicated by the yellow arrow (Figure 16 D). In Y235T cells featuring TKS5 knockdown, less clear invadopodia/podosomes were observed (Figure 16 H, L). These results indicate that formation of invadopodia/podosomes was impaired in TKS5 knockdown cells. The quantification shows the number of puncta of invadopodia/podosomes were reduced significantly compared to control cells (Figure 16 M).

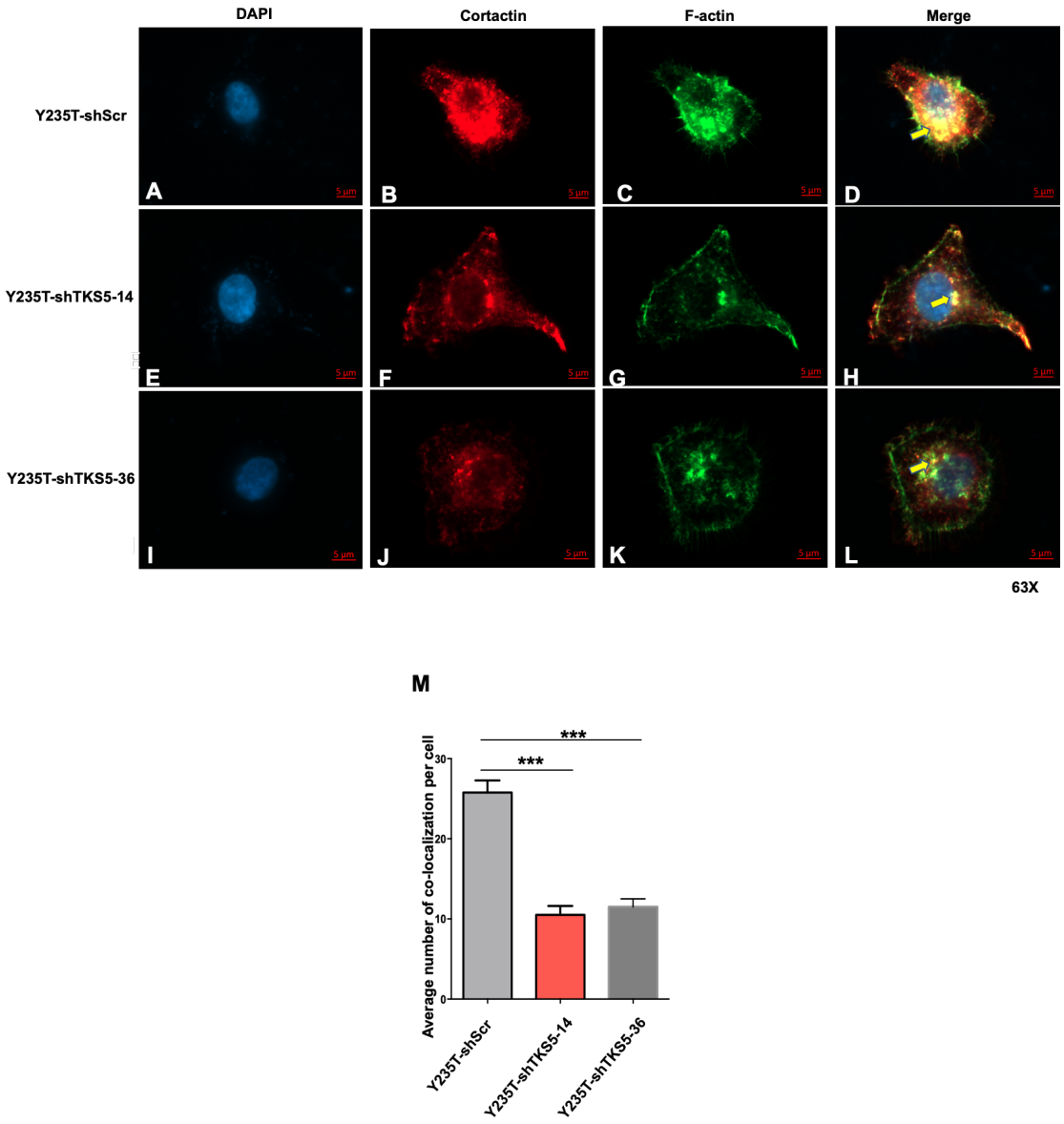

Figure 16. Invadopodia/podosomes formation ability was reduced in TKS5 knockdown Y235T cells. A, E, I) Cells' nuclei were stained with 4',6-diamidino-2-phenylindole (DAPI). **B, F, J, C, G, K**) Invadopodia/podosomes were visualized by cortactin and phalloidin staining. **D, H, L)** Yellow (yellow arrow) dots indicate the co-localization of F-actin and cortactin. **M)** The histogram shows that invadopodia/podosomes formation ability was significantly reduced in TKS5 knockdown Y235T cells compared to scramble control cells (***P<0.001). Pictures were taken with 63X objective. The experiments are technically repeated for two times. Student's t-test is used to analyze statistical significance. Error bars represent mean +/- SEM.

Cortactin plays an important role in cancer cell invasion and migration. Therefore, cortactin expression was analyzed by Western blot in TKS5 knockdown and overexpression cells. While the knockdown of TKS5 led to reduced cortactin expression, both in Y235T cells (Y235T-shTKS5, Figure 17 A) and in non-

invasive BC cell line RT4 (RT4-shTKS5, Figure 17 B). However, cortactin protein levels did not change in UMUC-3 cells upon overexpression of TKS5 (Figure 17 C). These results suggest that TKS5 may influence cortactin expression upon knockdown but a further increase of cortactin in cells with high cortactin levels (such as highly invasive BC cell line UMUC-3) is not possible by forced TKS5 expression.

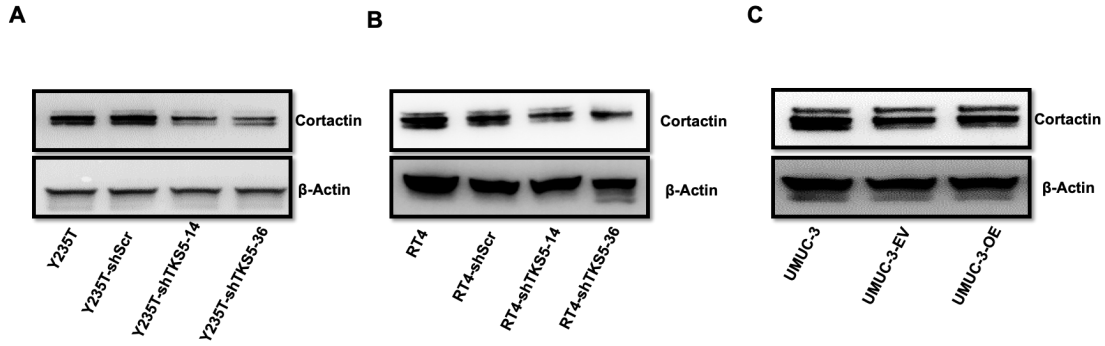

Figure 17. Expression of cortactin in Y235T, RT4 and UMUC-3 cells. A) Expression of cortactin in Y235T cell lines at protein levels. **B)** Expression of cortactin in RT4 cell lines at protein level. **C)** Protein expression of cortactin in UMUC-3 cell lines. Cortactin was down-regulated in Y235T-shTKS5 cells and RT4-shTKS5 cells, but there is no change in UMUC-3 TKS5 overexpression cells. The molecular weight of cortactin is at around 80kDa. B-Actin served as loading control appears at around 42kDa. The experiments are repeated twice from different lysates.

3.3.5 TKS5 regulates matrix degradation and invasion ability

Because degradation of ECM is a key process for malignant tumor cells to invade surrounding tissues, the degradation ability of ECM was examined in UMUC-3 cells by gelatin degradation assay. UMUC-3-EV cells and UMUC-3-OE cells were seeded onto the coverslips coated with FITC-labeled gelatin for 48 hours and then stained with Alexa 568-phalloidin for F-actin. Alexa Fluor® 488 Phalloidin is a marker with high affinity for filamentous actin (F-actin) that is conjugated with a bright, photo-stable, green fluorescent dye Alexa Fluor® 488. Gelatin degradation is visualized as black areas on FITC-gelatin. The degraded black area in the UMUC-3 ectopically expressing TKS5 is significantly larger than the black area produced by the control cells (Figure 18 A). The quantification result

of gelatin degradation assay indeed confirms that TKS5 overexpression is associated with significantly increased degradation compared to control cells (Figure 18 B). The Boyden chamber assay was performed to clarify the function of TKS5 on the invasive capacity in BC cells. Compared with RT4 control cells, the invasive ability in RT4 TKS5 knockdown cells was decreased significantly (Figure 18 C). Similarly, TKS5 overexpression in UMUC-3 cells promote the invasive ability significantly compared to UMUC-3 control cells (Figure 18 D).

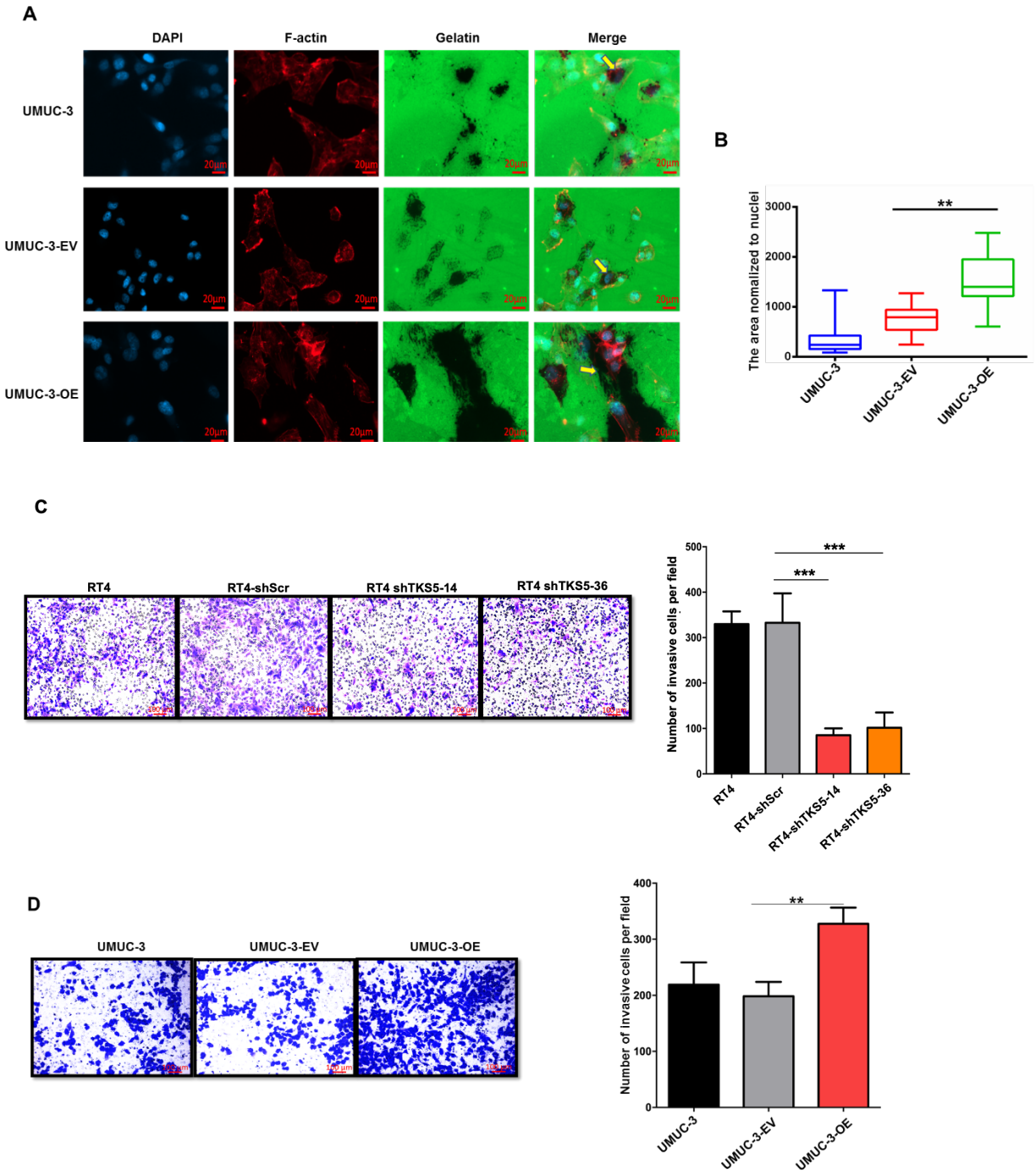

Figure 18. TKS5 promotes matrix degradation and invasive abilities of cells. A, B) Gelatin degradation assay showed that TKS5 overexpression in UMUC-3 cells increases degradation ability of extra cellular matrix significantly. **C)** TKS5 knockdown in RT4 cell is associated with a decrease in the invasive ability. **D)** Representative images of Boyden chamber experiment in UMUC-3 TKS5 overexpression cells showed increased invasion ability. Gelatin pictures were taken with 40X objective and Boyden chamber pictures were taken with 10X objectives. Gelatin degradation assay was repeated for two times independently and Boyden chamber assay was repeated for three times independently. Student's t-test is used to analyze statistical significance. Error bars represent mean +/- SEM (**P<0.01, **P<0.001).

3.3.6 TKS5 regulates migration ability of RT4 cells and UMUC-3 cells in wound healing assay

The wound healing assay (also called the scratch assay) was performed with RT4-shScr, RT4-shTKS5 and UMUC-3-EV and UMUC-3-OE cells to characterize the role of TKS5 in the migration of BC tumor cells.

Compared with RT4-shScr cells, the wound gap closed slower in RT4-shTKS5 cells, which means migration ability was reduced in RT4-shTKS5 cells (Figure 19 A, B). The wound gap was completely closed within 4 days in RT4-shScr cells, but not in the RT4-shTKS5 cells. Similarly, TKS5 overexpression in UMUC-3 cells promotes the migratory capacity (Figure 19 C, D).

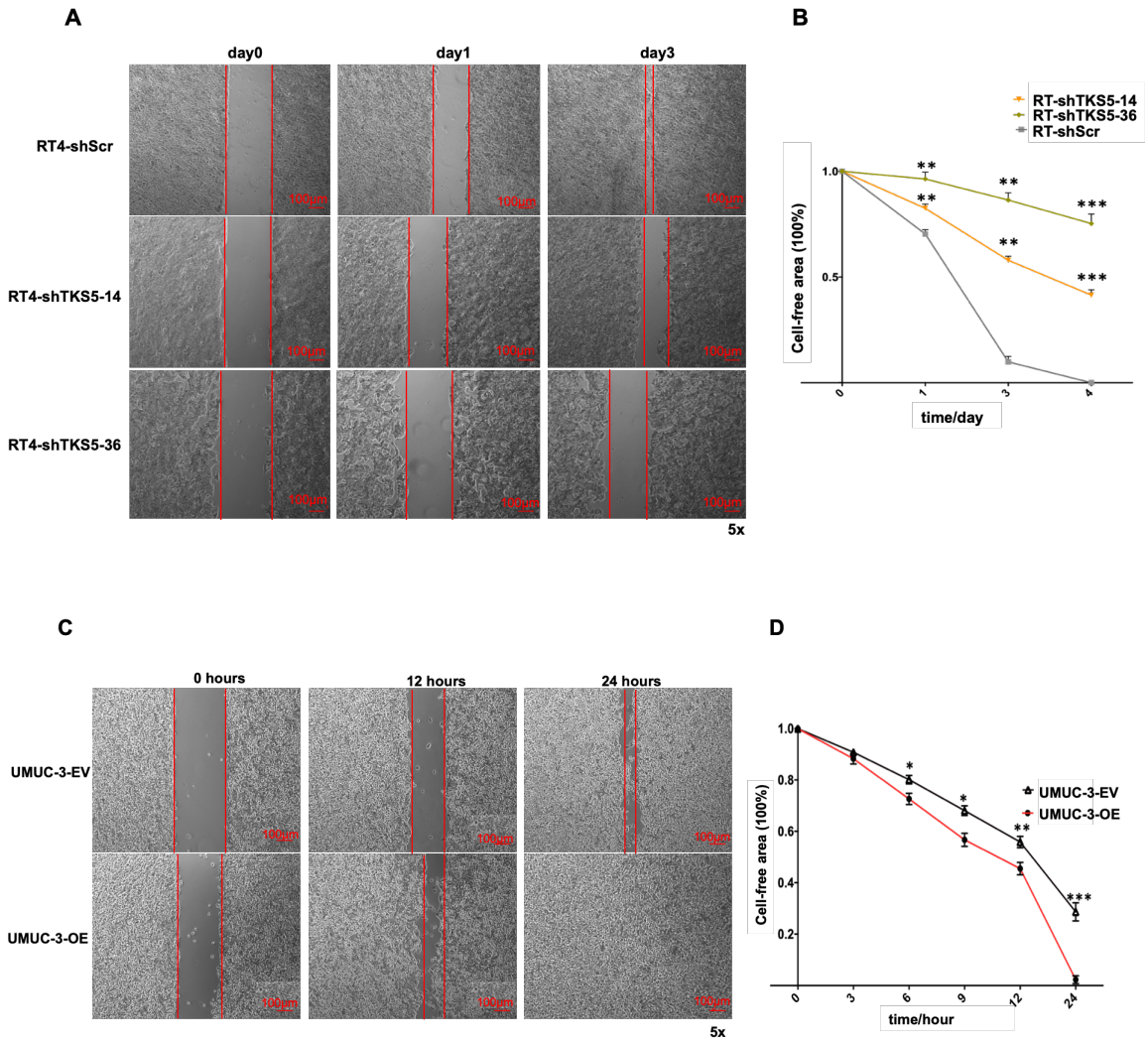

Figure 19. TKS5 regulates migration ability of bladder cancer cells in wound healing assay. **A，B)** Representative images showing wound gap closure of RT4-shScr and RT4-shTKS5 cells different time points. The wound gap in RT4-shTKS5 closed slower than that of RT4 control cells. **C, D)** Images demonstrate that the wound gap in UMUC-3 TKS5 overexpression cells closed fast than that of UMUC-3 control cells. Quantification of the cell-free area from both UMUC-3 control and UMUC-3 TKS5 overexpression cells with time. At each time point, less cell-free area means a stronger migratory capacity. Pictures were taken with 5X objective. The experiment was repeated for two times independently. Student's t-test is used to analyze statistical significance. Error bars represent mean +/- SEM (*P<0.05, **P<0.01, ***P<0.001).

In summary, the results of the invasion and migration experiments are in line with the expectation that TKS5 expression improves invasion/migration capacity of cells. However, these results are in apparent contrast to the above described expression levels showing reduced TKS5 expression in invasive cancer cell lines compared to immortal but non-tumorigenic cells, such as Y235T, HBLAK (data

presented in Figure 11). These results may indicate another, yet unknown cellular function of TKS5.

3.4 Pathway analysis in Y235T, RT4 and UMUC-3 cells

BC is associated with downregulation of two main signal transduction pathways, namely AKT and the MAPK/ERK. These pathways control cell proliferation and/or cell survival and cell migration/invasion. In order to study whether TKS5 is involved in the regulation of these pathways, Western blot experiments were performed (Figure 20). Western blot analysis shows reduced AKT phosphorylation at serine (Ser473) and threonine (Thr308) residues by TKS5 abrogation in Y235T cells, while the total amount of AKT is the same, indicating epistatic post-translational modulation of the AKT protein in downstream of TKS5. Equal protein loading control was confirmed by the detection of β-Actin levels (Figure 20 A). Similarly, TKS5 knockdown resulted in reduced AKT phosphorylation (i.e. pathway activation) was observed at Ser473 in non-invasive RT4 BC cell line while total AKT and β-Actin remained unaffected (Figure 20 B). Although, lower pThr308 levels were also seen in TKS5 knockdown cells, this result needs to be taken with care as scrambled shRNA-control cells also show reduced pThr308-AKT. Importantly, in concordance with the reduced AKT phosphorylation upon TKS5 knockdown, Western blot result shows enhanced phosphorylation of Ser473 and Thr308 residues by TKS5 overexpression in UMUC-3 cells while total AKT and β-Actin levels do not change (Figure 20 C). In summary, the data show that TKS5 is involved in AKT pathway regulation. On the other hand, no obvious difference was observed in the MAPK/ERK pathway upon investigation of p-ERK1/2 (Thr202/Tyr204) in Y235T or RT4 cells with TKS5 knockdown (Figure 21 A, B).

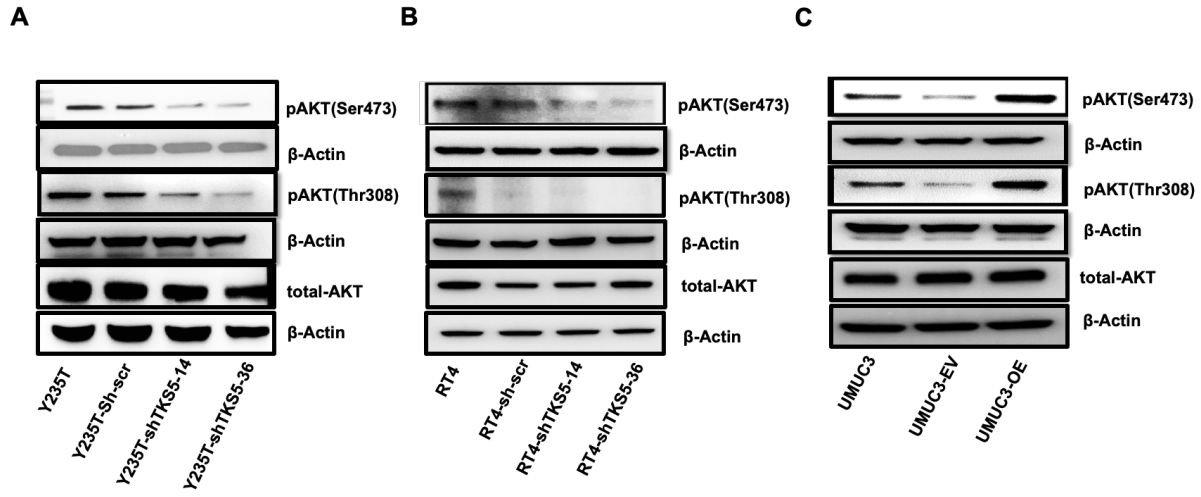

Figure 20. Expression of AKT in Y235T, RT4 and UMUC-3 cells. A) Expression of phosphor-AKT (Ser473), phosphor-AKT (Thr308), and total-AKT in Y235T cell lines at protein levels. The protein expression of phosphor-AKT is reduced in Y235T cells. **B)** Activation of AKT signaling is impaired in RT4 cells with TKS5 knockdown. Phospho-AKT (Ser473) is reduced in RT4-shTKS5 cells. **C)** Ectopic TKS5 expression induces AKT pathway activation. As determined by phosphor-AKT (Ser473), phosphor-AKT (Thr308) and total-AKT in UMUC-3 cell line at protein level. The molecular weight of total-AKT and phosphor-AKT is at around 60kDa. The target protein and the internal reference protein were used the same lysates and same membrane. All experiments were repeated for three times with different lysates.

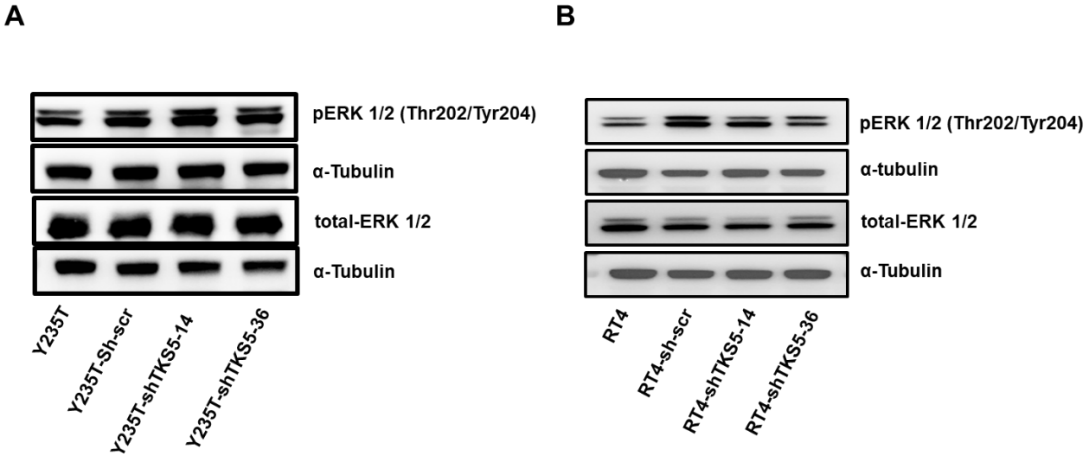

Figure 21. Expression of ERK protein in Y235T cells and RT4 cells. A) Expression of pERK1/2 (Thr202/Tyr204) and total ERK1/2 in Y235T cell lines at protein level. **B**）Protein expression of pERK1/2 (Thr202/Tyr204) and total ERK1/2 in RT4 cell lines. The result showed that there is no obvious difference in the expression of pERK1/2 (Thr202/Tyr204) between TKS5 knockdown cells and control cells. Total-ERK1/2 and pERK1/2 (Thr202/Tyr204) appears at around 42 and 44kDa. A-Tubulin was used as loading control appears at around 50kDa. The target protein and the internal reference protein were used the same lysates and same membrane.

4. Discussion

There are ample evidences that the adaptor protein TKS5 is involved in actin remodeling and cellular protease secretion and is an essential component of invadopodia or podosome. Recent studies have demonstrated TKS5's relevance for the prognosis of glial-derived brain tumors [110], lung adenocarcinomas [68], and prostate cancer [14]. Although previous studies demonstrated involvement of TKS5 in a variety of physiological and pathological processes, the role of TKS5 in urothelial tumors has not been addressed before. Also, the role of TKS5 in ploidy control and genome stability is not investigated in previous studies. The data provided in this thesis bring to light a role of TKS5 in genome stability control and provide experimental evidence for a potential role in BC. These data revealed that TKS5 downregulation induces aneuploidy in the ureter-derived immortal Y235T cell strain. Moreover, the results show that the knockdown of TKS5 inhibits the invasion and migration ability of RT4 cells. On the other hand, ectopic TKS5 expression increases migratory and invasive capacities of UMUC-3 cells. In summary, this study identifies a new, previously unknown role for TKS5 in bladder carcinogenesis and genome stability.

4.1 The expression of TKS5 in normal and tumor tissues or cells

It is known that the adapter protein TKS5 is involved in invadosome formation, ECM degradation and invasiveness of some cancer cells. The study by Stylli et al. demonstrated that TKS5 expression in brain tumor gliomas predicts reduced overall survival of patients [110]. TKS5 can be utilized as a marker protein for the staging of prostate cancer [56]. TKS5 expression was shown to be higher in many cancer cell lines, including cell lines from breast cancer and melanoma. Moreover, strong TKS5 staining was found by immunohistochemistry on paraffin embedded samples from breast cancer and melanoma [104]. These observations suggest that increased TKS5 expression is associated with tumor progression.

Interestingly, high-throughput sequencing (HTS) data from The Cancer Genome Atlas (TCGA), analyzed and provided by the UALCAN database showed that the mRNA expression level of TKS5 is higher in healthy urothelial tissues than in urothelial tumors, and that TKS5 expression decreases during BC progression to later stages of lymph node metastasis [24] (Suppl. Figure 1). These observations rather suggest that TKS5 plays an important role for normal tissue function and TKS5 downregulation is associated with tumor progression. The RT-qPCR and Western blotting results presented in this thesis are in line with the latter observations, showing that TKS5 is highly expressed in normal or untransformed bladder urothelial cells while its expression is downregulated in cells with low malignant potential, and is almost absent in invasive BC cells. Importantly, these results are in contrast to findings in other cancer types, including melanoma, breast cancer, and lung cancer. As indicated above, these previous studies showed that increased TKS5 expression correlates with tumor progression. Furthermore, it is important to note that the survival curve analysis from human protein atlas database based on TCGA HTS data indicates that urothelial cancer patients with high TKS5 expression have a poorer survival rate [115, 118-119] (suppl. Figure 2 A). This finding is consistent with that reported in other cancers, showing that uveal melanoma patients with high TKS5 expression have poorer outcome than patients with low TKS5 expression [24] (Suppl. Figure 2B). These contradictory observations cannot satisfactorily be explained at the moment. It was suggested by Burger et al. that TKS5 phosphorylation is crucial for the development of invadopodia in prostate cancer [14]. It is possible that phosphorylated TKS5 plays an important role in BC progression, rather than total amount of TKS5. In this study, phosphorylated TKS5 levels could not be determined, despite the use of several antibodies. This aspect remains to be elucidated in future studies. Another important aspect that remains to be investigated in future studies is the impact of mutant TKS5 proteins that were observed in human cancer samples. Based on the sequencing data from the TCGA database in cBioPortal, TKS5 mutations or alterations were found in

around 3% (Suppl. Figure 3 B) of samples from urinary tract cancer and in more than 13% of samples from uterine carcinosarcoma [23, 45] (Suppl. Figure 3 A). It remains to be experimentally proven, whether these are loss or gain of function mutations. Assuming that these are commonly loss of function mutations, these results would be in line with the lower expression level of TKS5 in bladder cancer samples.

Recent studies have shown that the gene expression and mutation landscape of the BBN model is similar to that of human MIBC [38]. BBN feeding was used to construct a mouse tumor model, and then the mouse bladder tissue of the constructed model was used for RT-qPCR detection. According to histology examination, bladder cancer models cannot be formed until four weeks after BBN treatment [74]. Tissue expression data from mice bladder tumor and human bladder tumor appear to be in agreement with the expression analysis results from cell lines, suggesting that primary and immortalized but untransformed epithelial cells (e.g. Y235T, HBLAK) express higher TKS5 levels compared to BC cell lines with higher tumorigenic potential (UROtsa) or invasive BC cell lines (T24, UMUC-3). Aside from this, it was found that RT4 cells, which are non-invasive, expressed a higher level of TKS5 than the most aggressive and migratory cancer cell lines T24 or UMUC-3. This apparent contradiction may indicate a new, yet unknown role of TKS5 in cancer.

4.2 The roles of TKS5 in cell viability/survival

The present results indicate that the abrogation of TKS5 inhibits viability/survival of non-tumorigenic Y235T cells, but not of the BC cell line RT4. Similarly, TKS5 overexpressing in UMUC-3 cells do not have an altered growth ability. Interestingly, growth ability of Y235T-shTKS5 cells is consistent with previously published cell proliferation of TKS5 siRNA-transfected BEAS-2B cell line, derived from normal bronchial epithelium obtained from autopsy of a non-cancerous

individual, showing that TKS5 downregulation inhibits proliferation [79]. In addition, TKS5 knockdown of melanoma cells B16F10 resulted in a decreased proliferation in 3-dimensional (3-D) collagen matrix, but not in 2-dimensional (2-D) cultures [56]. Blouw et al. also proved that breast cancer cells MDA-MB-231 with TKS5 abrogation have decreased growth, both in 3-D culture and *in vivo* [9]. In the present studies, all proliferation experiments were conducted under 2-D-culture conditions. It seems that TKS5 influences proliferation/survival of non-tumorigenic cells (Y235T or BEAS-2B) in 2-D and 3-D conditions, but of cancer cell lines only in 3-D culture conditions. It is important to note that TKS5, related to the formation of invadopodia and the degradation of ECM, will provide a more bionic microenvironment for the growth of cells in 3-D culture. Nevertheless, future studies are required in order to evaluate the effect of TKS5 on BC viability in 3-D culture and *in vivo*.

It is mentioned in the introduction that TKS5 plays a vital role in many normal physiological processes and embryonic development. It supports the research results that the knockdown of TKS5 in Y235T cells leads to reduced viability/survival. Moreover, in the study of *Tks5* KO mouse model, Cejudo-Martin et al. found that in the background of C57BL/6J mice, the neonatal mortality rate and the incidence of cleft palate rose to 90%, although the remaining 10% of mice did not have a cleft palate, but they die of unknown causes shortly after birth [22]. In addition, research data from the International Mouse Phenotyping Consortium (IMPC) in an online database mousephenotype showed that all mice with homozygous loss of *Tks5* showed pre-weaning lethality [34]. Although, data on the proliferation capacity of cells *in vivo* are not provided in these studies, the phenotype information indicate that TKS5 is essential for survival and development. The causal link between the cellular functions of TKS5, its role in genome instability and survival remains to be elucidated in future studies.

4.3 The roles of TKS5 in invasion, migration and invadosome formation

Y235T cells deficient in TKS5 show a significant reduction in the formation of invadosomes, thus indicating that TKS5 plays a critical role in the formation of invadosomes in immortalized urothelial cells. It has been demonstrated that TKS5 is a podosome marker and functions to regulate macrophage invasion [13]. Additionally, the scaffold protein Tks5 is localized to podosomes in SRC-transformed fibroblasts and in smooth muscle cells, and serves as a recruitment adapter for various components during podosome formation [29]. The TKS5 knockdown was also shown to decrease invadosome formation in both human and mouse melanoma cells by Iizuka et al. [56]. Previous studies show that TKS5 is involved in invadosome formation not only in cancer cells but also in many healthy cells. Based on the results, it can be concluded that TKS5 is essential for invadosome formation of urothelial cells. Unfortunately, staining of TKS5 with cortactin or F-actin by immunofluorescence could not get satisfactory result at the moment, to further confirm the localization of TKS5 to invodosomes in Y235T cells.

Previous researches have already shown TKS5 is important in cancer progression and metastasis by increasing cell invasion and migration, for instance, it has been suggested the importance of TKS adaptor proteins in melanoma metastasis *in vivo* and *in vitro* [56]. Burger et al. showed TKS5 promotes prostate cancer cells invasion via the formation of invadopodia [14]. It can be concluded that TKS5 promotes tumor progression in BC. Similar results were obtained in the research of this paper. Based on the results of the experiment, elevated TKS5 expression significantly promoted invasion/migration in UMUC-3 cells. Moreover, RT4 cells are generally considered as a non-invasive BC cell line. However, these cells exhibit low invasion capacity at long-term culture in the Boyden chamber experiment. But the TKS5 knockdown in RT4 cells lead to reduced migration/invasion ability in Boyden chamber and wound healing

assay. In fact, the cells were described to have some low invasion capacity [100]. However, more work is still needed in the future to explain that TKS5 is low expressed in invasive BC cells UMUC-3, but elevated expression can promote cell migration.

A study also demonstrated that elevated TKS5 expression in LNCaP cells was also associated with matrix degradation [14]. This is in agreement with the results found by gelatin degradation assays that TKS5 overexpression in BC cells UMUC-3 facilitates the degradation of matrix. It is essential for tumor cells to degrade and pass through the ECM during migration/invasion processes. The above results further confirmed the important role of TKS5 in the invasion and migration process.

It is already known that TKS5 plays a vital role in the formation of invadopodia in many tumors. In prostate cancer cell line LNCaP, it has been showed that elevated TKS5 expression promotes invadopodia formation [14]. In the thesis, it was shown that the absence of TKS5 in Y235T reduce invadosome formation ability. Yamamoto et al. examined the invasive bladder tumor cell lines YTS-1 and T24, and noninvasive bladder tumor cell line RT4 for invadopodia formation with phalloidin to visualize F-actin cores of invadopodia and revealed that there were a lot of F-actin puncta observed in YTS-1 and T24 cells but no F-actin puncta was observed in most RT4 cells [129]. It was also observed that strong invadopodia formation in T24 and UMUC-3 cells in my experiments. Moreover, elevated TKS5 expression in UMUC-3 cells did not increase the formation of invadopodia during my experiments. There is a possibility that TKS5 contributes to the degradation of excess extracellular matrix, but not to the formation of invadopodia. One of the possible explanations is that UMUC-3 cells already have a very strong ability to form invadopodia and the overexpression of TKS5 will not have a more obvious promotion effect. This phenomenon is still not fully understood. However, results of RT-qPCR showed TKS5 is generally poorly

expressed in BC cells especially invasive cells T24 and UMUC-3. There may be another gene that is responsible for invadopodia formation instead of TKS5, or that TKS5 is not the main gene for invadopodia formation in some BC cells. Yamamoto et al. previously showed that FBP17 act as a critical role in the process of bladder tumor cell invasion by mediating invadopodia formation, the EFC domain of FBP17 was shown to bind strongly to the PI (4,5) P2 of cell membrane [106, 117]. Same as the PX domain of TKS5, it binds to PI (4,5) P2 of the membrane which is essential for the formation of invadopodia. That means FBP17 may has the overlapping mechanism of invadopodia formation with TKS5 and their differences and connections are not very clear.

As described in introduction, Invadopodia is a sign that tumor cells undergo systemic spread and metastasis. However, there are various mechanisms involved in tumor invasion and metastasis via invadopodia. The actin regulators cortactin is one of the key components of invadosomes. A study demonstrated that extravasation of bladder cancer cells into the lungs is reduced when cortactin is knockdown, such findings suggest that formation of invadopodia is key to extravasation [116]. Imanishi and colleagues showed that cortactin knockdown reduced invadopodia formation and reduced cancer cell invasion significantly, which indicates the importance of invadopodia in trans-urothelial invasion [57]. This study is consistent with the results of the thesis. In the thesis, it was shown that the absence of TKS5 in RT4 cells results in reduced cortactin level.

As mentioned above, TKS5 is expressed not only in cancer cells or tissues, but it is also required for physiological functions in some cells. This has been observed in cells of the macrophage/monocyte lineage. For example, podosomes formed in osteoclasts as they differentiate [32], and formed in dendritic cells as they initiate migration in response to a stimulus [15]. Y235T cell line is a new type of immortalized urothelial cell line with high TKS5 expression and strong formation ability of podosomes. Furthermore, my experiments also showed

Y235T cells exhibited robust migratory/invasion ability. This is probably a consequence of that migratory behaviors of cells play a vital role in homeostasis and is employed by many different types of cells throughout the life cycle of organisms, including embryonic development, immune surveillance and response, and wound healing [46, 98]. On the whole, the results imply that TKS5 promotes BC progression but it is not essential for BC progression, there may be alternative genes with overlapping functions with TKS5 in invasive BC cells. On the other hand, TKS5 also play important role in normal urothelial cells with strong formation of invadosomes.

4.4 TKS5 knockdown causes chromosome instability

Unpublished data from previous experiments of our lab have revealed that TKS5 knockdown results in aneuploidy in human skin fibroblasts cells. In this study, evidence is provided for the first time that TKS5 knockdown leads to aneuploidy in human the ureter derived, telomerase-immortalized epithelial cell strain with a normal karyotype (46 chromosomes). TKS5 knockdown causes a substantially greater variation in chromosome number and a decrease in TKS5 expression increases the number of micronuclei, a consequence of defects in chromosome segregation. Importantly, TKS5 knockdown in Y235T cells also causes abnormal chromosome segregation defects and formation of multiple centrosomes. Importantly, experimental evidence shown here indicates a co-localization of TKS5 with γ-tubulin in Y235T cells. As γ-tubulin is the localized at the centrosomes and is the priming site for spindle formation, aneuploidy induction in response to TKS5 downregulation is likely due to be the consequence of deregulated microtubule function. In fact, the interaction of TKS5 with tubulin via its third SH3 domain has been reported previously, although a link to microtubule function in the context of ploidy-control was not mentioned [84]. As a component of microtubules, tubulin plays a number of roles that are essential for the regulation of cellular processes, including cell division, differentiation, intracellular

transport, and motility [93]. It is also conceivable that the impact of TKS5 on cell migration and invasion is connected to this interaction with microtubule components. This aspect could not directly be addressed in this study and remains to be studied in future experiments. In summary, data presented in this study provide convincing evidence for the first time that TKS5 plays a crucial role in chromosome segregation and potentially in genome stability.

4.5 Possible signal pathways and gene regulation that TKS5 involved

Activated AKT regulates a variety of substrates, which are involved in the functions of cell survival, cell cycle progression and cell growth. Components of the phosphoinositide 3-kinase (PI3K)/AKT pathway are frequently altered in human cancers [42]. A number of genes regulate cell proliferation, invasion, and migration via the PI3K/AKT pathway, for instance, adipose differentiation-related protein (ADFP) stimulated cell proliferation and increased the pAKT/AKT ratio in A549 and NCI-H1299 cells *in vitro* [75]. Insulin receptor substrate 4 (IRS-4) enhanced the proliferation and migration of the hepatoblastoma cells via PI3K/AKT pathways [124]. Moodley et al. observed that down-regulation of XB130 and/or Tks5 inhibited SRC activation and downstream PI3K and AKT phosphorylation [79]. They also showed that Tks5, similar to XB130, plays a vital role in cell proliferation and cell survival [79]. According to studies from Wang and his colleagues, activated AKT plays an important role in enabling arsenic-transformed human bronchial epithelial cell (HBEC) migration and invasion by upregulating zinc finger E-box binding homeobox 1 (ZEB1) and zinc finger E-box binding homeobox 2 (ZEB2) expression [121]. The changes in the AKT activation in response to TKS5 levels shown in this study could thus influence proliferation of urothelial cells and invasion and migration of BC cell lines.

The results showed that pAKT protein levels were reduced in Y235T-shTKS5 cells. Furthermore, pAKT staining appears to be co-localized with microtubules

in immunofluorescence in my experiments. Maybe TKS5 affects cell mitosis by regulating AKT, leading to chromosomal instability. It has been shown that the reduction of AKT activity in drosophila embryos appears to effect centrosome separation and spindle orientation [19]. In previous studies, AKT was shown to play a role in the mitotic process of epithelial cells [107]. In mouse oocytes, AKT activity is required for correct chromosome alignment and spindle organization, and in drosophila embryonic cells with low levels of AKT, spindles divide almost perpendicular to the epithelial structure [19, 55]. It has been shown that active AKT is located around the mitotic spindle and centrosome in some cells' prophase and metaphase, as well as at the telophase, at the central position of the centrosome [20]. To some extent, these results are consistent with the results of this thesis, but further research is required to determine the precise mechanism of TKS5 involved in regulating cell division.

Cortactin is SRC substrate that plays crucial roles in cell migration and invasion by regulating branched actin assembly through multiple diverse mechanism [62]. Moreover, cortactin is also an important component of invadopodia/podosomes [62]. Clark et al. showed that three different head and neck squamous cell carcinoma cell lines with cortactin knockdown developed significantly smaller tumors *in vivo* when compared to control tumors [27]. Crimaldi et al. demonstrated that TKS5 plays a central role in the recruitment of cortactin to drive podosome formation [29]. In order to clarify whether TKS5 is involved in regulating cortactin in BC and normal urothelium, the expression of cortactin was analysed in TKS5 knockdown and overexpression cell lines. The cortactin protein expression in TKS5 knockdown Y235T and RT4 cells was decreased obviously. This might be explained by the involvement of TKS5 in BC cell invasion and migration via cortactin regulation. However, TKS5 overexpression in UMUC-3 cells has no impact on cortactin expression. It is possible that UMUC-3 cells are already an invasive BC with strong formation of invadopodia. Moreover, it has been shown that deletion or knockdown of Akt1 in mouse embryonic fibroblasts

(MEF) significantly reduces Src-induced formation of podosomes and rosettes, and ECM digestion [37]. Cortactin may also be involved in regulating the formation of invadosomes by the regulation of the AKT pathway.

5. Summary

The present study reveals that TKS5 plays an important role in proliferation and genome stability of urothelial cells, and that it is involved in migration/invasion processes of bladder cancer (BC) cell lines. The results show that *TKS5* mRNA and protein expression levels are higher in non-cancer cells compared to those in cancer cells. Importantly, lower TKS5 levels are observed in invasive BC cell lines. These results are in line with The Cancer Genome Atlas (TCGA) sequencing data showing lower *TKS5* mRNA levels in tumors compared to normal tissue samples. On the other hand, the gene expression results stand in some contrast to the well-described role of TKS5 in invadopodia formation and the results of functional studies presented here showing that TKS5 promotes invadopodia formation and higher TKS5 levels are associated with increased cell migration and invasion. TKS5 knockdown in RT4 cells impairs their invasion and migration ability, while TKS5 overexpression in invasive BC cells UMUC-3 increases their invasion and migration ability. These results are in concordance with the observation demonstrating that TKS5 knockdown results in lower cortactin levels, a component of invadopodia. Furthermore, the results suggest that TKS5 may regulate invasion and migration of BC cells via AKT pathway. Serine-phosphorylated AKT (pSer478-AKT) is decreased in Y235T-shTKS5 and RT4-shTKS5 cells and phosphorylated serine and threonine AKT (pSer478/pThr308-AKT) are increased in UMUC-3 cells with TKS5 overexpression.

Importantly, the presented results show for the first time that TKS5 may play a crucial role in the control of cell division of urothelial cell. Decreased TKS5 expression results in abnormal cell division and chromosome instability in Y235T cells, which was confirmed by the observation and analysis of abnormal chromosome segregation and multiple centrosome during mitosis, as well as metaphase counting and increased micronucleus.

It remains to be shown in future studies how TKS5 is involved in the regulation of cell division. It was demonstrated that AKT is located at spindle microtubuli thus changes in AKT pathway activation through TKS5 may impair accurate chromosome segregation. Potentially, modulation of the AKT signaling pathway may be involved here as well.

6. Bibliography

1. Ádám C, Fekete A, Bőgel G, Németh Z, Tőkési N, Ovádi J, Liliom K, Pesti S, Geiszt M, Buday L. Accumulation of the PX domain mutant Frank-ter Haar syndrome protein Tks4 in aggresomes. Cell Commun Signal 13:33 (2015)
2. Abram CL, Seals DF, Pass I, Salinsky D, Maurer L, Roth TM, Courtneidge SA. The adaptor protein fish associates with members of the ADAMs family and localizes to podosomes of Src-transformed cells. J Biol Chem 278:16844-16851 (2003)
3. Anderhub SJ, Krämer A, Maier B. Centrosome amplification in tumorigenesis. Cancer Lett 322:8-17 (2012)
4. Aquila L, Ohm J, Woloszynska-Read A. The role of STAG2 in bladder cancer. Pharmacol Res 131:143-149 (2018)
5. Artym VV, Zhang Y, Seillier-Moiseiwitsch F, Yamada KM, Mueller SC. Dynamic interactions of cortactin and membrane type 1 matrix metalloproteinase at invadopodia: defining the stages of invadopodia formation and function. Cancer Res 66:3034-3043 (2006)
6. Bastians H. Causes of Chromosomal Instability. Recent Results Cancer Res 200: 95-113 (2015)
7. Bernstein HG, Keilhoff G, Dobrowolny H, Lendeckel U, Steiner J. From putative brain tumor marker to high cognitive abilities: Emerging roles of a disintegrin and metalloprotease (ADAM) 12 in the brain. J Chem Neuroanat 109:101846 (2020)
8. Bisson N, James DA, Ivosev G, Tate SA, Bonner R, Taylor L, Pawson T. Selected reaction monitoring mass spectrometry reveals the dynamics of signaling through the GRB2 adaptor. Nat Biotechnol 29:653-688 (2011)
9. Blouw B, Patel M, Iizuka S, Abdullah C, You WK, Huang X, Li JL, Diaz B, Stallcup WB, Courtneidge SA. The invadopodia scaffold protein Tks5 is required for the growth of human breast cancer cells in vitro and in vivo. PLoS One 10:e0121003 (2015)

10. Bögel G, Gujdár A, Geiszt M, Lányi Á, Fekete A, Sipeki S, Downward J, Buday L. Frank-ter Haar syndrome protein Tks4 regulates epidermal growth factor-dependent cell migration. J Biol Chem 287:31321-31329 (2012)
11. Boveri T. Concerning the origin of malignant tumours by Theodor Boveri. Translated and annotated by Henry Harris. J Cell Sci 121 Suppl 1:1-84 (2008)
12. Bromann PA, Korkaya H, Courtneidge SA. The interplay between Src family kinases and receptor tyrosine kinases. Oncogene 23:7957-7968 (2004)
13. Burger KL, Davis AL, Isom S, Mishra N, Seals DF. The podosome marker protein Tks5 regulates macrophage invasive behavior. Cytoskeleton (Hoboken) 68:694-711 (2011)
14. Burger KL, Learman BS, Boucherle AK, Sirintrapun SJ, Isom S, Díaz B, Courtneidge SA, Seals DF. Src-dependent Tks5 phosphorylation regulates invadopodia-associated invasion in prostate cancer cells. Prostate 74:134-148 (2014)
15. Burns S, Hardy SJ, Buddle J, Yong KL, Jones GE, Thrasher AJ. Maturation of DC is associated with changes in motile characteristics and adherence. Cell Motil Cytoskeleton 57:118-132 (2004)
16. Burns S, Thrasher AJ, Blundell MP, Machesky L, Jones GE. Configuration of human dendritic cell cytoskeleton by Rho GTPases, the WAS protein, and differentiation. Blood 98:1142-1149 (2001)
17. Burrell RA, McClelland SE, Endesfelder D, Groth P, Weller MC, Shaikh N, Domingo E, Kanu N, Dewhurst SM, Gronroos E, Chew SK, Rowan AJ, Schenk A, Sheffer M, Howell M, Kschischo M, Behrens A, Helleday T, Bartek J, Tomlinson IP, Swanton C. Replication stress links structural and numerical cancer chromosomal instability. Nature 494:492-496 (2013)
18. Buschman MD, Bromann PA, Cejudo-Martin P, Wen F, Pass I, Courtneidge SA. The novel adaptor protein Tks4 (SH3PXD2B) is required for functional podosome formation. Mol Biol Cell 20:1302-1311 (2009)

19. Buttrick GJ, Beaumont LM, Leitch J, Yau C, Hughes JR, Wakefield JG. Akt regulates centrosome migration and spindle orientation in the early Drosophila melanogaster embryo. J Cell Biol 180:537-548 (2008)
20. Buttrick GJ, Wakefield JG. PI3-K and GSK-3: Akt-ing together with microtubules. Cell Cycle 7:2621-2625 (2008)
21. Cao Y. Opinion: emerging mechanisms of tumour lymphangiogenesis and lymphatic metastasis. Nat Rev Cancer 5:735-743 (2005)
22. Cejudo-Martin P, Yuen A, Vlahovich N, Lock P, Courtneidge SA, Díaz B. Genetic disruption of the sh3pxd2a gene reveals an essential role in mouse development and the existence of a novel isoform of tks5. PLoS One 9:e107674 (2014)
23. Cerami E, Gao J, Dogrusoz U, Gross BE, Sumer SO, Aksoy BA, Jacobsen A, Byrne CJ, Heuer ML, Larsson E, Antipin Y, Reva B, Goldberg AP, Sander C, Schultz N. The cBio cancer genomics portal: an open platform for exploring multidimensional cancer genomics data. Cancer Discov 2:401-404 (2012)
24. Chandrashekar DS, Bashel B, Balasubramanya SAH, Creighton CJ, Ponce-Rodriguez I, Chakravarthi BVSK, Varambally S. UALCAN: A Portal for Facilitating Tumor Subgroup Gene Expression and Survival Analyses. Neoplasia19:649-658 (2017)
25. Cimini D. Merotelic kinetochore orientation, aneuploidy, and cancer. Biochim Biophys Acta 1786:32-40 (2008)
26. Cines DB, Pollak ES, Buck CA, Loscalzo J, Zimmerman GA, McEver RP, Pober JS, Wick TM, Konkle BA, Schwartz BS, Barnathan ES, McCrae KR, Hug BA, Schmidt AM, Stern DM. Endothelial cells in physiology and in the pathophysiology of vascular disorders. Blood 91:3527-3561 (1998)
27. Clark ES, Brown B, Whigham AS, Kochaishvili A, Yarbrough WG, Weaver AM. Aggressiveness of HNSCC tumors depends on expression levels of cortactin, a gene in the 11q13 amplicon. Oncogene 28:431-444 (2009)
28. Courtneidge SA. Cell migration and invasion in human disease: the Tks adaptor proteins. Biochem Soc Trans 40:129-132 (2012)

29. Crimaldi L, Courtneidge SA, Gimona M. Tks5 recruits AFAP-110, p190RhoGAP, and cortactin for podosome formation. Exp Cell Res 315:2581-2592 (2009)
30. David-Pfeuty T, Singer SJ. Altered distributions of the cytoskeletal proteins vinculin and alpha-actinin in cultured fibroblasts transformed by Rous sarcoma virus. Proc Natl Acad Sci U S A 77:6687-6691(1980)
31. Destaing O, Block MR, Planus E, Albiges-Rizo C. Invadosome regulation by adhesion signaling. Curr Opin Cell Biol 23:597-606 (2011)
32. Destaing O, Saltel F, Géminard JC, Jurdic P, Bard F. Podosomes display actin turnover and dynamic self-organization in osteoclasts expressing actin-green fluorescent protein. Mol Biol Cell 14:407-416 (2003)
33. Di Martino J, Henriet E, Ezzoukhry Z, Goetz JG, Moreau V, Saltel F. The microenvironment controls invadosome plasticity. J Cell Sci 129:1759-1768 (2016)
34. Dickinson ME, Flenniken AM, Ji X, Teboul L, Wong MD, White JK, Meehan TF, Weninger WJ, Westerberg H, Adissu H, Baker CN, Bower L, Brown JM, Caddle LB, Chiani F, Clary D, Cleak J, Daly MJ, Denegre JM, Doe B, Dolan ME, Edie SM, Fuchs H, Gailus-Durner V, Galli A, Gambadoro A, Gallegos J, Guo S, Horner NR, Hsu CW, Johnson SJ, Kalaga S, Keith LC, Lanoue L, Lawson TN, Lek M, Mark M, Marschall S, Mason J, McElwee ML, Newbigging S, Nutter LM, Peterson KA, Ramirez-Solis R, Rowland DJ, Ryder E, Samocha KE, Seavitt JR, Selloum M, Szoke-Kovacs Z, Tamura M, Trainor AG, Tudose I, Wakana S, Warren J, Wendling O, West DB, Wong L, Yoshiki A; International Mouse Phenotyping Consortium; Jackson Laboratory; Infrastructure Nationale PHENOMIN, Institut Clinique de la Souris (ICS); Charles River Laboratories; MRC Harwell; Toronto Centre for Phenogenomics; Wellcome Trust Sanger Institute; RIKEN BioResource Center, MacArthur DG, Tocchini-Valentini GP, Gao X, Flicek P, Bradley A, Skarnes WC, Justice MJ, Parkinson HE, Moore M, Wells S, Braun RE, Svenson KL, de Angelis MH, Herault Y, Mohun T, Mallon AM, Henkelman RM, Brown SD, Adams DJ, Lloyd

KC, McKerlie C, Beaudet AL, Bućan M, Murray SA. High-throughput discovery of novel developmental phenotypes. Nature 537:508-514 (2016)

35. Eddy RJ, Weidmann MD, Sharma VP, Condeelis JS. Tumor Cell Invadopodia: Invasive Protrusions that Orchestrate Metastasis. Trends Cell Biol 27:595-607 (2017)
36. Ertych N, Stolz A, Stenzinger A, Weichert W, Kaulfuß S, Burfeind P, Aigner A, Wordeman L, Bastians H. Increased microtubule assembly rates influence chromosomal instability in colorectal cancer cells. Nat Cell Biol 16:779-791 (2014)
37. Eves R, Oldham R, Jia L, Mak AS. The roles of akt isoforms in the regulation of podosome formation in fibroblasts and extracellular matrix invasion. Cancers (Basel) 7:96-111 (2015)
38. Fantini D, Glaser AP, Rimar KJ, Wang Y, Schipma M, Varghese N, Rademaker A, Behdad A, Yellapa A, Yu Y, Sze CC, Wang L, Zhao Z, Crawford SE, Hu D, Licht JD, Collings CK, Bartom E, Theodorescu D, Shilatifard A, Meeks JJ. A Carcinogen-induced mouse model recapitulates the molecular alterations of human muscle invasive bladder cancer. Oncogene 37:1911-1925 (2018)
39. Fekete A, Bőgel G, Pesti S, Péterfi Z, Geiszt M, Buday L. EGF regulates tyrosine phosphorylation and membrane-translocation of the scaffold protein Tks5. J Mol Signal 7;8:8 (2013)
40. Florl AR, Schulz WA. Chromosomal instability in bladder cancer. Arch Toxicol 82:173-182 (2008)
41. Foxall E, Pipili A, Jones GE, Wells CM. Significance of kinase activity in the dynamic invadosome. Eur J Cell Biol 95:483-492 (2016)
42. Fresno Vara JA, Casado E, de Castro J, Cejas P, Belda-Iniesta C, González-Barón M. PI3K/Akt signalling pathway and cancer. Cancer Treat Rev 30:193-204 (2004)
43. Gaidano G, Bergui L, Schena M, Gaboli M, Cremona O, Marchisio PC, Caligaris-Cappio F. Integrin distribution and cytoskeleton organization in normal and malignant monocytes. Leukemia 4:682-687 (1990)

44. Ganem NJ, Godinho SA, Pellman D. A mechanism linking extra centrosomes to chromosomal instability. Nature 460:278-282 (2009)
45. Gao J, Aksoy BA, Dogrusoz U, Dresdner G, Gross B, Sumer SO, Sun Y, Jacobsen A, Sinha R, Larsson E, Cerami E, Sander C, Schultz N. Integrative analysis of complex cancer genomics and clinical profiles using the cBioPortal. Sci Signal 6:pl1 (2013)
46. Gardel ML, Schneider IC, Aratyn-Schaus Y, Waterman CM. Mechanical integration of actin and adhesion dynamics in cell migration. Annu Rev Cell Dev Biol 26:315-333 (2010)
47. Gawden-Bone C, Zhou Z, King E, Prescott A, Watts C, Lucocq J. Dendritic cell podosomes are protrusive and invade the extracellular matrix using metalloproteinase MMP-14. J Cell Sci 123:1427-1437 (2010)
48. Gianni D, Diaz B, Taulet N, Fowler B, Courtneidge SA, Bokoch GM. Novel p47(phox)-related organizers regulate localized NADPH oxidase 1 (Nox1) activity. Sci Signal 2:ra54 (2009)
49. Guardavaccaro D, Frescas D, Dorrello NV, Peschiaroli A, Multani AS, Cardozo T, Lasorella A, Iavarone A, Chang S, Hernando E, Pagano M. Control of chromosome stability by the beta-TrCP-REST-Mad2 axis. Nature 452:365-369 (2008)
50. Hai CM, Hahne P, Harrington EO, Gimona M. Conventional protein kinase C mediates phorbol-dibutyrate-induced cytoskeletal remodeling in a7r5 smooth muscle cells. Exp Cell Res 280:64-74 (2002)
51. Hansemann, D. Ueber pathologische Mitosen. Virchows Archiv : an international journal of pathology 123, 356–370 (1891)
52. Hautmann RE, de Petriconi RC, Pfeiffer C, Volkmer BG. Radical cystectomy for urothelial carcinoma of the bladder without neoadjuvant or adjuvant therapy: long-term results in 1100 patients. Eur Urol 61:1039-1047 (2012)

53. Hinsch A, Chaker A, Burdelski C, Koop C, Tsourlakis MC, Steurer S, Rink M, Eichenauer TS, Wilczak W, Wittmer C, Fisch M, Simon R, Sauter G, Büschek F, Clauditz T, Minner S, Jacobsen F. βIII-tubulin overexpression is linked to aggressive tumor features and genetic instability in urinary bladder cancer. Hum Pathol 61:210-220 (2017)
54. Hoffmann MJ, Koutsogiannouli E, Skowron MA, Pinkerneil M, Niegisch G, Brandt A, Stepanow S, Rieder H, Schulz WA. The New Immortalized Uroepithelial Cell Line HBLAK Contains Defined Genetic Aberrations Typical of Early Stage Urothelial Tumors. Bladder Cancer 2:449-463 (2016)
55. Hoshino Y, Sato E. Protein kinase B (PKB/Akt) is required for the completion of meiosis in mouse oocytes. Dev Biol 314:215-223 (2008)
56. Iizuka S, Abdullah C, Buschman MD, Diaz B, Courtneidge SA. The role of Tks adaptor proteins in invadopodia formation, growth and metastasis of melanoma. Oncotarget 7:78473-78486 (2016)
57. Imanishi K, Yoneyama MS, Hatakeyama S, Yamamoto H, Koie T, Saitoh H, Yamaya K, Funyu T, Nakamura T, Ohyama C, Tsuboi S. Invadopodia are essential in transurothelial invasion during the muscle invasion of bladder cancer cells. Mol Med Rep 9:2159-2165 (2014)
58. Jemal A, Siegel R, Ward E, Hao Y, Xu J, Thun MJ. Cancer statistics, 2009. CA Cancer J Clin 59:225-249 (2009)
59. Kanehisa J, Yamanaka T, Doi S, Turksen K, Heersche JN, Aubin JE, Takeuchi H. A band of F-actin containing podosomes is involved in bone resorption by osteoclasts. Bone 11:287-293 (1990)
60. Karaman S, Detmar M. Mechanisms of lymphatic metastasis. J Clin Invest 124:922-928 (2014)
61. Kelley LC, Ammer AG, Hayes KE, Martin KH, Machida K, Jia L, Mayer BJ, Weed SA. Oncogenic Src requires a wild-type counterpart to regulate invadopodia maturation. J Cell Sci 123:3923-3932 (2010)
62. Kirkbride KC, Sung BH, Sinha S, Weaver AM. Cortactin: a multifunctional regulator of cellular invasiveness. Cell Adh Migr 5:187-198 (2011)

63. Knowles MA, Hurst CD. Molecular biology of bladder cancer: new insights into pathogenesis and clinical diversity. Nat Rev Cancer 15:25-41 (2015)
64. Kudlik G, Takács T, Radnai L, Kurilla A, Szeder B, Koprivanacz K, Merő BL, Buday L, Vas V. Advances in Understanding TKS4 and TKS5: Molecular Scaffolds Regulating Cellular Processes from Podosome and Invadopodium Formation to Differentiation and Tissue Homeostasis. Int J Mol Sci 21:8117 (2020)
65. Kurochkina N, Guha U. SH3 domains: modules of protein-protein interactions. Biophys Rev 5:29-39 (2013)
66. Lányi Á, Baráth M, Péterfi Z, Bogel G, Orient A, Simon T, Petrovszki E, Kis-Tóth K, Sirokmány G, Rajnavölgyi É, Terhorst C, Buday L, Geiszt M. The homolog of the five SH3-domain protein (HOFI/SH3PXD2B) regulates lamellipodia formation and cell spreading. PLoS One 6:e23653 (2011)
67. Lara-Gonzalez P, Westhorpe FG, Taylor SS. The spindle assembly checkpoint. Curr Biol 20;22: R966-980 (2012)
68. Li CM, Chen G, Dayton TL, Kim-Kiselak C, Hoersch S, Whittaker CA, Bronson RT, Beer DG, Winslow MM, Jacks T. Differential Tks5 isoform expression contributes to metastatic invasion of lung adenocarcinoma. Genes Dev 27:1557-1567 (2013)
69. Linder S, Wiesner C, Himmel M. Degrading devices: invadosomes in proteolytic cell invasion. Annu Rev Cell Dev Biol 27:185-211(2011)
70. Lock P, Abram CL, Gibson T, Courtneidge SA. A new method for isolating tyrosine kinase substrates used to identify fish, an SH3 and PX domain-containing protein, and Src substrate. EMBO J 17:4346-4357 (1998)
71. Malinin NL, Wright S, Seubert P, Schenk D, Griswold-Prenner I. Amyloid-beta neurotoxicity is mediated by FISH adapter protein and ADAM12 metalloprotease activity. Proc Natl Acad Sci U S A 102:3058-3063 (2005)

72. Marchisio PC, Cirillo D, Teti A, Zambonin-Zallone A, Tarone G. Rous sarcoma virus-transformed fibroblasts and cells of monocytic origin display a peculiar dot-like organization of cytoskeletal proteins involved in microfilament-membrane interactions. Exp Cell Res 169:202-214 (1987)
73. Martinez Rodriguez RH, Buisan Rueda O, Ibarz L. Bladder cancer: Present and future. Med Clin (Barc) 149:449-455 (2017)
74. Meessen, Sabine; Rother, Jan; Zheng, Xi; Eckstein, Markus; Kriegmair, Maximilian C.; Hernandez, David; Grychtol, Bartłomiej; Deliolanis, Nikolaos C.; Bolenz, Christian; Günes, Cagatay. Establishment of Real-Time Multispectral Imaging for the Detection of bladder cancer Using a Preclinical in Vivo Model 2020: 285-294 (2020)
75. Meng X, Sun R, Wang W, Zhang N, Cao S, Liu B, Fang P, Deng S, Yang S. ADFP promotes cell proliferation in lung adenocarcinoma via Akt phosphorylation. J Cell Mol Med 25:827-839 (2021)
76. Meraldi P, Nigg EA. The centrosome cycle. FEBS Lett 521:9-13 (2002)
77. Michel LS, Liberal V, Chatterjee A, Kirchwegger R, Pasche B, Gerald W, Dobles M, Sorger PK, Murty VV, Benezra R. MAD2 haplo-insufficiency causes premature anaphase and chromosome instability in mammalian cells. Nature 409:355-359 (2001)
78. Miyauchi A, Hruska KA, Greenfield EM, Duncan R, Alvarez J, Barattolo R, Colucci S, Zambonin-Zallone A, Teitelbaum SL, Teti A. Osteoclast cytosolic calcium, regulated by voltage-gated calcium channels and extracellular calcium, controls podosome assembly and bone resorption. J Cell Biol 111:2543-2552 (1990)
79. Moodley S, Hui Bai X, Kapus A, Yang B, Liu M. XB130/Tks5 scaffold protein interaction regulates Src-mediated cell proliferation and survival. Mol Biol Cell 26:4492-4502 (2015)
80. Moreau V, Tatin F, Varon C, Génot E. Actin can reorganize into podosomes in aortic endothelial cells, a process controlled by Cdc42 and RhoA. Mol Cell Biol 23:6809-6822 (2003)

81. Murphy DA, Courtneidge SA. The 'ins' and 'outs' of podosomes and invadopodia: characteristics, formation and function. Nat Rev Mol Cell Biol 12:413-426 (2011)
82. Murphy DA, Diaz B, Bromann PA, Tsai JH, Kawakami Y, Maurer J, Stewart RA, Izpisúa-Belmonte JC, Courtneidge SA. A Src-Tks5 pathway is required for neural crest cell migration during embryonic development. PLoS One 6:e22499 (2011)
83. Musacchio A. Spindle assembly checkpoint: the third decade. Philos Trans R Soc Lond B Biol Sci 366:3595-3604 (2011)
84. Oikawa T, Itoh T, Takenawa T. Sequential signals toward podosome formation in NIH-src cells. J Cell Biol 182:157-169 (2008)
85. Oikawa T, Oyama M, Kozuka-Hata H, Uehara S, Udagawa N, Saya H, Matsuo K. Tks5-dependent formation of circumferential podosomes/invadopodia mediates cell-cell fusion. J Cell Biol 197:553-568 (2012)
86. Oser M, Yamaguchi H, Mader CC, Bravo-Cordero JJ, Arias M, Chen X, Desmarais V, van Rheenen J, Koleske AJ, Condeelis J. Cortactin regulates cofilin and N-WASp activities to control the stages of invadopodium assembly and maturation. J Cell Biol 186:571-587 (2009)
87. P. etzoldt JL, Leigh IM, Duffy PG, Sexton C, Masters JR. Immortalisation of human urothelial cells. Urol Res 23:377-380 (1995)
88. Patel A, Dash PR. Formation of atypical podosomes in extravillous trophoblasts regulates extracellular matrix degradation. Eur J Cell Biol 91:171-179 (2012)
89. Paterson EK, Courtneidge SA. Invadosomes are coming: new insights into function and disease relevance. FEBS J 285:8-27 (2018)
90. Peters JM, Tedeschi A, Schmitz J. The cohesin complex and its roles in chromosome biology. Genes Dev 22:3089-3114 (2008)
91. Pino MS, Chung DC. The chromosomal instability pathway in colon cancer. Gastroenterology 138:2059-2072 (2010)

92. Podgrabinska S, Skobe M. Role of lymphatic vasculature in regional and distant metastases. Microvasc Res 95:46-52 (2014)
93. Prassanawar SS, Panda D. Tubulin heterogeneity regulates functions and dynamics of microtubules and plays a role in the development of drug resistance in cancer. Biochem J 476:1359-1376 (2019)
94. Prout GR Jr, Barton BA, Griffin PP, Friedell GH. Treated history of noninvasive grade 1 transitional cell carcinoma. The National Bladder Cancer Group. J Urol 148:1413-1419 (1992)
95. Remeseiro S, Cuadrado A, Losada A. Cohesin in development and disease. Development 140:3715-3718 (2013)
96. Revach OY, Geiger B. The interplay between the proteolytic, invasive, and adhesive domains of invadopodia and their roles in cancer invasion. Cell Adh Migr 8:215-225 (2014)
97. Revach OY, Sandler O, Samuels Y, Geiger B. Cross-Talk between Receptor Tyrosine Kinases AXL and ERBB3 Regulates Invadopodia Formation in Melanoma Cells. Cancer Res 79:2634-2648 (2019)
98. Ridley AJ, Schwartz MA, Burridge K, Firtel RA, Ginsberg MH, Borisy G, Parsons JT, Horwitz AR. Cell migration: integrating signals from front to back. Science 302:1704-1709 (2003)
99. Rieder CL, Cole RW, Khodjakov A, Sluder G. The checkpoint delaying anaphase in response to chromosome monoorientation is mediated by an inhibitory signal produced by unattached kinetochores. J Cell Biol 130:941-948 (1995)
100. Rigby CC, Franks LM. A human tissue culture cell line from a transitional cell tumour of the urinary bladder: growth, chromosone pattern and ultrastructure. Br J Cancer 24(4):746-754 (1970)
101. Saltel F, Daubon T, Juin A, Ganuza IE, Veillat V, Génot E. Invadosomes: intriguing structures with promise. Eur J Cell Biol 90:100-107 (2011)
102. Sanes JR, Yamagata M. Formation of lamina-specific synaptic connections. Curr Opin Neurobiol 9:79-87 (1999)

103. Schoumacher M, Goldman RD, Louvard D, Vignjevic DM. Actin, microtubules, and vimentin intermediate filaments cooperate for elongation of invadopodia. J Cell Biol 189:541-556 (2010)
104. Seals DF, Azucena EF Jr, Pass I, Tesfay L, Gordon R, Woodrow M, Resau JH, Courtneidge SA. The adaptor protein Tks5/Fish is required for podosome formation and function, and for the protease-driven invasion of cancer cells. Cancer Cell 7:155-165 (2005)
105. Sharma VP, Eddy R, Entenberg D, Kai M, Gertler FB, Condeelis J. Tks5 and SHIP2 regulate invadopodium maturation, but not initiation, in breast carcinoma cells. Curr Biol 23:2079-2089 (2013)
106. Shimada A, Niwa H, Tsujita K, Suetsugu S, Nitta K, Hanawa-Suetsugu K, Akasaka R, Nishino Y, Toyama M, Chen L, Liu ZJ, Wang BC, Yamamoto M, Terada T, Miyazawa A, Tanaka A, Sugano S, Shirouzu M, Nagayama K, Takenawa T, Yokoyama S. Curved EFC/F-BAR-domain dimers are joined end to end into a filament for membrane invagination in endocytosis. Cell 129:761-772 (2007)
107. Shtivelman E, Sussman J, Stokoe D. A role for PI 3-kinase and PKB activity in the G2/M phase of the cell cycle. Curr Biol 12:919-924 (2002)
108. Silkworth WT, Nardi IK, Scholl LM, Cimini D. Multipolar spindle pole coalescence is a major source of kinetochore mis-attachment and chromosome mis-segregation in cancer cells. PLoS One 10;4: e65-64 (2009)
109. Solomon DA, Kim JS, Bondaruk J, Shariat SF, Wang ZF, Elkahloun AG, Ozawa T, Gerard J, Zhuang D, Zhang S, Navai N, Siefker-Radtke A, Phillips JJ, Robinson BD, Rubin MA, Volkmer B, Hautmann R, Küfer R, Hogendoorn PC, Netto G, Theodorescu D, James CD, Czerniak B, Miettinen M, Waldman T. Frequent truncating mutations of STAG2 in bladder cancer. Nat Genet 45:1428-1430 (2013)
110. Stylli SS, I ST, Kaye AH, Lock P. Prognostic significance of Tks5 expression in gliomas. J Clin Neurosci 19:436-442 (2012)

111. Stylli SS, Luwor RB, Kaye AH, I ST, Hovens CM, Lock P. Expression of the adaptor protein Tks5 in human cancer: prognostic potential. Oncol Rep 32:989-1002 (2014)
112. Stylli SS, Stacey TT, Verhagen AM, Xu SS, Pass I, Courtneidge SA, Lock P. Nck adaptor proteins link Tks5 to invadopodia actin regulation and ECM degradation. J Cell Sci 122:2727-2740 (2009)
113. Thompson SL, Bakhoum SF, Compton DA. Mechanisms of chromosomal instability. Curr Biol 20:R285-295 (2010)
114. Thompson SL, Compton DA. Examining the link between chromosomal instability and aneuploidy in human cells. J Cell Biol 180:665-672 (2008)
115. Thul PJ, Åkesson L, Wiking M, Mahdessian D, Geladaki A, Ait Blal H, Alm T, Asplund A, Björk L, Breckels LM, Bäckström A, Danielsson F, Fagerberg L, Fall J, Gatto L, Gnann C, Hober S, Hjelmare M, Johansson F, Lee S, Lindskog C, Mulder J, Mulvey CM, Nilsson P, Oksvold P, Rockberg J, Schutten R, Schwenk JM, Sivertsson Å, Sjöstedt E, Skogs M, Stadler C, Sullivan DP, Tegel H, Winsnes C, Zhang C, Zwahlen M, Mardinoglu A, Pontén F, von Feilitzen K, Lilley KS, Uhlén M, Lundberg E. A subcellular map of the human proteome. Science 356:eaal3321 (2017)
116. Tokui N, Yoneyama MS, Hatakeyama S, Yamamoto H, Koie T, Saitoh H, Yamaya K, Funyu T, Nakamura T, Ohyama C, Tsuboi S. Extravasation during bladder cancer metastasis requires cortactin mediated invadopodia formation. Mol Med Rep 9:1142-1146 (2014)
117. Tsujita K, Suetsugu S, Sasaki N, Furutani M, Oikawa T, Takenawa T. Coordination between the actin cytoskeleton and membrane deformation by a novel membrane tubulation domain of PCH proteins is involved in endocytosis. J Cell Biol 172:269-279 (2006)

118. Uhlén M, Fagerberg L, Hallström BM, Lindskog C, Oksvold P, Mardinoglu A, Sivertsson Å, Kampf C, Sjöstedt E, Asplund A, Olsson I, Edlund K, Lundberg E, Navani S, Szigyarto CA, Odeberg J, Djureinovic D, Takanen JO, Hober S, Alm T, Edqvist PH, Berling H, Tegel H, Mulder J, Rockberg J, Nilsson P, Schwenk JM, Hamsten M, von Feilitzen K, Forsberg M, Persson L, Johansson F, Zwahlen M, von Heijne G, Nielsen J, Pontén F. Proteomics. Tissue-based map of the human proteome. Science 347:1260419 (2015)

119. Uhlen M, Zhang C, Lee S, Sjöstedt E, Fagerberg L, Bidkhori G, Benfeitas R, Arif M, Liu Z, Edfors F, Sanli K, von Feilitzen K, Oksvold P, Lundberg E, Hober S, Nilsson P, Mattsson J, Schwenk JM, Brunnström H, Glimelius B, Sjöblom T, Edqvist PH, Djureinovic D, Micke P, Lindskog C, Mardinoglu A, Ponten F. A pathology atlas of the human cancer transcriptome. Science 357:eaan2507 (2017)

120. Van Batavia J, Yamany T, Molotkov A, Dan H, Mansukhani M, Batourina E, Schneider K, Oyon D, Dunlop M, Wu XR, Cordon-Cardo C, Mendelsohn C. Bladder cancers arise from distinct urothelial sub-populations. Nat Cell Biol 16:982-991 (2014)

121. Wang Z, Yang J, Fisher T, Xiao H, Jiang Y, Yang C. Akt activation is responsible for enhanced migratory and invasive behavior of arsenic-transformed human bronchial epithelial cells. Environ Health Perspect 120:92-97 (2012)

122. Weaver AM. Regulation of cancer invasion by reactive oxygen species and Tks family scaffold proteins. Sci Signal 2:pe56 (2009)

123. Wu XR. Urothelial tumorigenesis: a tale of divergent pathways. Nat Rev Cancer 5:713-725 (2005)

124. Xia Z, Zhang N, Ding D. Proliferation and migration of hepatoblastoma cells are mediated by IRS-4 via PI3K/Akt pathways. Int J Clin Exp Med 7:3763-3769 (2014)

125. Xiang Y, Cheng Y, Li X, Li Q, Xu J, Zhang J, Liu Y, Xing Q, Wang L, He L, Zhao X. Up-regulated expression and aberrant DNA methylation of LEP and SH3PXD2A in pre-eclampsia. PLoS One 8:e59753 (2013)
126. Xiao H, Bai XH, Wang Y, Kim H, Mak AS, Liu M. MEK/ERK pathway mediates PKC activation-induced recruitment of PKCζ and MMP-9 to podosomes. J Cell Physiol 228:416-427 (2013)
127. Yamaguchi H, Lorenz M, Kempiak S, Sarmiento C, Coniglio S, Symons M, Segall J, Eddy R, Miki H, Takenawa T, Condeelis J. Molecular mechanisms of invadopodium formation: the role of the N-WASP-Arp2/3 complex pathway and cofilin. J Cell Biol 168:441-452 (2005)
128. Yamaguchi H, Yoshida S, Muroi E, Yoshida N, Kawamura M, Kouchi Z, Nakamura Y, Sakai R, Fukami K. Phosphoinositide 3-kinase signaling pathway mediated by p110α regulates invadopodia formation. J Cell Biol 193:1275-1288 (2011)
129. Yamamoto H, Sutoh M, Hatakeyama S, Hashimoto Y, Yoneyama T, Koie T, Saitoh H, Yamaya K, Funyu T, Nakamura T, Ohyama C, Tsuboi S. Requirement for FBP17 in invadopodia formation by invasive bladder tumor cells. J Urol 185:1930-1938 (2011)
130. Yamamoto Y, Matsuyama H, Chochi Y, Okuda M, Kawauchi S, Inoue R, Furuya T, Oga A, Naito K, Sasaki K. Overexpression of BUBR1 is associated with chromosomal instability in bladder cancer. Cancer Genet Cytogenet 174:42-47 (2007)
131. Yamamoto Y, Matsuyama H, Kawauchi S, Matsumoto H, Nagao K, Ohmi C, Sakano S, Furuya T, Oga A, Naito K, Sasaki K. Overexpression of polo-like kinase 1 (PLK1) and chromosomal instability in bladder cancer. Oncology 70:231-237 (2006)
132. Youssef RF, Raj GV. Lymphadenectomy in management of invasive bladder cancer. Int J Surg Oncol 2011:7581-7589 (2011)

7. Appendix

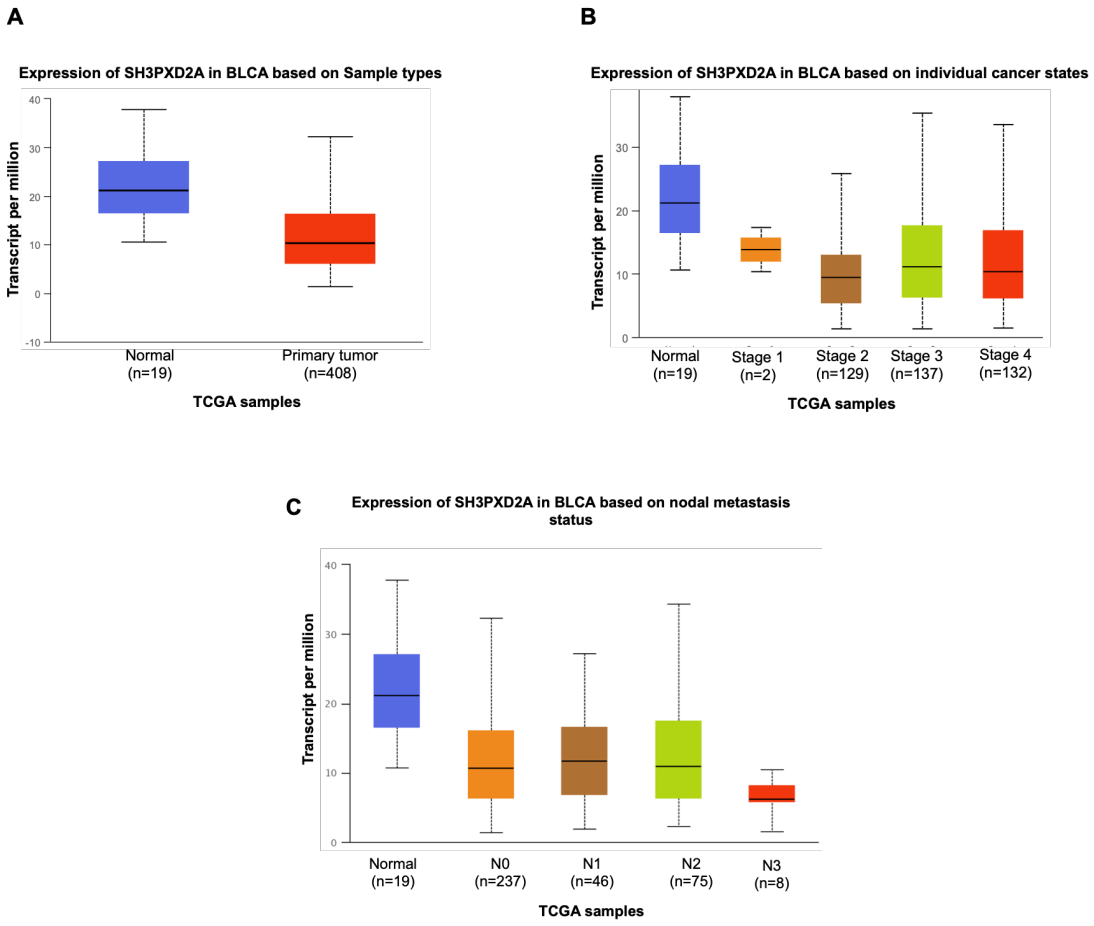

Suppl. Figure 1. It shows the expression of TKS5 in normal and cancerous bladder tissues. **A)** TKS5 expression in healthy bladder tissues is higher than bladder cancer samples. **B)** The expression of TKS5 in healthy bladder tissues is higher than different stages of bladder cancer samples. **C)** The expression of TKS5 in different lymph node metastasis stages of bladder cancer is lower than that of normal bladder tissue, and the expression tends to be lower the later the stage is. Figures are obtained with permission use from online database UALCAN (http://ualcan.path.uab.edu/analysis.html).

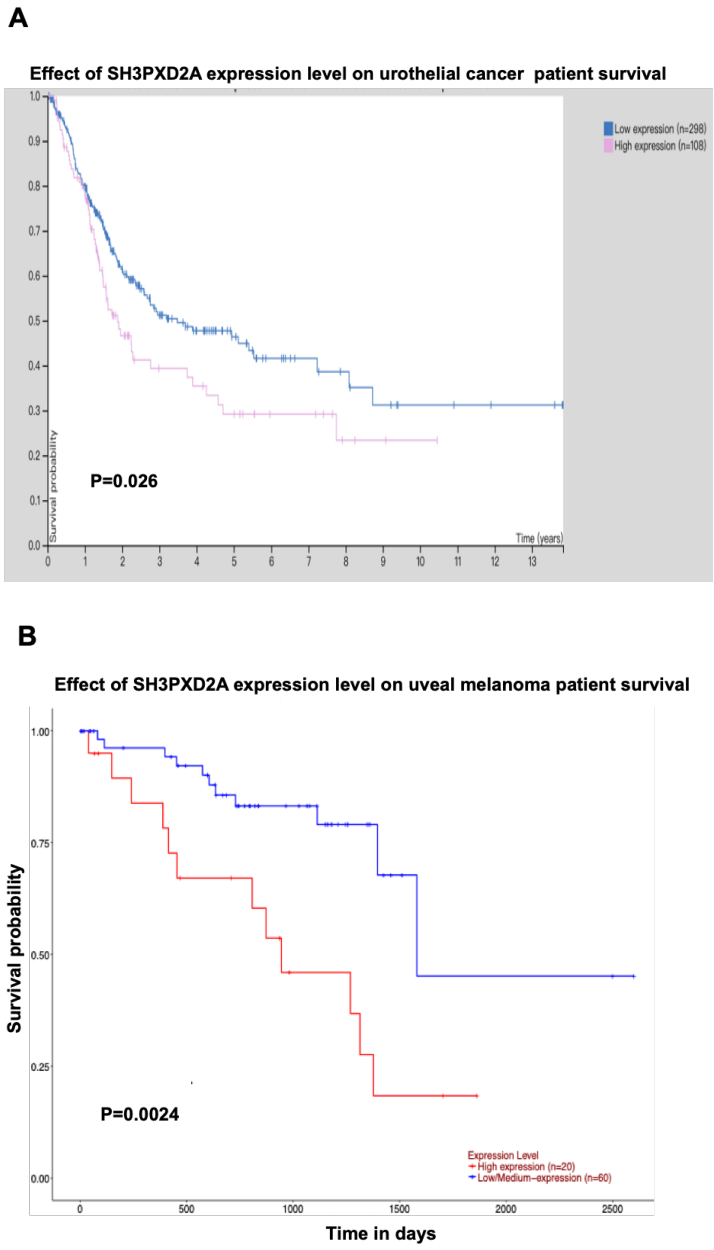

Suppl. Figure 2. The effect of TKS5 expression level on the survival outcome of urothelial cancer patients and uveal melanoma patients. A) Urothelial cancer patient with high TKS5 expression have shorter survival time compared with low TKS5 expression (P=0.026). **B)** Uveal melanoma patients with high TKS5 expression have worse survival probability compared with low TKS5 expression (P=0.0024). Figure A and B were obtained from Proteinatlas database (https://www.proteinatlas.org) and UALCAN (http://ualcan.path.uab.edu/analysis.html) respectively and also got the permission for use.

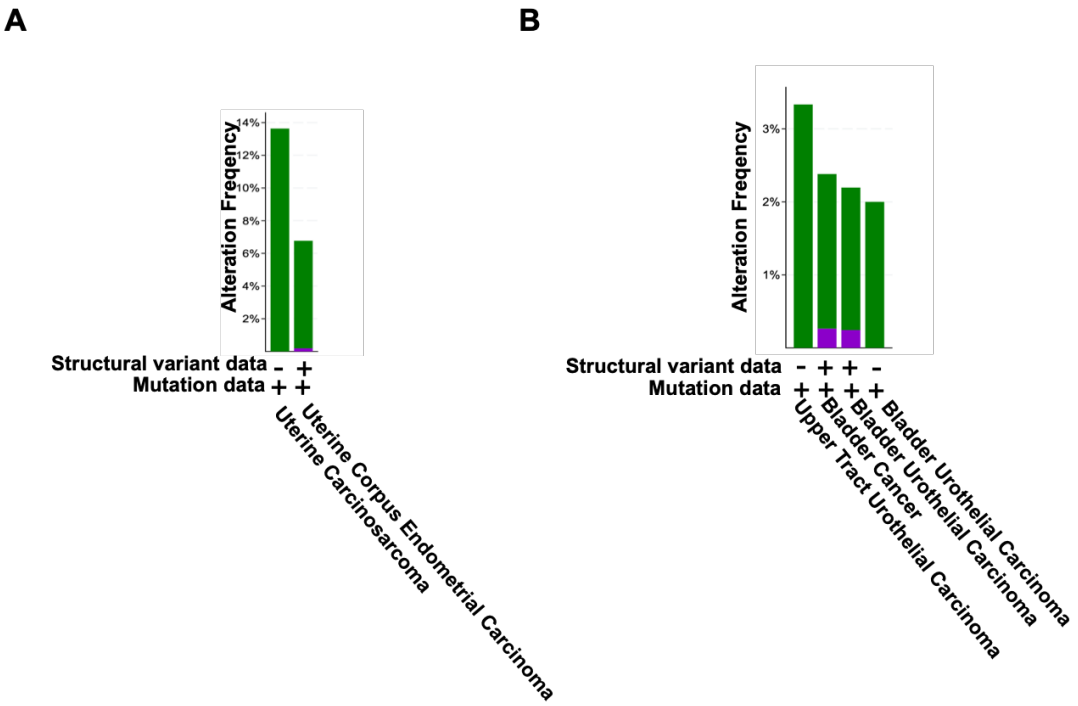

Suppl. Figure 3. The mutation of TKS5 in some cancer studies. A) It shows TKS5 mutation in uterine carcinosarcoma studies. **B)** It shows TKS5 mutation in different urothelial cancer studies. Green represents the mutation rate of the sample, blue represents the deep deletion rate of the sample. Data graph was obtained from cBioPortal (http://www.cbioportal.org) with permission for use.

The source URL and download date of the appendix:

Suppl. Figure 1

http://ualcan.path.uab.edu/cgi-bin/TCGAExResultNew2.pl?genenam=SH3PXD2A&ctype=BRCA (21-07-2021)

Suppl. Figure 2 A

https://www.proteinatlas.org/ENSG00000107957-SH3PXD2A/pathology/urothelial+cancer (20-07-2021)

Suppl. Figure 2 B

http://ualcan.path.uab.edu/cgi-bin/TCGA-survival1.pl?genenam=SH3PXD2A&ctype=UVM (21-07-2021)

Suppl. Figure 3 A

https://bit.ly/3Al0aY3 (21-07-2021)

Suppl. Figure 3 B

https://bit.ly/3aghdje (21-07-2021)

8. Acknowlegements

Foremost, I would like to express my gratitude to my supervisor prof. Dr. Cagatay Günes for the continuous of my MD study and research, for his motivation, enthusiasm, and immense knowledge. Thanks to the guidance of the professor, I made great progress on the road of scientific research and finally completed this thesis. I would also thank Prof. Dr. med. Christian Bolenz for kind support.

I also want to express my appreciation to Dr. rer. nat. Anca Azoitei. She is a good teacher in experimental research and a good friend in daily life. I would like to thank her for her friendship, empathy, and great sense of humor. I would also like to thank Xi Zheng, Junnan Liu and Xue Wang in particular. With their company and help, my experimental research process will not take so many detours, and my life in Germany will not be so boring. I would like also to thank other laboratory members, Xue Kong, Mingquan Chen, Cheng Zhang, Qianyu Kang, Iris Holzheu, Gregoire Najjar and Viktor Zehe, for a good communicative and encouraging atmosphere. I also would like to express my sincere thanks to my grandparents, parents and other family members. Thanks for raising me up and give me completely support for mine pursue in life.

Thanks to Mrs. Lina Zaveleva, from the international school of Ulm University, and Mrs. Katrin Mihr, from the medical faculty of Ulm University, for their help and support regarding my thesis writing and my studies.

9. Curriculum Vitae

The Curriculum Vitae has been removed due to data privacy protection.